



3 4456 0004232 6

ORNL/TM-9749

ornl

**OAK RIDGE
NATIONAL
LABORATORY**

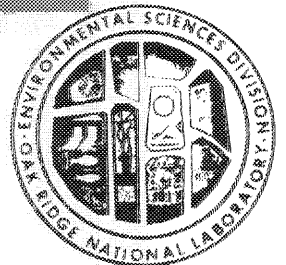
MARTIN MARIETTA

Site-Specific Seasonal Models of Carbon Fluxes in Terrestrial Biomes

A. W. King
D. L. DeAngelis

Environmental Sciences Division
Publication No. 2515

OAK RIDGE NATIONAL LABORATORY
CENTRAL RESEARCH LIBRARY
CIRCULATION SECTION
4500N ROOM 175
LIBRARY LOAN COPY
DO NOT TRANSFER TO ANOTHER PERSON
If you wish someone else to see this
report, send in name with report and
the library will arrange a loan.



OPERATED BY
MARTIN MARIETTA ENERGY SYSTEMS, INC.
FOR THE UNITED STATES
DEPARTMENT OF ENERGY

Printed in the United States of America. Available from
National Technical Information Service
U.S. Department of Commerce
5285 Port Royal Road, Springfield, Virginia 22161
NTIS price codes—Printed Copy: A08; Microfiche A01

This report was prepared as an account of work sponsored by an agency of the United States Government. Neither the United States Government nor any agency thereof, nor any of their employees, makes any warranty, express or implied, or assumes any legal liability or responsibility for the accuracy, completeness, or usefulness of any information, apparatus, product, or process disclosed, or represents that its use would not infringe privately owned rights. Reference herein to any specific commercial product, process, or service by trade name, trademark, manufacturer, or otherwise, does not necessarily constitute or imply its endorsement, recommendation, or favoring by the United States Government or any agency thereof. The views and opinions of authors expressed herein do not necessarily state or reflect those of the United States Government or any agency thereof.

ORNL/TM-9749

ENVIRONMENTAL SCIENCES DIVISION

SITE-SPECIFIC SEASONAL MODELS OF CARBON
FLUXES IN TERRESTRIAL BIOMES

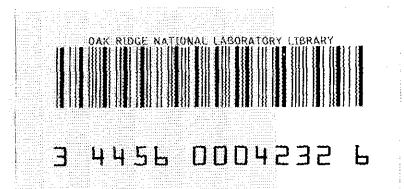
A. W. King and D. L. DeAngelis

Environmental Sciences Division
Publication No. 2515

Date of Issue -- January 1986

Prepared for the
Carbon Dioxide Research Division
Office of Energy Research

Prepared by the
OAK RIDGE NATIONAL LABORATORY
Oak Ridge, Tennessee 37831
operated by
MARTIN MARIETTA ENERGY SYSTEMS, INC.
for the
U.S. DEPARTMENT OF ENERGY
under Contract No. DE-AC05-84OR21400



CONTENTS

	<u>Page</u>
LIST OF FIGURES	vii
LIST OF TABLES	xi
ACKNOWLEDGMENTS	xiii
ABSTRACT	xv
INTRODUCTION	1
1. MODEL COLLECTION	4
2. MODEL DESCRIPTIONS	7
2.1 Temperate Deciduous Forest Model - <u>Liriodendron</u> Stand	7
2.1.1 Structure of the Model	8
2.1.1.1 Compartments	8
2.1.1.2 Driving variables	13
2.1.1.3 Flows or rate processes	13
2.1.1.4 Photosynthesis and respiration	16
2.1.1.5 Release of carbon through decomposition	17
2.1.2 Seasonal Photosynthesis and Respiration	18
2.2 Temperate Deciduous Forest Model - Oak/Ash Stand	18
2.2.1 Structure of the Model	21
2.2.1.1 Compartments	21
2.2.1.2 Driving variables	23
2.2.1.3 Flows or rate processes	23
2.2.1.4 Photosynthesis and respiration	24
2.2.1.5 Release of carbon through decomposition	26
2.2.2 Seasonal Photosynthesis and Respiration	26

	<u>Page</u>
2.3 Northern Coniferous Forest Model	27
2.3.1 Structure of the Model	27
2.3.1.1 Compartments	27
2.3.1.2 Driving variables	32
2.3.1.3 Flows or rate processes	33
2.3.1.4 Indirect interactions of compartments . .	35
2.3.1.5 Photosynthesis and respiration	35
2.3.1.6 Release of carbon through decomposition	38
2.3.2 Seasonal Photosynthesis and Respiration	39
2.4 Temperate Broadleaf Evergreen Forest Model	39
2.4.1 Structure of the Model	42
2.4.1.1 Compartments	42
2.4.1.2 Driving variables	42
2.4.1.3 Flows or rate processes	44
2.4.1.4 Photosynthesis and respiration	45
2.4.1.5 Release of carbon through decomposition	46
2.4.2 Seasonal Photosynthesis and Respiration	47
2.5 Tropical Deciduous Forest Model	47
2.5.1 Structure of the Model	50
2.5.1.1 Compartments	50
2.5.1.2 Driving variables	50
2.5.1.3 Flows or rate processes	50
2.5.1.4 Photosynthesis and respiration	52
2.5.1.5 Release of carbon through decomposition	53
2.5.2 Seasonal Photosynthesis and Respiration	53

	<u>Page</u>
2.6 Tropical Rain Forest Model	56
2.6.1 Structure of the Model	56
2.6.1.1 Compartments	56
2.6.1.2 Driving variables	56
2.6.1.3 Flows or rate processes	58
2.6.1.4 Photosynthesis and respiration	59
2.6.1.5 Release of carbon through decomposition	60
2.6.2 Seasonal Photosynthesis and Respiration	60
2.7 Temperate Grassland Model	63
2.7.1 Structure of the Model	63
2.7.1.1 Compartments	63
2.7.1.2 Driving variables	65
2.7.1.3 Flows or rate processes	66
2.7.1.4 Photosynthesis and respiration	67
2.7.1.5 Release of carbon through decomposition	69
2.7.2 Seasonal Photosynthesis and Respiration	70
2.8 Arid Lands Model	72
2.8.1 Structure of the Model	72
2.8.1.1 Compartments	72
2.8.1.2 Driving variables	77
2.8.1.3 Flows or rate processes	78
2.8.1.4 Photosynthesis and respiration	83
2.8.1.5 Release of carbon through decomposition	85
2.8.2 Seasonal Photosynthesis and Respiration	86

	<u>Page</u>
2.9 Tundra Model	86
2.9.1 Structure of the Model	89
2.9.1.1 Compartments	89
2.9.1.2 Driving variables	89
2.9.1.3 Flows or rate processes	91
2.9.1.4 Photosynthesis and respiration	93
2.9.1.5 Release of carbon through decomposition	94
2.9.2 Seasonal Photosynthesis and Respiration	95
2.10 Pine Flatwoods Model	98
2.10.1 Structure of the Model	98
2.10.1.1 Compartments	98
2.10.1.2 Driving variables	102
2.10.1.3 Flows or rate processes	102
2.10.1.4 Photosynthesis and respiration	104
2.10.1.5 Release of carbon through decomposition	105
2.10.2 Seasonal Photosynthesis and Respiration	105
3. EXTRAPOLATION OF SITE-SPECIFIC MODELS TO BIOME-LEVEL MODELS	109
4. CONCLUDING REMARKS	124
REFERENCES	127

LIST OF FIGURES

<u>Figure</u>		<u>Page</u>
2.1.1a	Compartmental structure of the temperate deciduous forest model - <u>Liriodendron</u> stand (ecosystem overview) . . .	9
2.1.1b	Compartmental structure of the temperate deciduous forest model - <u>Liriodendron</u> stand (canopy subsystem) . . .	10
2.1.1c	Compartmental structure of the temperate deciduous forest model - <u>Liriodendron</u> stand (understory subsystem)	11
2.1.1d	Compartmental structure of the temperate deciduous forest model - <u>Liriodendron</u> stand (litter/soil subsystem)	12
2.1.2	Seasonal total ecosystem photosynthesis and respiration for a <u>Liriodendron</u> stand	19
2.1.3	Seasonal net CO ₂ exchange between the atmosphere and a <u>Liriodendron</u> stand	20
2.2.1	Compartmental structure of the temperate deciduous forest model - oak-ash stand	22
2.2.2	Seasonal total ecosystem photosynthesis and respiration for an oak-ash stand	28
2.2.3	Seasonal net CO ₂ exchange between the atmosphere and an oak-ash stand	29
2.3.1a	Compartmental structure of the northern coniferous forest model - carbon budget	30
2.3.1b	Compartmental structure of the northern coniferous forest model - water budget	31
2.3.2	Seasonal total ecosystem photosynthesis and respiration for a northern coniferous forest stand	40
2.3.3	Seasonal net CO ₂ exchange between the atmosphere and a northern coniferous forest stand	41
2.4.1	Compartmental structure of the temperate broadleaf evergreen forest model	43
2.4.2	Seasonal total ecosystem photosynthesis and respiration for a temperate broadleaf evergreen forest stand	48

<u>Figure</u>	<u>Page</u>
2.4.3 Seasonal net CO ₂ exchange between the atmosphere and a temperate broadleaf evergreen forest stand	49
2.5.1 Compartmental structure of the tropical deciduous forest model	51
2.5.2 Seasonal total ecosystem photosynthesis and respiration for a tropical deciduous forest stand	54
2.5.3 Seasonal net CO ₂ exchange between the atmosphere and a tropical deciduous forest stand	55
2.6.1 Compartmental structure of the tropical rain forest model	57
2.6.2 Seasonal total ecosystem photosynthesis and respiration for a tropical rain forest stand	61
2.6.3 Seasonal net CO ₂ exchange between the atmosphere and a tropical rain forest stand	62
2.7.1 Compartmental structure of the temperate grassland model	64
2.7.2 Seasonal total ecosystem photosynthesis and respiration for a temperate grassland plot	71
2.7.3 Seasonal net CO ₂ exchange between the atmosphere and a temperate grassland plot	73
2.8.1 Compartmental structure of the arid lands model - production submodel	74
2.8.2 Compartmental structure of the arid lands model - decomposition submodel	75
2.8.3 Compartmental representation of carbon components in living plant compartments of the arid lands model	82
2.8.4 Seasonal total ecosystem photosynthesis and respiration for a stand of arid land vegetation	87
2.8.5 Seasonal net CO ₂ exchange between the atmosphere and a stand of arid land vegetation	88

<u>Figure</u>	<u>Page</u>
2.9.1	Compartment structure of the tundra model, ABISCO II 90
2.9.2	Seasonal total ecosystem photosynthesis and respiration for a tundra ecosystem model 96
2.9.3	Seasonal net CO ₂ exchange between the atmosphere and a tundra ecosystem 97
2.10.1	Compartmental structure of pine flatwoods carbon flow submodel 99
2.10.2	Compartmental structure of pine flatwoods phosphorus cycling submodel 100
2.10.3	Compartmental structure of pine flatwoods water flow submodel 101
2.10.4	Seasonal total ecosystem photosynthesis and respiration for a pine flatwoods ecosystem 107
2.10.5	Seasonal net CO ₂ exchange between the atmosphere and a pine flatwoods ecosystem 108
3.1	World distribution of the site-specific models collected to date 113

LIST OF TABLES

<u>Table</u>		<u>Page</u>
2.3.1	Interactions among modules of CONIFER	36
3.1	List of available seasonal terrestrial carbon flux models that have been collected to date up to present time	110
3.2	Regional classification of the site-specific models according to Olson, Watts, and Allison (1983)	114
3.3	Descriptions of the Olson, Watts, and Allison (1983) regional classifications represented by the site-specific models	116

ACKNOWLEDGMENTS

The authors gratefully acknowledge the critical reviews by W. M. Post and J. S. Olson of Oak Ridge National Laboratory.

ABSTRACT

KING, A. W. and D. L. DEANGELIS. 1986. Site-specific seasonal models of carbon fluxes in terrestrial biomes. ORNL/TM-9749. Oak Ridge National Laboratory, Oak Ridge, Tennessee. 155 pp.

A set of site-specific computer simulation models of seasonal terrestrial carbon exchange has been assembled from open-literature sources. This collection is designed to facilitate the development of biome-level models for each of the principal terrestrial vegetation biomes on earth, for their integration into a global model of seasonal CO₂ variation in the atmosphere. The models are described in sufficient detail that their underlying assumptions can be compared. Descriptions include the following aspects of each model: (1) the compartments, (2) the carbon fluxes between compartments, and (3) the climatic variables that drive the carbon fluxes. In particular, the functional forms of the dependencies of respiration and photosynthesis on the driving variables are described. The methods by which these models will be extrapolated to biome-level models are also discussed.

INTRODUCTION

The atmospheric CO₂ records at Mauna Loa Observatory (Bacastow and Keeling 1981) and elsewhere (Pearman and Hyson 1981) document a seasonality, which appears as nearly sinusoidal excursions around the increasing average annual concentration of CO₂. This periodicity in atmospheric CO₂ is largely attributable to the seasonality of terrestrial biomass metabolism in the Northern Hemisphere, which is characterized by net carbon fixation during the summer and net decomposition during the winter. This terrestrial effect on atmospheric seasonality is only partially offset by a seasonality of smaller amplitude (with a 180° phase difference) of CO₂ flux from the oceans (Fung et al. 1983).

The amplitude of the seasonal excursions of CO₂ remained roughly constant at about 5 ppm in the measured data up until about 1975 (Hall, Ekdahl, and Wartenburg 1975), but has apparently increased since that time (Bacastow and Keeling 1981, Bacastow et al. 1981). There are several possible explanations for this phenomenon, including increased storage of carbon in terrestrial biota or faster CO₂-stimulated photosynthesis.

As far as possible long-term effects of increasing CO₂ on the climate are concerned, the seasonal variations in atmospheric CO₂ may be of minor importance. However, data on this seasonality may reveal new information on terrestrial-atmospheric carbon fluxes in general. A modeling effort to describe seasonality may improve our general understanding of the global carbon cycle in the following ways: (1) it

may help determine if the increasing amplitude of the seasonality of atmospheric CO₂ concentration (Bacastow et al. 1981) is related to effects that could be of long-term importance, such as CO₂-stimulated high rates of terrestrial photosynthesis; (2) it may contribute to our knowledge of whether various terrestrial ecosystems are acting as sources or sinks, and whether climatic changes could alter the present situation; (3) it may contribute to our understanding of the seasonal cycle as a possible monitor of biotic metabolism and provide insight into the health and productivity of the biosphere (Hall, Ekdahl, and Wartenburg 1975).

Mathematical modeling efforts to describe the seasonality of atmospheric CO₂ may approach the problem in a number of different ways: (1) Empirical relationships can be derived between the seasonality of photosynthetic and respiratory fluxes and climatic variables. This method usually makes no attempt to model the terrestrial standing crops. (2) Standardized compartment models can be applied to each biome, life-zone type, or latitudinal zone. These models may be simple, containing several biomass and soil variables averaged over each of the zones. (3) Models already developed for specific sites may be borrowed and modified so that they apply to wider areas than the particular sites for which they were originally designed.

Each of the above procedures has advantages and disadvantages. We will discuss here the relative advantages and disadvantages of approach (3), the elaboration of site-specific models.

Advantages:

1. A large number of site-specific models have already been developed. Computer simulation of these is usually fairly simple.
2. These site-specific models were developed by experts on the particular biome type; in many cases the models have been validated.
3. Detailed site-specific compartment models have the flexibility to incorporate a variety of scenarios of possible interest in any attempt to investigate changes in seasonal fluxes. These include (a) land-use changes, (b) changes in harvesting rates, (c) growth stimulation by enhanced CO₂, (d) changes in climate, and (e) effects of other stresses such as acid rain.
4. It is easy to incorporate new ecological data into improvements on site-specific models.
5. Site-specific models will provide "ground-truth" data against which other modeling approaches can be compared.

Disadvantage:

1. The primary disadvantage of site-specific models is that it may be difficult to extend such models to cover whole biomes. This is because of the great amount of heterogeneity, both climatic and edaphic, within a biome.

This report documents a set of site-specific models that will later be incorporated into a global seasonal carbon flux model. We also outline a method for extrapolating the site-specific models to biome-level models.

1. MODEL COLLECTION

The assembly of a set of terrestrial carbon flux models is made possible by the recent appearance of a number of volumes synthesizing the extensive data collected during the International Biological Program (IBP). Examples include compilations or summaries of information on forests (Reichle 1981), grasslands (Bremeyer and Van Dyne 1980), arid lands (Goodall and Perry 1979), and tundra (Weilgolaski 1975). Although these summaries sometimes do not contain detailed seasonal information, many of the primary sources on which they are based do contain such information; many of the 116 IBP sites compiled by DeAngelis, Gardner, and Shugart (1981) are good examples.

A compendium on seasonal terrestrial carbon fluxes has been compiled to serve as a compact source for constructing, modifying, and improving models of seasonal terrestrial carbon fluxes (King and DeAngelis 1985). This compendium includes much of the available IBP data, plus information from other literature sources. The data are organized by general biome type.

In addition to the large amount of data collected, many site-specific models of seasonal carbon dynamics have been constructed, both within and outside the various IBP projects. These models are also reviewed by King and DeAngelis (1985). Most of the models are process-oriented compartment models. Seasonality is built into the models through both empirical information on phenology and mechanistic driving of photosynthesis, respiration, and decomposition by climatic variables. These models, and others like them, are being scrutinized

for their applicability to the problem of modeling the seasonal carbon dynamics of the terrestrial biosphere.

In collecting site-specific models for ultimate integration into an overall model of global carbon, we have directed our search towards coverage of ten major ecosystem types: tropical rain forest, tropical deciduous forest, temperate deciduous forest, temperate broadleaved evergreen forest, temperate grassland, tropical grassland/savanna, northern coniferous forest, boreal tundra, arid lands, and warm coniferous (pine) forest. From this compiled set of models, we select representative models for as many ecosystem types (or subtypes) as possible. The criteria used in the selection process are outlined below.

1. Availability: The selection of representative models is determined by the number of suitable models. For some ecosystem types, few appropriate models are available; for others, such as the temperate grasslands, there is a relatively large selection of models dealing with some aspect of carbon dynamics.
2. Abiotic driving variables: Models in which seasonal carbon dynamics are driven by seasonally varying climatic factors are favored. For example, decomposition might be modeled as a function of litter (or soil) temperature and moisture. Models in which seasonal dynamics are determined by time-varying rate coefficients specific only to a certain site or data set are not selected. This selection criterion reflects the demands of the site-to-biome extrapolation process described later (Sect. 3).
3. Simplicity: Preference is given to models with relatively few state variables and parameters (unless the state variables are repetitive, such as many soil layers). Thus, exceptionally complex or detailed models are omitted.

4. Completeness: In general, the models chosen are those that trace the flux of carbon from the assimilation of CO₂ via photosynthesis, through translocation of photosynthate, to the release of CO₂ during respiration and organic matter decomposition. When such models are not available, we select submodels of photosynthetic production and decomposition. These independently derived submodels require coupling in some manner to provide complete models of carbon fluxes for some of the ecosystem types.
5. General applicability: Preference is given to those models that have already been applied to two or more sites within the ecosystem type or biome, in contrast to those models having been applied to only one site or vegetation stand. This criterion often distinguishes between models developed for general application and those developed with only a single site in mind.
6. Validation: Preference is given to models that have been validated against independent data sets, or those for which model output has been compared against field observations.

2. MODEL DESCRIPTIONS

This section describes a set of site-specific models that we have implemented on the computer facilities at Oak Ridge National Laboratory, Oak Ridge, Tennessee. The models are only a subset of the models that we have identified as potentially useful (according to the criteria of Sect. 1). We expect that several more models will eventually be implemented.

Model descriptions present the compartmental structure, the intercompartmental carbon or biomass fluxes, the climatic driving forces, and the way in which the driving forces are assumed to affect the fluxes. Special emphasis is given to the effect of driving forces on photosynthesis, respiration, and the release of CO_2 during decomposition; these fluxes are the most critical in simulating CO_2 exchange between the atmosphere and the terrestrial biosphere.

The descriptions also include plots of total stand (or ecosystem), photosynthesis, and respiration (including both live plant respiration and decomposer respiration), as generated by the models. Photosynthesis represents the assimilation of atmospheric CO_2 by the vegetation; the respiration represents the ecosystem's contribution to atmospheric CO_2 . The simulations are the results of model implementation runs and should be considered illustrative and characteristic of the ecosystem type, but preliminary.

2.1 TEMPERATE DECIDUOUS FOREST MODEL - LIRIODENDRON STAND

A model of organic matter transfer in a second-growth deciduous forest at Oak Ridge, Tennessee, was developed by Sollins, Reichle, and

Olson (1973). This forest ecosystem is dominated by the tulip poplar, Liriodendron tulipifera L. The purpose of their model was to improve the ability to predict the effects of forest perturbation. We use the model to predict seasonal carbon dynamics in forests for which we believe the model to be appropriate.

2.1.1 Structure of the Model

2.1.1.1 Compartments. The overall compartmental structure of the model is shown in Fig. 2.1.1a. There are four subsystems:

- (1) subsystem A - tulip poplar compartment of the stand (Fig. 2.1.1b),
- (2) subsystem B - other miscellaneous canopy species (Fig. 2.1.1b),
- (3) subsystem C - understory species (Fig. 2.1.1c), and
- (4) subsystem D - soil, litter, and decomposers (Fig. 2.1.1d).

The state variables corresponding to these compartments are listed below. Values of all state variables are in units of kilograms biomass per square meter. These do not completely correspond to the compartments in Fig. 2.1.1 in a one-to-one manner.

- X₁ - tulip poplar leaves
- X₂ - tulip poplar active tissues
- X₃ - tulip poplar woody tissues
- X₄ - tulip poplar buds
- X₅ - other overstory leaves
- X₆ - other overstory active tissues
- X₇ - other overstory woody tissues
- X₈ - other overstory buds
- X₉ - understory leaves
- X₁₀ - understory active tissues
- X₁₁ - understory woody tissues
- X₁₂ - understory buds
- X₁₃ - ground cover
- X₁₄ - standing dead
- X₁₅ - canopy consumers
- X₁₆ - fine roots
- X₁₇ - quickly decomposing O₁ layer
- X₁₈ - slowly decomposing O₁ layer

ORNL - DWG 70-12021AR

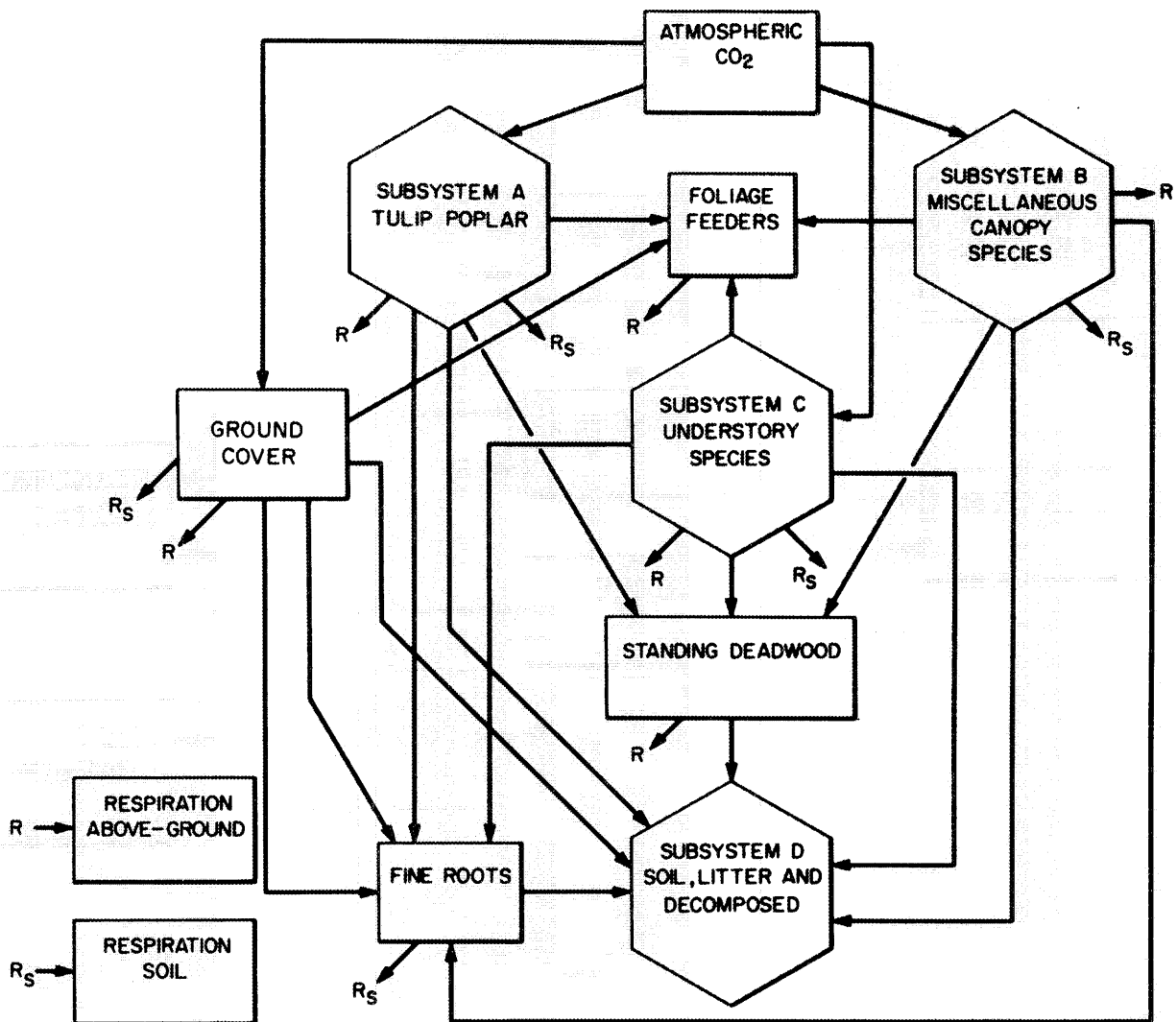


Fig. 2.1.1a. Compartmental structure of the temperate deciduous forest model - *Liriodendron* stand. Ecosystem overview showing four major subsystems (A-D) and various other compartments. R, aboveground respiration; R_s , belowground respiration. From Sollins, Reichle, and Olson (1973).

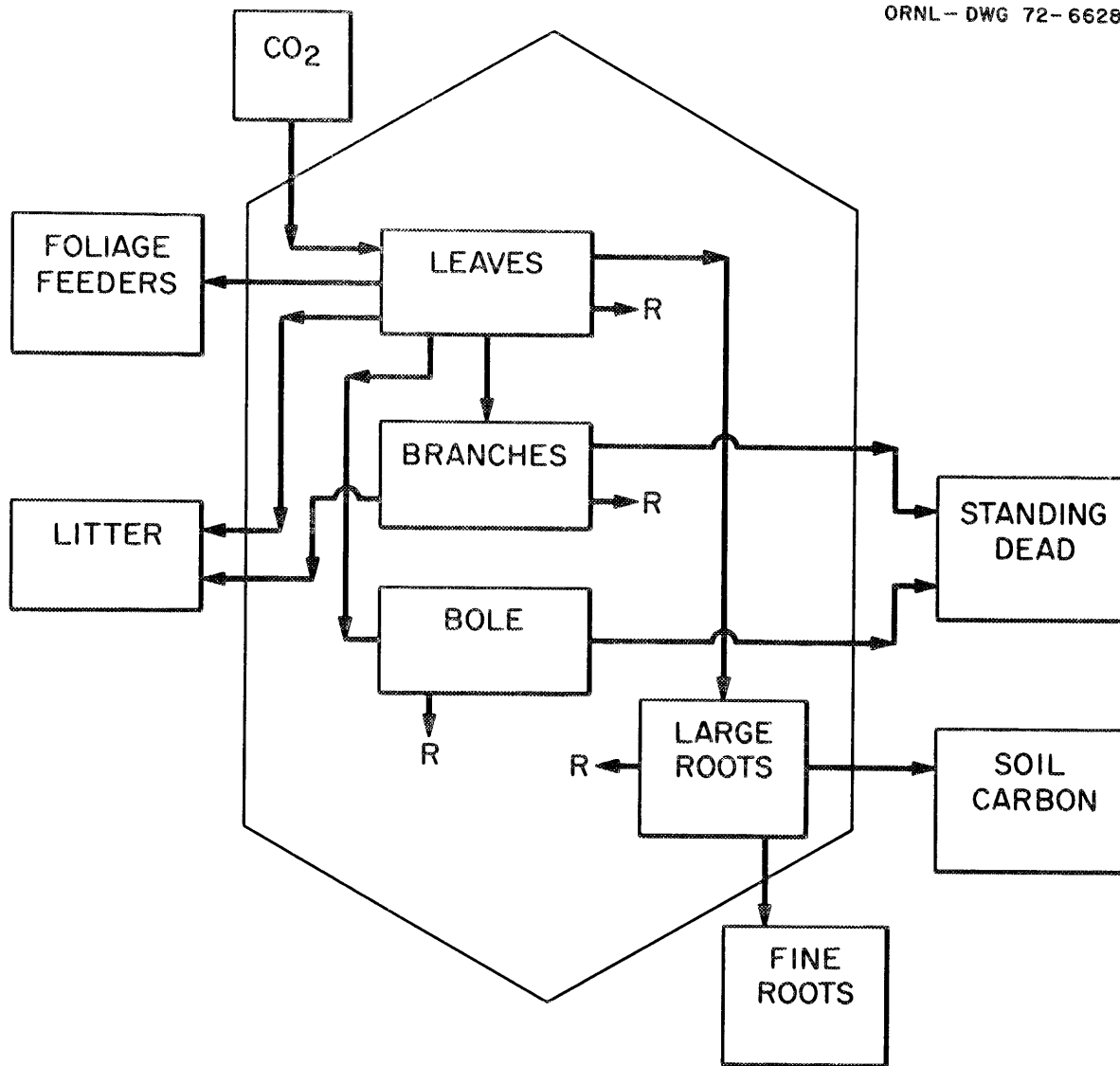


Fig. 2.1.1b. Compartmental structure of the temperate deciduous forest model - *Liriodendron* stand, canopy subsystems A and B. Subsystem A -- the dominant species *L. tulipifera* including all individuals greater than 10 m in height. Subsystem B -- other overstory trees 10 m in height. R, aboveground respiration. From Sollins, Reichle, and Olson (1973).

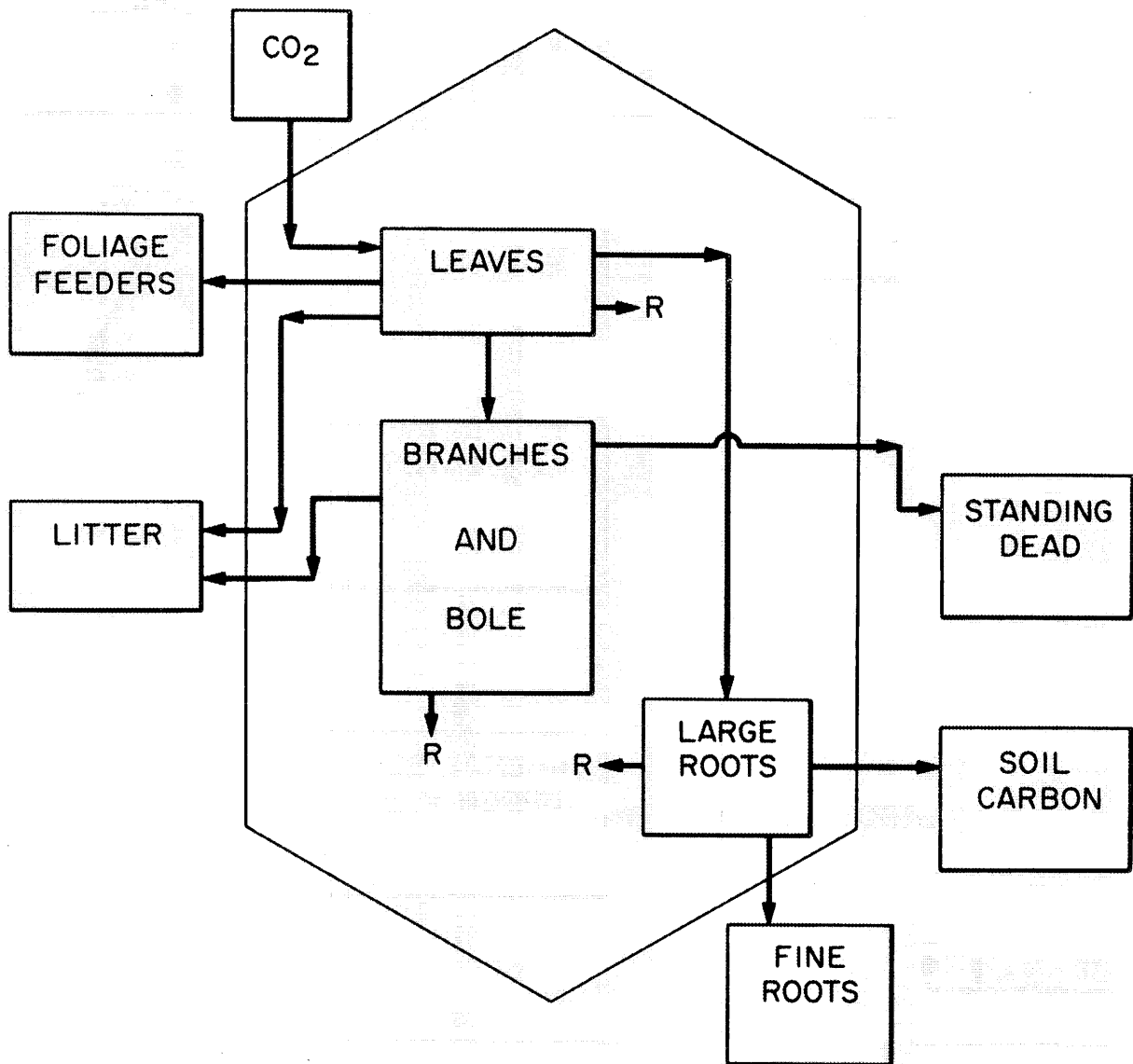


Fig. 2.1.1c. Compartmental structure of the temperate deciduous forest model - *Liriodendron* stand, understory subsystem. Understory includes trees 1-10 m height. R, aboveground respiration. From Sollins, Reichle, and Olson (1973).

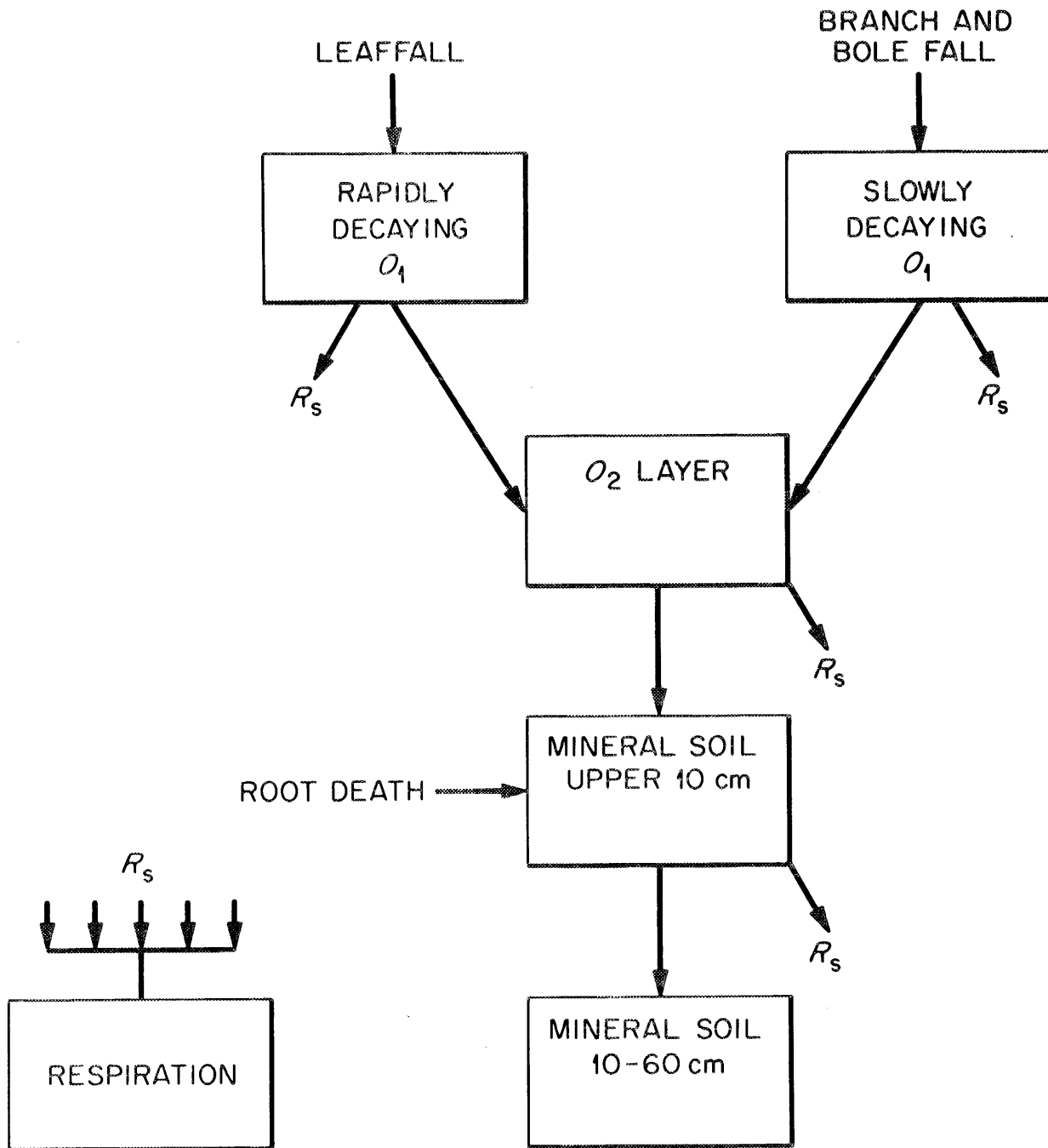


Fig. 2.1.1d. Compartmental structure of the temperate deciduous forest model - Liriodendron stand, litter and soil compartments. Decomposer organisms are conceptually combined with their substrate. R, belowground respiration. From Sollins, Reichle, and Olson (1973).

X_{19} - O_2 layer
 X_{20} - soil organic matter (0-10 cm depth)
 X_{21} - soil organic matter (10-60 cm depth)

2.1.1.2 Driving variables. There are three exogenous driving variables in the model:

Z_1 - temperature ($^{\circ}C$)
 Z_2 - light intensity (langleys min)
 Z_3 - soil moisture (% wet weight)

Daily values of soil moisture and temperature are interpolated from mean monthly empirical values read into the computer program as input data. An average value of light intensity is taken during the growing season.

2.1.1.3 Flows or rate processes. The flows of organic matter correspond to the arrows between compartments in Fig. 2.1.1a-d. The detailed functional representation of these flows and the assumptions involved are described in Sollins, Reichle, and Olson (1973); here we define the flows and provide their basic functional representation. The model representation of photosynthesis and respiration is discussed further in Sect. 2.1.1.4. The notation $F(i,j)$ indicates the flow of material from compartment i to compartment j . The number 99 refers to a compartment external to the system. All flows into the system are labeled $F(99,j)$, and all flows out of the system are labeled $F(i,99)$. In the list that follows, the A_{ij} 's, R_{ij} 's, C_i 's, and K_i 's are constants; the G_j 's represent photosynthesis as a function of light, Z_2 , and F_T is a temperature, Z_1 , function (these latter two functions are described in Sect. 2.1.1.4). The units of all flows are kilograms biomass per square meter per year.

Tulip poplar trees

- F(99,1) - photosynthesis of leaves: $(1 - R_{12})G_A$
 F(1,2) - translocation of organic matter from leaves
 to active tissue: $A_{12}X_1$
 F(1,15) - consumption of leaves: $A_{152}C_A X_1$
 F(1,17)₁ - frass production: $(1 - A_{152})C_A X_1$
 F(1,17)₂ - litterfall to quickly decomposing O₁ layer:
 $A_{14}X_1$ during dormant season, 0 during
 growing season
 F(1,99) - respiration of leaves: $R_4 F_T X_1$
 F(2,1) - translocation of organic matter from active
 tissue to leaves: Φ_{21}
 F(2,3) - translocation of organic matter from active
 tissue to buds: $A_{23} F_T X_2$
 F(2,16) - translocation of organic matter from active
 tissue to fine roots: $A_{216} X_2$
 F(2,99) - respiration of active tissues: $R_{21} F_T X_2$
 F(3,14) - transfer to standing dead: $A_{36} X_3$
 F(3,17) - limbfall to quickly decomposing O₁ layer:
 $0.38 A_{34} X_3$
 F(3,18) - limbfall to slowly decomposing O₁ layer:
 $0.62 A_{34} X_3$
 F(3,20) - transfer of woody biomass to soil organic
 matter: $A_{37} X_3$
 F(4,99) - respiration of buds: $R_{41} F_T X_4$

Other overstory trees

- F(99,5) - photosynthesis of leaves: $(1 - R_{52})G_B$
 F(5,6) - translocation of organic matter from leaves to
 active tissues: $A_{56} X_5$
 F(5,15) - consumption of leaves: $A_{152} C_B X_5$
 F(5,17)₁ - frass production: $(1 - A_{152}) C_B X_5$
 F(5,17)₂ - litterfall to quickly decomposing O₁ layer:
 $A_{54} X_5$
 F(5,99) - respiration of leaves: $R_{51} F_T X_5$
 F(6,5) - translocation of organic matter from active
 tissues to leaves: Φ_{65}
 F(6,7) - translocation of organic matter from active
 tissue to woody tissue: $A_{67} F_T X_6$
 F(6,8) - translocation of organic matter from active
 tissue to buds: $A_{68} F_T X_6$
 F(6,16) - translocation of organic matter from active
 tissue to fine roots: $A_{611} X_6$
 F(6,99) - respiration of active tissues: $R_{61} F_T X_6$
 F(7,14) - transfer to standing dead: $A_{611} X_6$
 F(7,17) - limbfall to quickly decomposing O₁ layer:
 $0.38 A_{74} X_7$
 F(7,18) - limbfall to slowly decomposing O₁ layer:
 $0.62 A_{74} X_7$
 F(7,20) - transfer of woody biomass to soil organic
 matter: $A_{77} X_7$
 F(8,99) - respiration of buds: $R_{81} F_T X_8$

Understory trees

- F(99,9) - photosynthesis of leaves: $(1 - R_{92})G_C$
 F(9,10) - translocation of organic matter from leaves to active tissue: $A_{910}X_9$
 F(9,15) - consumption of leaves: $A_{152}C_C X_9$
 F(9,17)₁ - frass production: $(1 - A_{152})C_C X_9$
 F(9,17)₂ - litterfall to quickly decomposing O₁ layer: $A_{94}X_9$ during dormant season, 0 during growing season
 F(9,99) - respiration of leaves: $R_{91}F_T X_9$
 F(10,9) - translocation of organic matter from active tissue to leaves: Φ_{109}
 F(10,11) - translocation of organic matter from active tissue to woody tissue: $A_{1011}F_T X_{10}$
 F(10,12) - translocation of organic matter from active tissue to buds: $A_{1012}F_T X_{10}$
 F(10,99) - respiration of active tissue: $R_{101}F_T X_{10}$
 F(11,14) - transfer to standing dead: $A_{116}X_{11}$
 F(11,17) - limbfall to quickly decomposing O₁ layer: $0.38A_{114}X_{11}$
 F(11,18) - limbfall to slowly decomposing O₁ layer: $0.62A_{114}X_{11}$
 F(11,20) - transfer of organic matter from woody tissues to soil organic matter: $A_{117}X_{11}$
 F(12,99) - respiration of buds: $R_{121}F_T X_{12}$

Ground cover

- F(99,13) - photosynthesis of leaves: $(1 - R_{132})G_H$
 F(13,16) - transfer to fine roots: $A_{131}X_{13}$
 F(13,17) - litterfall to quickly decomposing O₁ layer: $A_{132}X_{13}$
 F(13,99) - respiration of leaves: $R_{131}F_T X_{13}$

Other components

- F(14,18) - transfer of biomass from standing dead to slowly decomposing O₁ layer: $A_{141}X_{14}$
 F(14,99) - decomposer respiration from standing dead: $R_{141} F_T X_{14}$
 F(15,99) - respiration of canopy consumers: $(M_{15} + R_{15} F_T) X_{15}$
 F(16,20) - transfer of fine roots to soil organic matter: $A_{161} (1 - F_{TM}) X_{16}$
 F(16,99) - respiration of fine roots: $R_{161} F_T X_{16}$
 F(17,19) - transfer of biomass from quickly decomposing O₁ layer to O₂ layer: $A_{1719} X_{17}$
 F(17,99) - decomposer respiration from quickly decomposing O₁ layer: $R_{17} F_{TM} X_{17}$
 F(18,19) - transfer of biomass from slowly decomposing O₁ layer to O₂ layer: $A_{1819} F_{TM} X_{18}$

- F(18,99) - decomposer respiration from slowly decomposing O₁ layer: $R_{18}F_{TM}X_{18}$
 F(19,20) - transfer of biomass from O₂ layer to soil organic matter: $A_{1920}F_{TM}X_{19}$
 F(19,99) - decomposer respiration from O₂ layer: $R_{19}F_{TM}X_{19}$
 F(20,21) - transfer of biomass from soil organic matter (0-10 cm) to soil organic matter (10-60 cm): $A_{2021}X_{20}$
 F(20,99) - decomposer respiration from soil organic matter (0-10 cm): $R_{20}X_{20}$
 F(21,99) - decomposer respiration from soil organic matter (10-60 cm): $R_{21}X_{21}$

In the fluxes above:

$$\Phi_{21} = X_4^* A_{21} X_2^{0.1} G_A^{-1},$$

$$\Phi_{65} = X_8^* A_{65} X_6^{0.1} G_B^{-1},$$

$$\Phi_{109} = X_{12}^* A_{109} X_{10}^{0.1} G_C^{-1},$$

X_i^* = value of X_i at the end of the dormant season,

M = soil moisture (% wet weight)

$$F_{TM} = 0.2 TM,$$

G_A , G_B , and G_C (see Sect. 2.1.1.4),

F_T (see Sect. 2.1.1.4).

2.1.1.4 Photosynthesis and respiration. There are four photosynthesis functions: (1) tulip poplar leaves, (2) other overstory leaves, (3) understory leaves, and (4) ground cover. The first three of these functions are similar, so we show only the photosynthesis of tulip poplar leaves, G_A :

$$G_A = \frac{X_4^* + A_{13}}{A_{13} + 0.005} \left(\frac{-3.914 B_1}{A_1 B_1} \right) \frac{X_1}{X_1 + X_5} \ln \left(\frac{1 + A_1 E_1}{1 + A_1 I(0)} \right), \quad (2.1.1)$$

where

$$E_1 = I(0) \exp[-1000 K_1 (X_1 + X_5)] \quad (2.1.2)$$

The photosynthesis of ground cover is G_H :

$$G_H = \frac{3.914}{A_{13}K_{13}} \ln \left(\frac{1 + A_{13}E_1E_2 \exp(-1000K_{13}X_{13})}{1 + A_{13}E_1E_2} \right) . \quad (2.1.3)$$

where E_1 is given by Eq. (2.1.2), and

$$E_2 = \exp(-1000K_9X_9) . \quad (2.1.4)$$

Respiration [e.g., $F(1,99)$] is dependent on temperature, T ($^{\circ}\text{C}$), in the following way:

$$F_T = 0.35(40 - T) \exp(-(40 - T)/8) , \quad (2.1.5)$$

where F_T is the temperature effect in the fluxes of Sect. 2.1.1.3.

The parameters used above are defined as follows:

- A_1 = light saturation coefficient,
- B_1 = maximum rate of photosynthesis,
- K_1 = light extinction coefficient for tulip poplar,
- A_{13} = light saturation coefficient for ground cover,
- K_{13} = light extinction coefficient for ground cover,
- K_9 = light extinction coefficient for understory leaves,
- $I(0)$ = light intensity (langleys/min).

2.1.1.5 Release of carbon through decomposition. As litter material decomposes, CO_2 is released through decomposer respiration. The Sollins, Reichle, and Olson (1973) model does not model decomposers directly, but it does allow for decomposer respiration. The loss of organic matter from the quickly decomposing O_1 layer through respiration of decomposers, $F(17,99)$, is described by

$$F(17,99) = R_{17}F_{TM}Q_{17} , \quad (2.1.6)$$

where F_{TM} is $0.2TM$ [T = litter temperature, M is litter moisture, (% wet weight)]; R_{17} is a rate constant, and Q_{17} is the organic

matter of the quickly decomposing O_1 layer. Decomposer respiratory losses from the slowly decomposing O_1 layer and the O_2 layer are of the same functional form, although the rates are numerically different. Decomposer loss from the upper soil organic matter layer is not dependent on temperature and moisture and is given by a constant proportion of the mass of soil organic matter in the 0-to-10 cm layer.

2.1.2 Seasonal Photosynthesis and Respiration

Values of temperature and soil moisture for the Liriodendron site at Oak Ridge were sampled by Sollins, Reichle, and Olson (1973) approximately twice a month during 1971. These values were used to interpolate approximate daily values of the functions for photosynthesis, G_A , G_B , G_C , and G_H , as well as respiration. Graphs of total ecosystem photosynthesis and respiration, as generated by the simulation, are shown in Fig. 2.1.2. The net flux of carbon dioxide (respiration minus photosynthesis) between the atmosphere and the forest stand is plotted in Fig. 2.1.3. A positive value indicates the stand is acting as a source of atmospheric CO_2 ; a negative value indicates the stand is acting as a sink. Biomass fluxes generated by the model were converted to CO_2 fluxes using a conversion factor of 1 g dry weight = 1.65 g CO_2 (Lieth 1978).

2.2 TEMPERATE DECIDUOUS FOREST MODEL - OAK/ASH STAND

A model of biomass dynamics in the managed oak-ash Virelles Forest, Belgium (Andersson et al. 1973), is the basis of a second

ORNL - DWG 85-14320

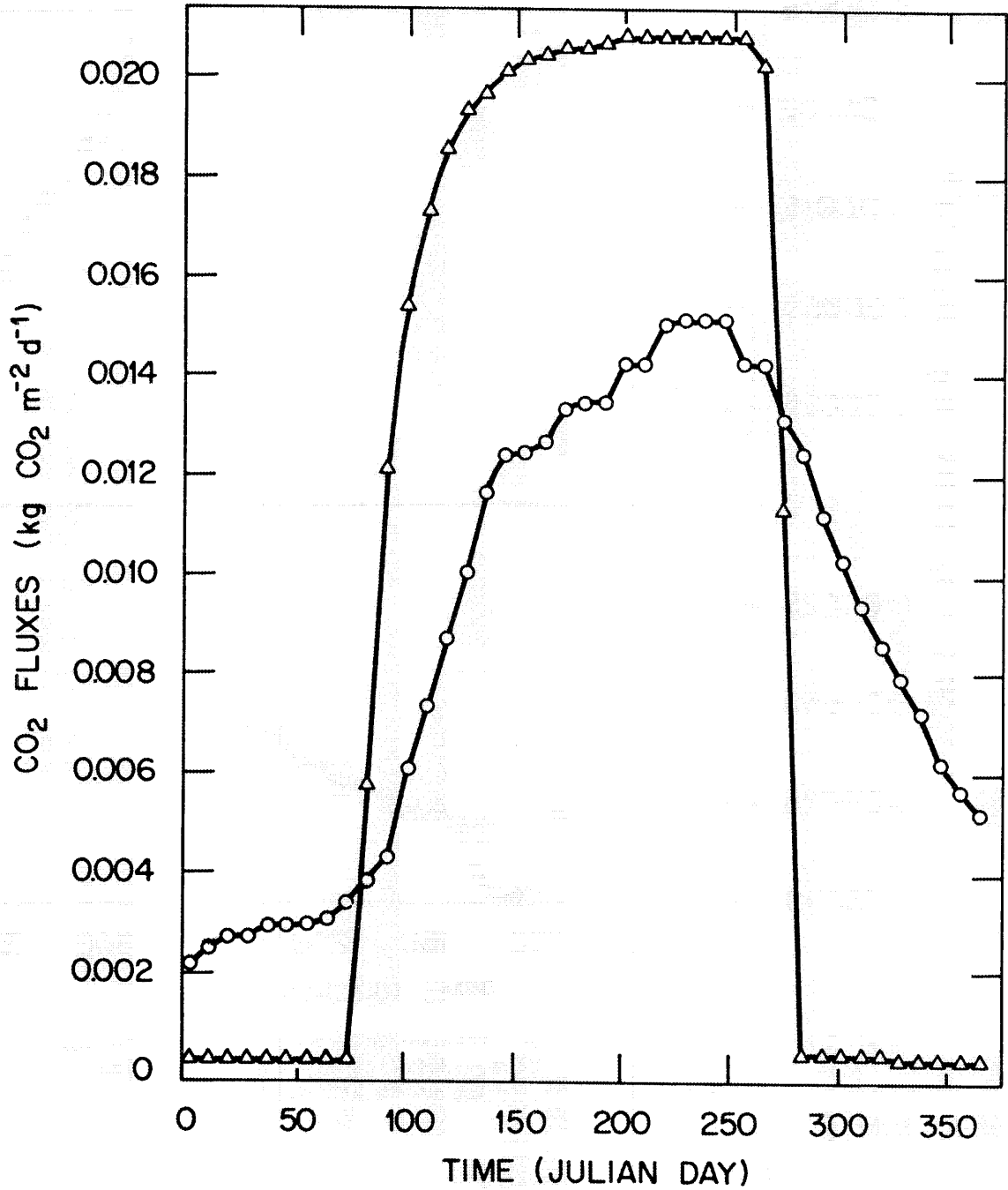


Fig. 2.1.2. Seasonal total ecosystem photosynthesis (Δ) and respiration (o) for a *Liriodendron* stand. Flux units are kg CO₂ m⁻² d⁻¹.

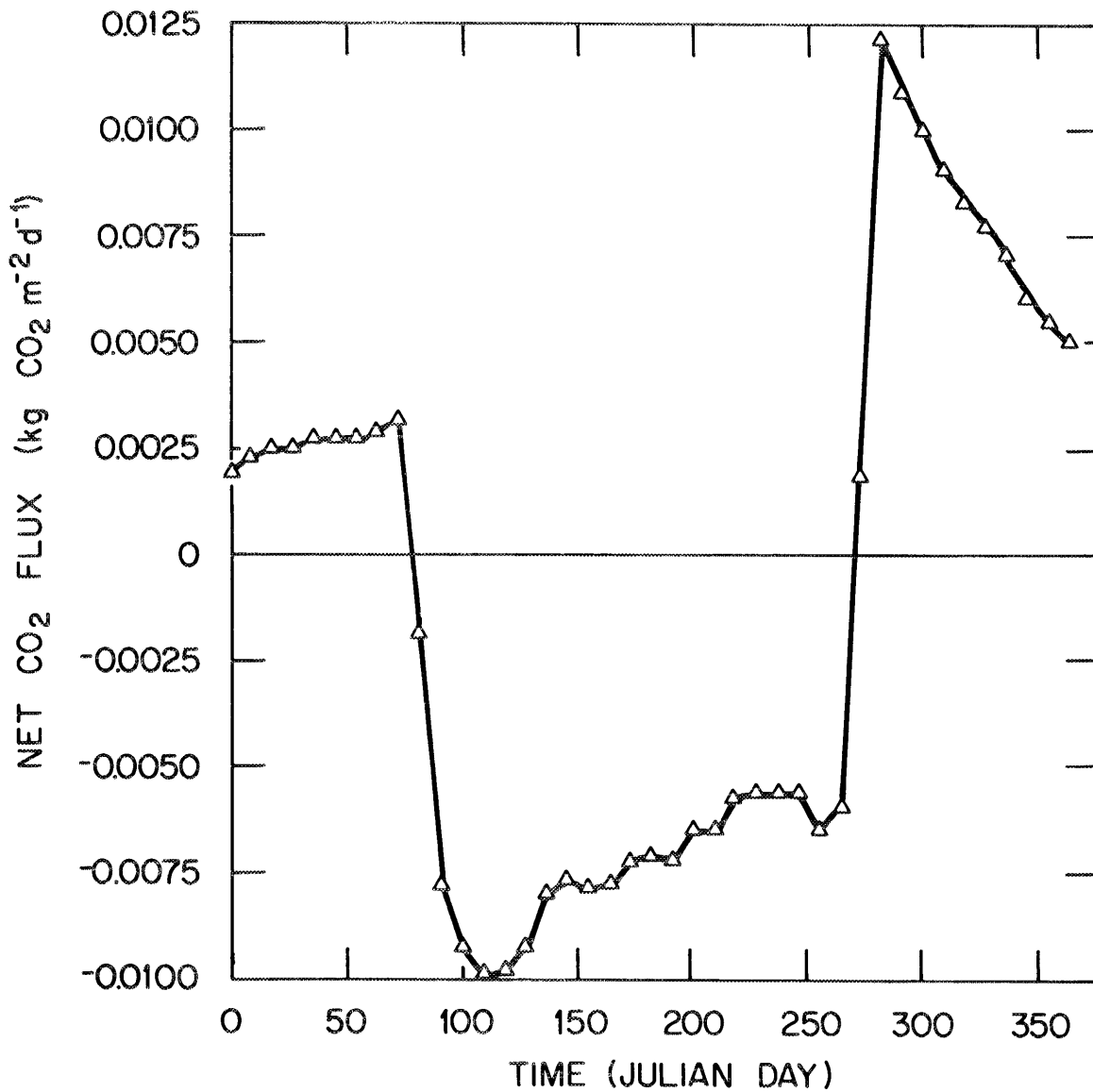


Fig. 2.1.3. Seasonal net CO₂ exchange between the atmosphere and a Liriodendron stand. Net flux is respiration minus photosynthesis. Flux units are kg CO₂ m⁻² d⁻¹.

temperate deciduous forest model. The Andersson et al. (1973) model was developed as part of the International Woodlands Workshop (Reichle et al. 1973). The model was initially constructed as an annual linear donor-controlled constant-coefficient model; seasonality was added in a series of subsequent steps. Seasonal effects were introduced through production forcings, biotic switches, and abiotic control of certain fluxes. The model distinguishes between trees and herbs but does not consider species or plant-type divisions within these categories. The model is implemented using first-order differential equations describing the rate of biomass change in the system compartments.

2.2.1 Structure of the Model

2.2.1.1 Compartments. Fourteen compartments are modeled (Fig. 2.2.1). Six of these are morphological divisions of trees and shrubs. All state variables are expressed in kilograms biomass per hectare. The state variables corresponding to the compartments are:

- X₁ - leaves of trees and shrubs
- X₂ - twigs and other parts (e.g., fruit) of trees and shrubs
- X₃ - branches of trees and shrubs
- X₄ - stems of trees and shrubs
- X₅ - large roots of trees and shrubs
- X₆ - fine roots of trees, shrubs, and herbs
- X₇ - herbivores
- X₈ - herb layer
- X₉ - litter layer leaves and miscellaneous
- X₁₀ - standing dead wood
- X₁₁ - litter layer wood
- X₁₂ - dead roots
- X₁₃ - decomposers
- X₁₄ - soil

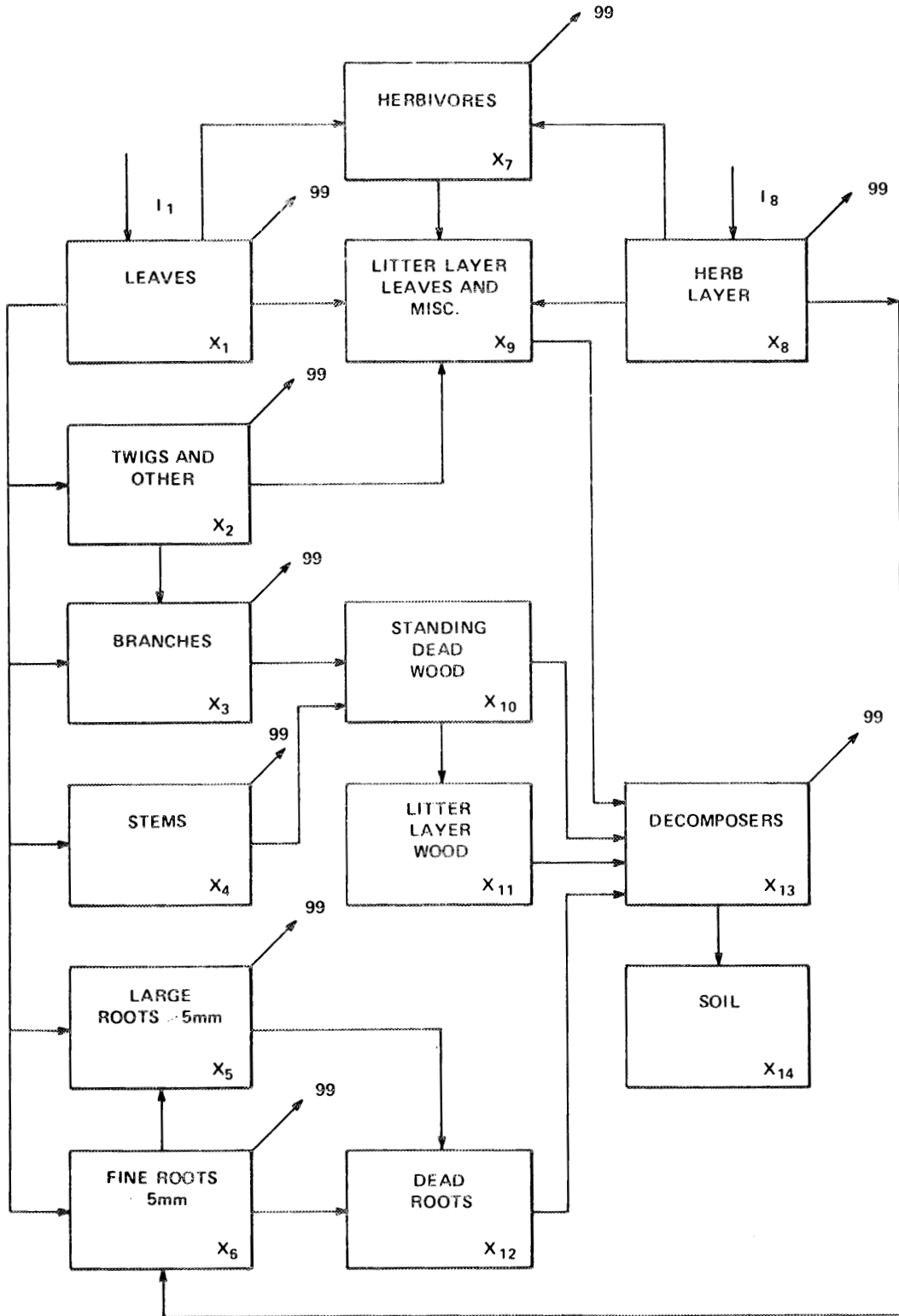


Fig. 2.2.1. Compartmental structure of the temperate deciduous forest model - oak-ash stand. The $F(i,j)$'s indicate the flux of biomass from compartment i to compartment j . The number 99 indicates a compartment external to the system.

2.2.1.2 Driving variables. Aspects of the forest biomass dynamics are driven exogenously by two abiotic driving variables:

Z_1 - a soil moisture index
 Z_2 - mean monthly air temperature ($^{\circ}\text{C}$)

Monthly empirical values of these variables are computer program input data.

Switches are also used to drive seasonal system dynamics, and are identified as:

CONS - an herbivory switch
FALL - a litterfall switch
GROW - a growing season switch

Seasonality is also driven by production forcings described in Section 2.2.1.4.

2.2.1.3 Flows or rate processes. Model treatment of fluxes between compartments and fluxes to and from the atmosphere are of varying complexity. Many are treated as constant donor control rate processes. Others are modified by step functions or on-off switches. A few are functions of abiotic factors such as soil moisture and air temperature (see Sect. 2.2.1.2). The precise representation of the flow equations and the assumptions behind them can be found in Andersson et al. (1973). The photosynthesis and respiration fluxes are described more fully in Sect. 2.2.1.4.

The arrows in Fig. 2.2.1 represent flows included in the model and are defined below. The number 99 refers to a compartment external to the system. The notation $F(i,j)$ indicates the flow of material from compartment i to compartment j . The a_{ij} and r_i are constants; the switches, CONS, FALL, and GROW, are defined in Sect. 2.2.1.2. The

symbol TF represents a temperature function (Section. 2.2.1.4) and MOIST is equivalent to Z_1 (Sect. 2.2.1.2). The units of flux are in kilograms per hectare per year.

- I_1 - net daytime tree photosynthesis forcing: see Sect. 2.2.1.4
- I_8 - net daytime herb layer photosynthesis forcing:
see Sect. 2.2.1.4
- F(1,99) - leaf dark respiration: $r_1TF(GROW)X_1$,
- F(1,2) - translocation from leaves to twigs: $a_{12}(GROW)X_1$
- F(1,3) - translocation from leaves to branches: $a_{13}(GROW)X_1$
- F(1,4) - translocation from leaves to stems: $a_{14}(GROW)X_1$
- F(1,5) - translocation from leaves to large roots: $a_{15}(GROW)X_1$
- F(1,6) - translocation from leaves to fine roots: $a_{16}(GROW)X_1$
- F(1,7) - herbivory: $(CONS)X_1$
- F(1,9) - leaf litterfall: $(FALL)X_1$
- F(2,99) - twigs and fruit respiration: r_2TFX_2
- F(2,3) - aging of twigs: $a_{23}X_2$
- F(2,9) - twig and fruit litterfall: $a_{29}(GROW)X_2$
- F(3,99) - branch respiration: r_3TFX_3
- F(3,10) - branch mortality: $a_{310}X_3$
- F(4,99) - stem respiration: r_4TFX_4
- F(4,10) - stem mortality: $a_{410}X_4$
- F(5,99) - large root respiration: r_5TFX_5
- F(5,12) - large root mortality: $a_{512}X_5$
- F(6,99) - fine root respiration: r_6TFX_6
- F(6,5) - aging of fine roots: $a_{65}X_6$
- F(6,12) - fine root mortality: $a_{612}(FALL)X_6$
- F(7,99) - herbivore respiration: r_7TFX_7
- F(7,9) - herbivore mortality and litterfall: $a_{79}X_7$
- F(8,99) - herb layer dark respiration: r_8TFX_8
- F(8,6) - translocation from herb layer leaves to fine
roots: $a_{86}(FALL)X_8$
- F(8,7) - herbivory on herb layer: $a_{87}X_8$
- F(8,9) - herb layer litterfall: $a_{89}X_8$
- F(9,13) - leaf litter decomposition: $a_{913}(MOIST)TFX_9$
- F(10,11) - fall of standing dead: $a_{1011}X_{10}$
- F(10,13) - decomposition of standing dead: $a_{1013}X_{10}$
- F(11,13) - decomposition of woody litter: $a_{1113}X_{11}$
- F(12,13) - decomposition of dead roots: $a_{1213}X_{12}$
- F(13,99) - decomposer respiration: $r_{13}TFX_{13}$
- F(13,14) - flux to soil carbon through decomposition: $a_{1314}X_{13}$

2.2.1.4 Photosynthesis and respiration. Photosynthesis is

modeled as external forcings, I_1 and I_8 , applied to the leaves (X_1) and herb layer (X_8) compartments, respectively. I_1 values

are interpolated from monthly photosynthesis values, PHOTA(m), obtained by multiplying Schulze's (1970) net assimilation values by leaf biomass. Herb layer photosynthesis is treated similarly. However, since 80% of the herb layer is assumed to be evergreen, I_g is calculated as the sum of a base-line yearly herb layer photosynthesis ($600 \text{ kg ha}^{-1} \text{ year}^{-1}$) and seasonal photosynthesis keyed to tree leaf photosynthesis:

$$I_g(m) = (600 + 0.36\text{PHOTA}(m))/365 \quad , \quad (2.2.1)$$

where $I_g(m)$ is the monthly forcing value, and PHOTA(m) is the monthly photosynthesis input data.

The photosynthesis forcings are best thought of as daytime assimilation. Net daily photosynthesis is the difference between daytime assimilation and nighttime respiration. Leaf and herb layer nighttime respiration, $F(1,0)$ and $F(8,0)$ respectively, are calculated by

$$F(1,0) = (0.4/365)\text{TF}(m)\text{GROW}(m)X_1 \quad , \quad (2.2.2)$$

and

$$F(8,0) = (0.4/365)\text{TF}(m)X_8 \quad , \quad (2.2.3)$$

where $\text{GROW}(m)$ is the monthly value of a , the growing season switch [$\text{GROW}(m) = 4.0$ for the months of April through September, otherwise $\text{GROW}(m) = 0.0$], and $\text{TF}(m)$ is the monthly temperature function. $\text{TF}(m)$ is a Q_{10} function relating a Q_{10} of 2.0 to mean monthly air temperature, Z_2 (m):

$$TF(m) = 0.92 \times 2.0[Z_2(m)-8.4]/10 \quad . \quad (2.2.4)$$

Respiration from other live compartments is given by:

$$F(i,0) = r_i TF(m) X_i \quad \text{for } i = 2, \dots, 8 \quad , \quad (2.2.5)$$

where r_i is a compartment specific constant, and $TF(m)$ is as in Eq. 2.2.4.

2.2.1.5 Release of carbon through decomposition. The release of carbon as CO_2 during decomposer metabolism of litter, standing dead, and dead roots is calculated by applying Eq. 2.2.5 to the decomposer compartment, X_{13} :

$$F(13,0) = r_{13} TF(m) X_{13} \quad . \quad (2.2.6)$$

The soil moisture index, $Z_1(m)$, is used to regulate the decomposition of litter layer leaves and miscellaneous litter [i.e., $F(9,13)$, the transfer of litter material to decomposers], but is assumed not to directly affect the rate of CO_2 evolution by the decomposers (see Eq. 2.2.6). This assumption is based on the idea that soil moisture rarely limits the respiratory metabolism of temperate deciduous forest litter decomposers. The amount of CO_2 evolved is, however, affected by soil moisture, since the mass of decomposers (X_{13} in Eq. 2.2.6) is dependent on the decomposition flux $F(9,13)$.

2.2.2 Seasonal Photosynthesis and Respiration

Seasonal input data for the driving variables, switches and forcings were provided by Andersson et al. (1973). These were used to generate total ecosystem photosynthesis and respiration values during

the year. A plot of daily fluxes sampled at 5-d intervals is shown in Fig. 2.2.2. Biomass fluxes generated by the model were converted to CO_2 fluxes using the conversion factor of 1 g dry matter = 1.65 g CO_2 (Lieth 1978). Seasonal net CO_2 exchange between the forest stand and the atmosphere is plotted in Fig. 2.2.3. Net exchange is respiration minus photosynthesis. Hence, a positive value indicates the stand is acting as a source of atmospheric CO_2 ; a negative value indicates the stand is acting as a sink for atmospheric CO_2 .

2.3 NORTHERN CONIFEROUS FOREST MODEL

To model the seasonal carbon dynamics of coniferous forests, we use the model CONIFER developed for the Coniferous Forest Biome of the United States (Coniferous Forest Biome Modeling Group 1977). CONIFER simulates both the carbon and the water dynamics of a coniferous forest stand using daily time steps.

2.3.1 Structure of the Model

2.3.1.1 Compartments. The compartmental structure of the model is shown in Fig. 2.3.1. Note that the carbon and water dynamics constitute separate parts of the model. The arrows indicate intercompartmental transfers of carbon and water, respectively, in the two parts of the model. What is not shown in Fig. 2.3.1, however, is the complex pattern of effects other than material transfers that occur between compartments. These are discussed in Sect. 2.3.1.4.

The state variables corresponding to these compartments and their measurement units are as follows:

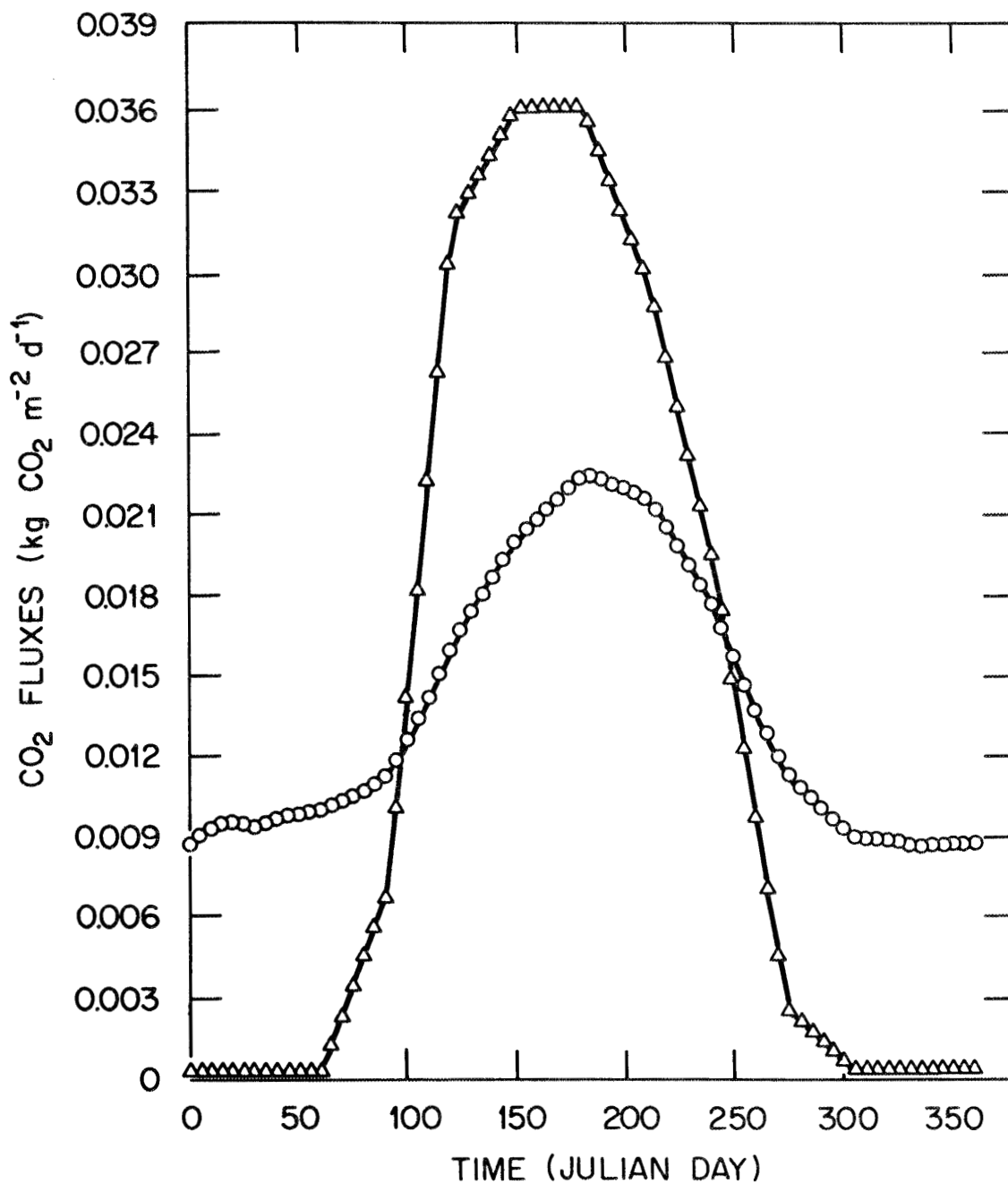


Fig. 2.2.2. Seasonal total ecosystem photosynthesis (Δ) and respiration (o) for an oak-ash stand. Flux units are kg CO₂ m⁻² d⁻¹.

ORNL-DWG 85-14323

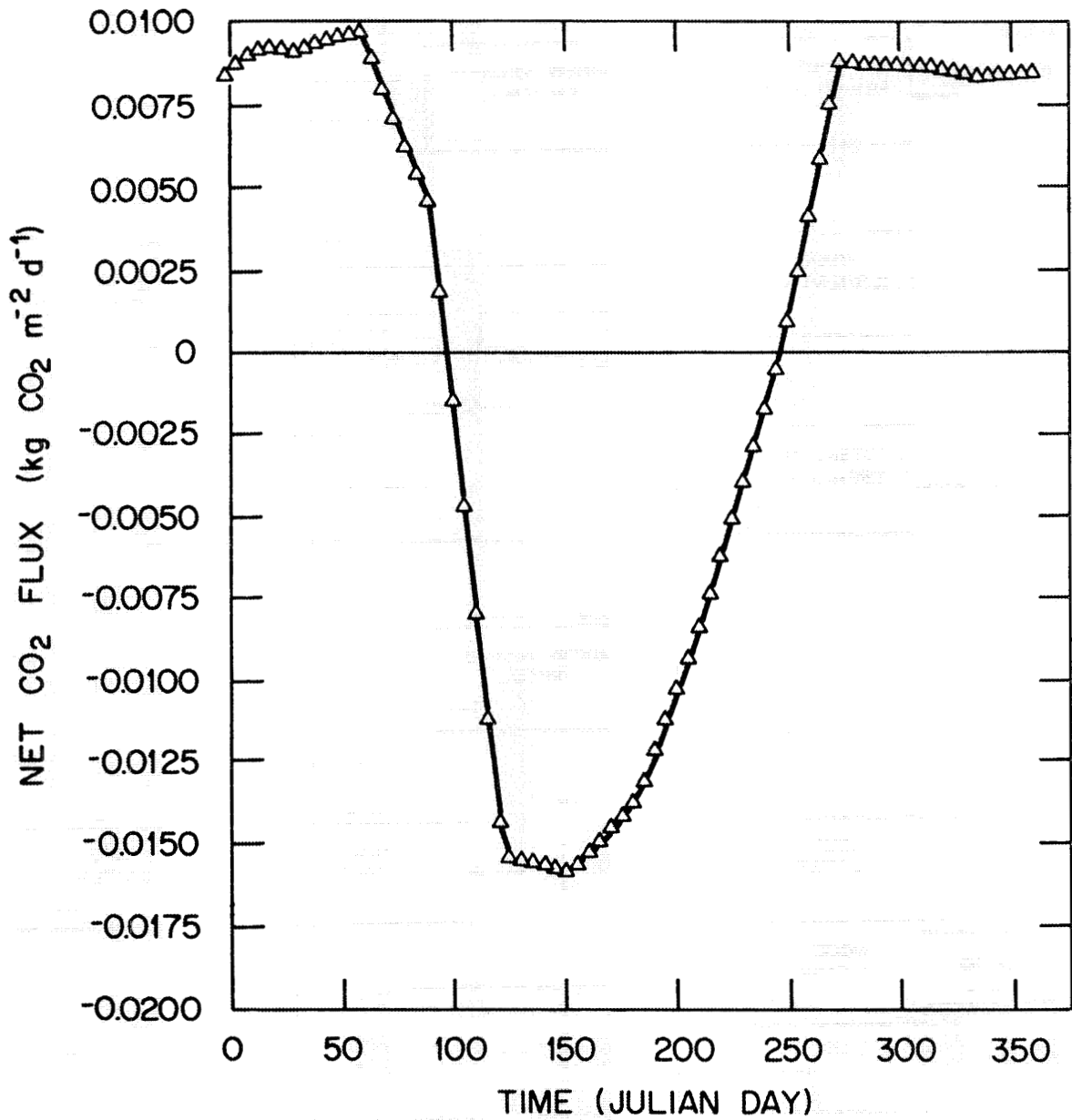
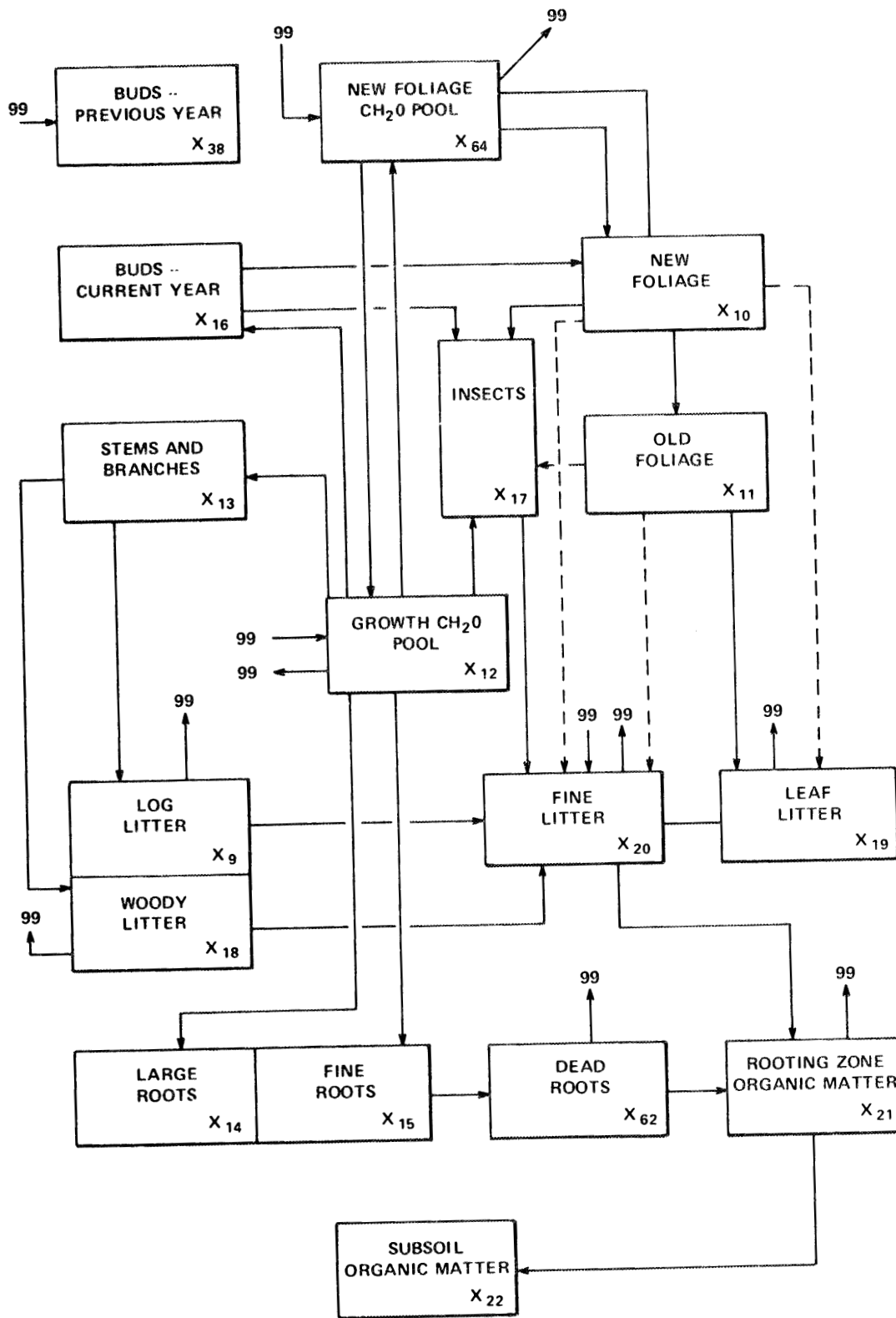


Fig. 2.2.3. Seasonal net CO₂ exchange between the atmosphere and an oak-ash stand. Net flux is respiration minus photosynthesis. Flux units are kg CO₂ m⁻² d⁻¹.



CARBON

Fig. 2.3.1a. Compartmental structure of the northern coniferous forest model. Arrows indicate the directional flow of carbon. Dashed lines indicate fluxes that occur only during perturbation. The 99's represent carbon sources and sinks. Adapted from Coniferous Forest Biome Modeling Group (1977).

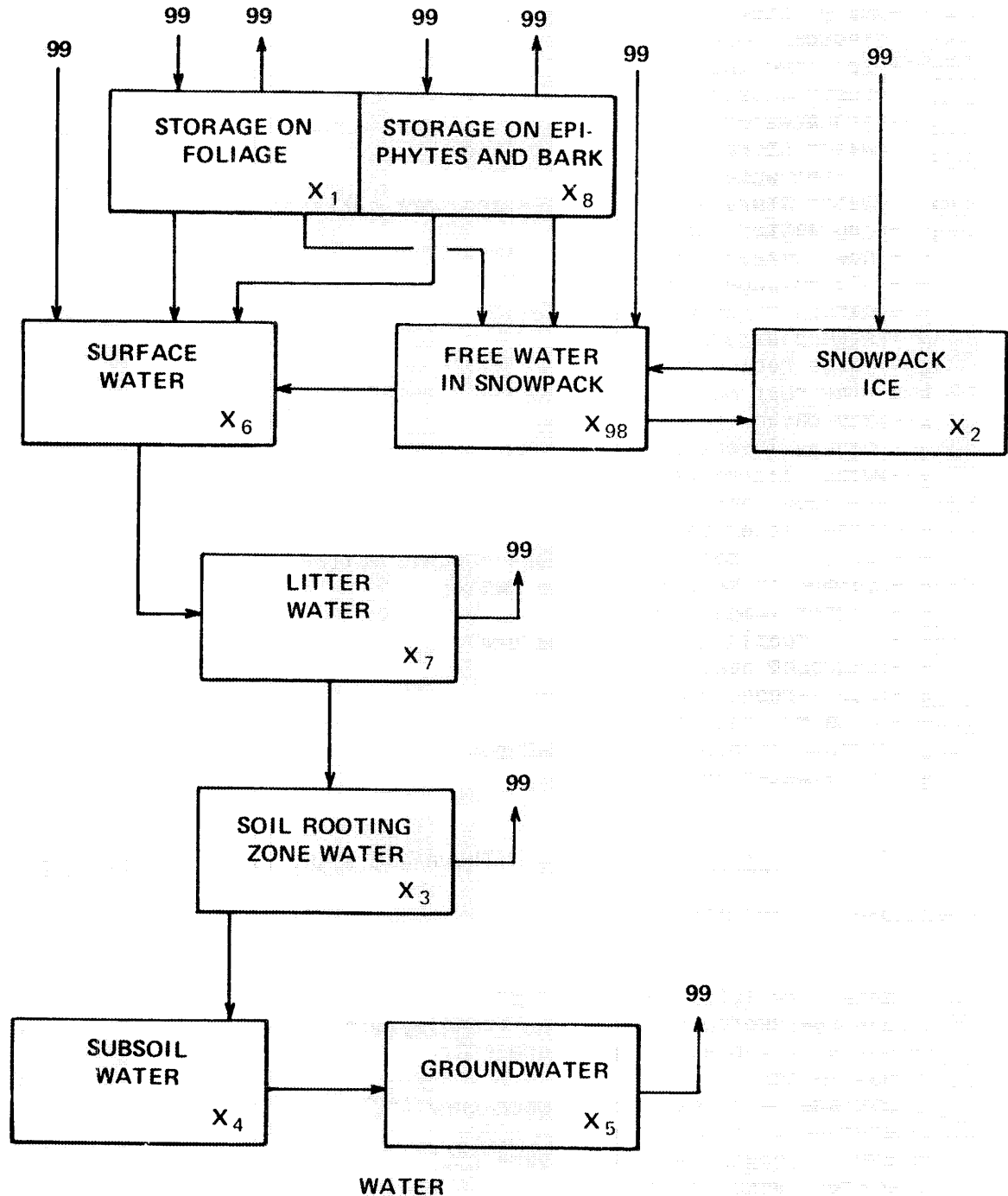


Fig. 2.3.1b. Compartmental structure of the northern coniferous forest model. Arrows indicate the directional flow of water. Dashed lines indicate fluxes that occur only during perturbation. The 99's represent water sources and sinks. Adapted from Coniferous Forest Biome Modeling Group (1977).

X ₁	- water storage on foliage	(m ³ /ha)
X ₂	- snowpack ice	"
X ₃	- soil rooting zone water	"
X ₄	- subsoil water	"
X ₅	- groundwater storage	"
X ₆	- water storage on litter surface	"
X ₇	- litter water	"
X ₈	- water storage on epiphytes and bark surfaces	"
X ₉	- log litter carbon	(t/ha)
X ₁₀	- new foliage carbon	"
X ₁₁	- old foliage carbon	"
X ₁₂	- carbon in growth CH ₂ O pool	"
X ₁₃	- stem plus branch carbon	"
X ₁₄	- large root carbon	"
X ₁₅	- fine root carbon	"
X ₁₆	- bud carbon (current year)	"
X ₁₇	- canopy insect carbon	"
X ₁₈	- woody litter carbon	"
X ₁₉	- foliage litter carbon	"
X ₂₀	- fine litter carbon	"
X ₂₁	- carbon in soil rooting zone organic matter	"
X ₂₂	- carbon in subsoil organic matter	"
X ₂₅	- litter temperature	(deg)
X ₂₆	- soil rooting zone temperature	"
X ₃₇	- snowpack heat deficit	"
X ₃₈	- bud carbon (previous year)	(t/ha)
X ₆₂	- dead root carbon	"
X ₆₄	- carbon in new foliage CH ₂ O pool	"
X ₉₈	- free water in snowpack	(m ³ /ha)

2.3.1.2 Driving variables. There are eight exogenous driving variables in the model:

Z ₁	- total precipitation (m ha ⁻¹ d ⁻¹)
Z ₂	- average shortwave radiation (langley/min)
Z ₃	- average 24-h air temperature (°C)
Z ₄	- day length
Z ₅	- average 24-h dew point temperature (°C)
Z ₆	- average daytime temperature (°C)
Z ₇	- average nighttime temperature (°C)
Z ₈	- average wind speed (m/s)

Daily empirical values of these data are read into the simulation program as input data.

2.3.1.3 Flows or rate processes. The model includes flow functions that correspond to the arrows in Fig. 2.3.1. The flow functions control the amounts of carbon or water being transferred from one compartment to another. The specific formulations for these often complicated functions can be found in the CONIFER documentation (Coniferous Forest Biome Modeling Group 1977). Here, we simply define the flows. The notation $F(i,j)$ indicates the flow of material from compartment i to compartment j . The number 99 refers to a compartment external to the system. All flows coming into the system are labeled $F(99,j)$, and all flows going out of the system are labeled $F(i,99)$. The units of the flows are cubic meters per hectare per year for water and tons per hectare per year for biomass.

- F(99,1) - rain input to foliar surfaces
- F(99,2) - precipitation as snow
- F(99,6) - rainfall passing directly to litter surface water
- F(99,8) - rain input to bark and epiphyte surfaces
- F(99,12) - input from old foliage photosynthesis to growth CH_2O pool
- F(99,20) - input to fine litter from microparticulate matter and carbon dissolved in precipitation
- F(99,25) - change in litter temperature
- F(99,26) - change in soil temperature
- F(99,37) - net increase in heat deficit of snowpack
- F(99,38) - change in last year's buds
- F(99,64) - input to new foliage CH_2O pool due to net new foliage photosynthesis
- F(99,98) - rainfall passing directly into free water in snowpack
- F(1,99) - evaporation from foliage
- F(1,6) - drip from foliage to litter surface
- F(1,98) - drip from foliage to free water in snowpack
- F(2,98) - transfer from ice to free water in snowpack
- F(3,99) - transpiration rate
- F(3,4) - water transfer from soil rooting zone to subsoil
- F(4,5) - water transfer from subsoil to groundwater
- F(5,99) - outflow from groundwater
- F(6,7) - water flow from surface to litter layer
- F(7,99) - evaporation from litter

- F(7,3) - water transfer from litter to soil rooting zone
- F(8,99) - evaporation from epiphyte and bark surfaces
- F(8,6) - water drip from epiphyte and bark surfaces
to storage on litter surface
- F(8,98) - drip from epiphytes and bark surfaces to
storage on litter surface
- F(9,99) - carbon loss from logs due to decomposer
respiration
- F(9,20) - carbon loss from logs due to fragmentation
- F(10,11) - carbon transfer with aging of new foliage
- F(10,17) - new foliage consumption by insects
- F(10,19) - carbon transfer from new foliage to leaf
litter due to acute defoliation
- F(10,20) - carbon transfer from new foliage to fine litter
due to acute defoliation
- F(10,64) - carbon transfer from new foliage to new foliage
CH₂O pool
- F(11,17) - old foliage consumption by insects
- F(11,19) - transfer from old foliage to leaf litter
due to leaf fall and acute defoliation
- F(11,20) - transfer from old foliage to fine litter
due to acute defoliation
- F(12,99) - total respiration loss from growth CH₂O pool
- F(12,13) - carbon transfer to stems plus branches from
growth CH₂O pool
- F(12,14) - carbon transfer to large roots from growth CH₂O
pool
- F(12,15) - carbon transfer to fine roots from growth CH₂O
pool
- F(12,16) - bud growth from growth CH₂O pool
- F(12,17) - consumption of growth CH₂O pool by insects
- F(12,64) - transfer of carbon from growth CH₂O pool
to new foliage CH₂O pool to meet foliar
respiration and growth demands
- F(13,9) - carbon transfer from stems plus branches
to log litter
- F(13,18) - carbon transfer from stems
plus branches to woody litter
- F(14,62) - large root mortality
- F(15,62) - fine root mortality
- F(16,10) - carbon transfer from buds to new foliage
- F(16,17) - bud consumption by insects
- F(17,20) - insect frass input to fine litter
- F(18,99) - carbon loss from woody litter due to
decomposer respiration
- F(18,20) - carbon loss from woody litter due to
fragmentation
- F(19,99) - carbon loss from foliage litter due to
decomposer respiration
- F(20,99) - carbon loss from fine litter due to
decomposer respiration

- F(20,21) - incorporation of fine litter into rooting zone organic matter
- F(21,99) - carbon loss from rooting zone due to decomposer respiration
- F(21,22) - carbon transfer from rooting zone to subsoil organic matter due to leaching
- F(62,99) - carbon loss from dead roots due to decomposer respiration
- F(62,21) - carbon loss from dead roots due to fragmentation
- F(64,99) - new foliage nighttime respiration from CH₂O pool
- F(64,10) - transfer of carbon to new foliage from new foliage CH₂O pool
- F(64,12) - transfer of surplus carbon from new foliage CH₂O pool to growth CH₂O pool
- F(98,2) - transfer from free water in snowpack to ice
- F(98,6) - water draining from snowpack to litter surface

2.3.1.4 Indirect interactions of compartments. The flow functions, F(i,j), designate only material flows between compartments, not the indirect actions of other compartments on these flows that are incorporated in the model. These indirect effects are detailed in the CONIFER report. Here, we simply list the indirect effects in Table 2.3.1.

2.3.1.5 Photosynthesis and respiration. Because of the importance of photosynthesis and respiration in calculating carbon fluxes between the conifer stand and the atmosphere, the detailed model components for these functions are described here.

Net daily photosynthesis is the sum of net new foliage photosynthesis (NNFP) and net old foliage photosynthesis (NOFP). NNFP is defined by

$$NNFP = \frac{B_{32} B_{33} G_{110} X_{10} G_{102}}{B_{35} G_{49} G_{61}} \ln \left(\frac{B_{34} + G_{109} \exp(-B_{35} G_{61})}{B_{34} + G_{109}} \right), \quad (2.3.1)$$

Table 2.3.1 Interactions among modules of CONIFER
(from Coniferous Forest Biome Modeling Group 1977)

Variables	Comments
<u>Effect of carbon variables on water and energy flows</u>	
A. Foliage biomass affects:	
1. Transpiration	
2. Fraction of rain incident to canopy that strikes foliage (and therefore also fraction striking nonfoliage)	(Numbers 2 through 4 affect drip, litter, and soil moisture dynamics. There are also indirect effects through percent cover)
3. Water retention capacity of canopy	
4. Distribution of retention capacity between foliage and nonfoliage	
5. Fraction of rainfall passing directly to forest floor	(Through percent cover)
6. Net longwave radiation input to canopy	(Through percent cover, which affects input and loss)
B. Stem biomass affects:	
1. Percent cover (and therefore numbers 2 through 6 above)	
C. Fine, leaf, and woody litter mass affects:	
1. Water retention capacity of litter	
<u>Effect of water variables on carbon and energy flows</u>	
A. Soil moisture affects:	
1. New and old foliage photosynthesis	(Via stomatal resistance)
2. Fine root death	(Via plant moisture stress)
3. Dead root plus soil organic matter decomposition processes	
B. Litter moisture affects:	
1. Litter decomposition processes	
C. Snowpack ice affects:	
1. Litter temperature	
D. Snowfall affects:	
1. Heat loss from snowpack due to snowfall	
2. Albedo of snowpack	
E. Drip plus direct rainfall affect:	
1. Litter and soil temperature	
<u>Effect of energy variables on carbon and water flows</u>	
A. Heat input to canopy affects:	
1. Potential evaporation from canopy	
2. Transpiration	
B. Litter temperature affects:	
1. Litter decomposition processes	
2. Potential evaporation from litter	

and where

- X_{10} = new foliage carbon (t/ha),
 G_{49} = average weekly stomatal resistance of new foliage (s/cm),
 G_{61} = total foliage carbon (t/ha),
 G_{102} = effect of temperature on photosynthesis ($\text{deg}^{-B_{177}}$),
 G_{109} = average weekly photosynthetically active solar radiation (langley/min),
 G_{110} = average weekly day length,
 B_{32} = ratio of net new foliage photosynthesis based on carbon budget to amount extrapolated from cuvette experiments (dimensionless),
 B_{33} = rate constant for new foliage photosynthesis ($\text{s cm}^{-1} \text{deg}^{-B_{177}} \text{ week}^{-1}$),
 B_{34} = light intensity at which new foliage photosynthesis is 1/2 maximum rate (langley/min),
 B_{35} = coefficient of attenuation of shortwave radiation by foliage (ha/t),
 B_{177} = coefficient.

A similar expression holds for NOFP. Photosynthates derived from NNFP accumulate in the new foliage CH_2O pool; NOFP photosynthates accumulate in the growth CH_2O pool.

The net daily respiration (NDR) from the stand is given by

$$\begin{aligned} \text{NDR} = G_{25} + G_{30} + G_{103} + G_{113} + G_{125} + G_{125} \\ + G_{131} + G_{133} + G_{138} + G_{139} + G_{140} \end{aligned} \quad (2.3.2)$$

where

- G_{25} = new foliage nighttime respiration ($\text{t ha}^{-1} \text{ week}^{-1}$),
 G_{30} = old foliage nighttime respiration ($\text{t ha}^{-1} \text{ week}^{-1}$),
 G_{103} = carbon loss from foliage litter due to decomposer respiration,
 G_{111} = carbon loss from woody litter due to decomposer respiration,
 G_{113} = carbon loss from log litter due to decomposer respiration,
 G_{125} = carbon loss from fine litter due to decomposer respiration,
 G_{131} = carbon loss from dead roots due to decomposer respiration,

G_{133} = carbon loss from rooting zone due to decomposer respiration,
 G_{138} = stem and branch respiration,
 G_{139} = large root respiration,
 G_{140} = fine root respiration.

The functional form of the individual respiration term for G_{25} is defined as:

$$G_{25} = B_{26}(1 - G_{110})X_{10}\exp(B_{145}G_{108}) \quad , \quad (2.3.3)$$

where

X_{10} = new foliage carbon (t/ha),
 G_{108} = average weekly nighttime air temperature ($^{\circ}\text{C}$),
 G_{110} = average weekly day length (dimensionless),
 B_{26} = foliar respiration rate constant (week^{-1}),
 B_{145} = coefficient for temperature effect on foliar respiration (deg^{-1}).

2.3.1.6 Release of carbon through decomposition. The release of carbon in CO_2 during the microbial decomposition of litter contributes to the total net daily respiration from the stand (Sect. 2.3.1.5). The term G_{103} , which represents carbon loss from foliage litter resulting from decomposer respiration, is an example of the functional form that describes decomposer respiratory fluxes and is defined by

$$G_{103} = (1 - B_{149})G_{81} \quad , \quad (2.3.4)$$

where B_{149} is the fraction of carbon loss from foliage litter because of fragmentation, and G_{81} is the foliage litter decomposition rate ($\text{t ha}^{-1} \text{ week}^{-1}$). The term G_{81} is given by

$$G_{81} = B_{62}G_{69}X_{19} \quad , \quad (2.3.5)$$

where X_{19} is foliage litter carbon, G_{69} is the effect of moisture and temperature on litter processes, and B_{62} is a rate constant. The effect of temperature and water on decomposition is described in the CONIFER documentation (Coniferous Forest Biome Modeling Group 1977).

2.3.2 Seasonal Photosynthesis and Respiration

Seasonal input data for the forcing functions (Z_i 's) were obtained from the CONIFER report, and used to generate (from the model) total ecosystem photosynthesis and respiration values during the year. A plot of weekly values for a particular year is shown in Fig. 2.3.2. The carbon fluxes generated by the model were converted to CO_2 fluxes using the conversion factor of 1 g carbon = 3.66 g CO_2 (Brown and Trlica 1974). Figure 2.3.3 is a plot of net carbon dioxide exchange between the stand and the atmosphere. Net exchange is calculated as respiration minus photosynthesis. Hence, a positive value indicates the stand is acting as source of atmospheric carbon; a negative value indicates the stand is acting as a sink for atmospheric carbon.

2.4 TEMPERATE BROADLEAF EVERGREEN FOREST MODEL

Seasonal carbon dynamics in a temperate broadleaf evergreen forest are studied using an model (originally Attiwill et al. 1973) of an Australian eucalyptus forest. Developed during the International Woodlands Workshop (Reichle et al. 1973), the seasonal compartment model simulates biomass dynamics using differential equations.

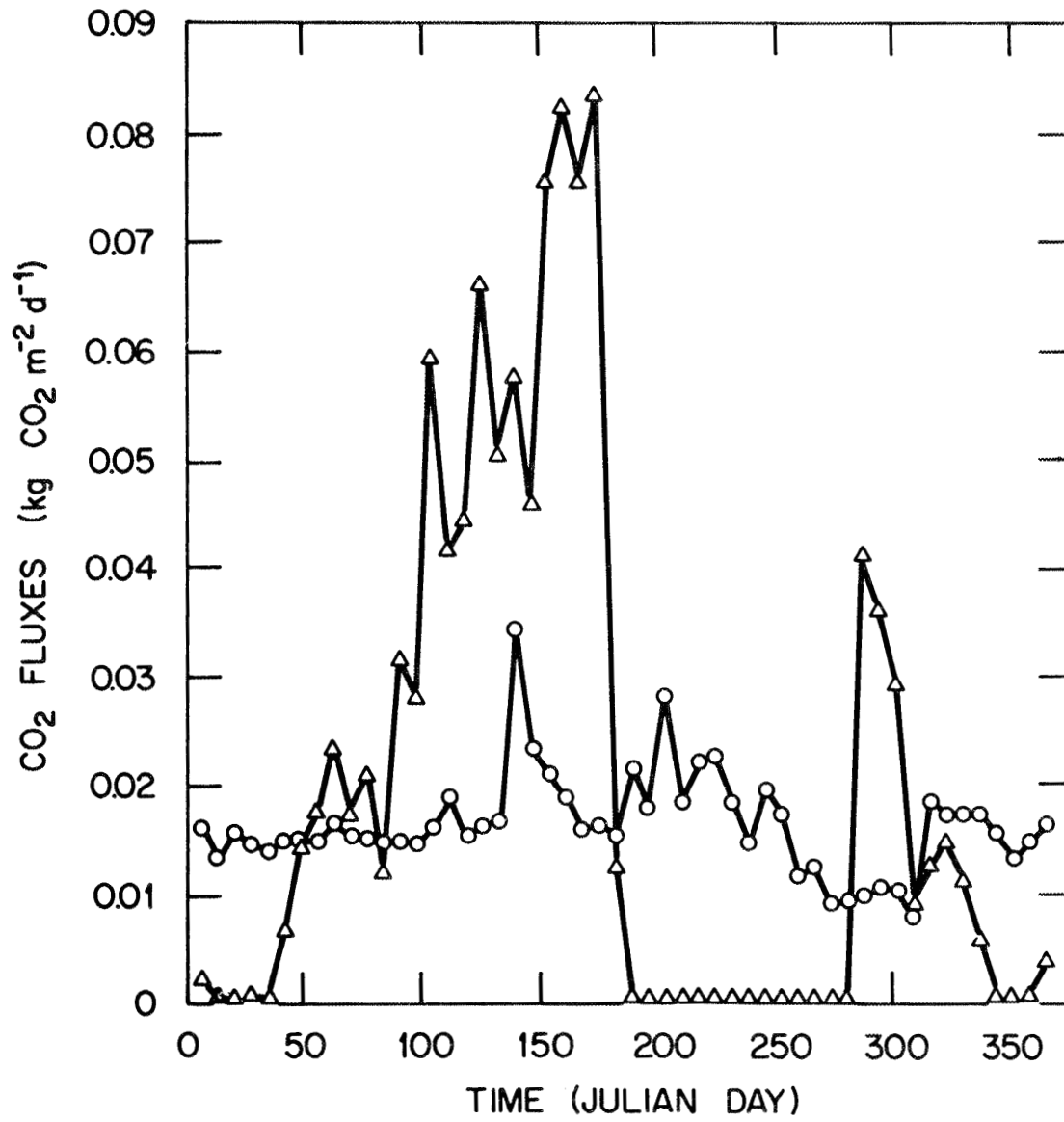


Fig. 2.3.2. Seasonal total ecosystem photosynthesis (Δ) and respiration (o) for a northern coniferous forest stand. Flux units are $\text{kg CO}_2 \text{ m}^{-2} \text{ d}^{-1}$.

ORNL-DWG 85-14325

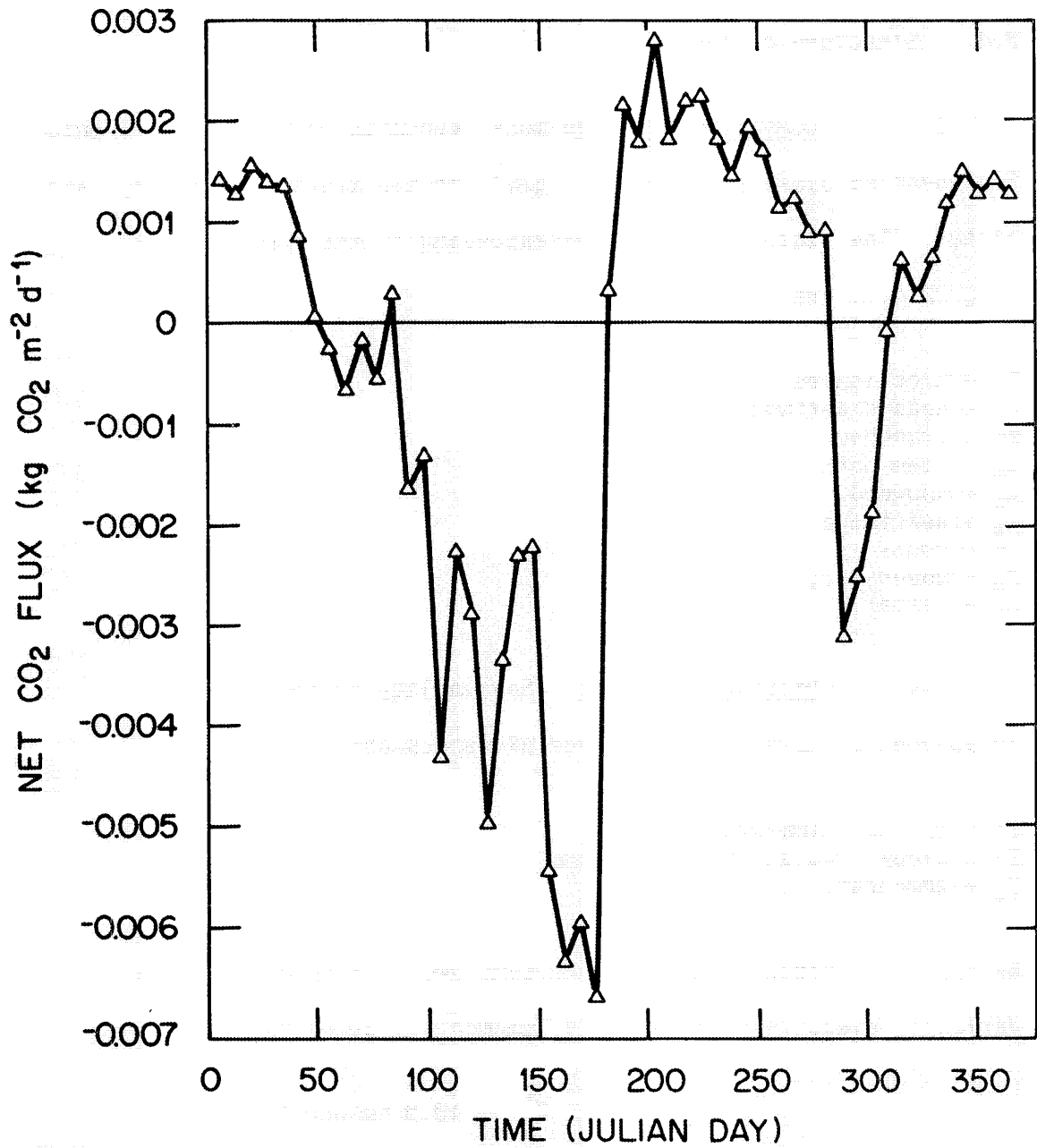


Fig. 2.3.3. Seasonal net CO₂ exchange between the atmosphere and a northern coniferous forest stand. Net flux is respiration minus photosynthesis. Flux units are kg CO₂ m⁻² d⁻¹.

2.4.1 Structure of the Model

2.4.1.1 Compartments. The model consists of nine compartments representing biomass reservoirs (g/m^2) in the trees, understory, and litter. The state variables corresponding to the compartments (Fig. 2.4.1) are:

X_1 - tree leaves
 X_2 - dead branchwood
 X_3 - branches
 X_4 - stem bark
 X_5 - sapwood
 X_6 - heartwood
 X_7 - roots
 X_8 - understory
 X_9 - litter.

2.4.1.2 Driving variables. Seasonality in the model is influenced by variations in three exogenous abiotic variables:

Z_1 - rainfall (mm/week),
 Z_2 - global radiation ($\text{kcal m}^{-2} \text{d}^{-1}$)
 Z_3 - temperature ($^{\circ}\text{C}$).

Rainfall and global radiation are combined to form a composite variable, evapotranspiration (EV, mm/month), using the equation:

$$EV = \begin{cases} a Z_2 & \text{if } Z_1 \geq 18.0 \text{ mm week}^{-1} \\ b Z_1 & \text{if } Z_1 < 18.0 \text{ mm week}^{-1} \end{cases}, \quad (2.4.1)$$

where b is the slope of evapotranspiration as a function of rainfall, and a is a time-varying coefficient relating evapotranspiration and global radiation (see Attiwill et al. 1973).

Rainfall at time t , $Z(t)$, is given by:

$$Z_1(t) = 19.25 + 7.25 \cos\{2\pi(t - 0.0633)\} \quad (0 \leq t \leq 1) \quad (2.4.2)$$

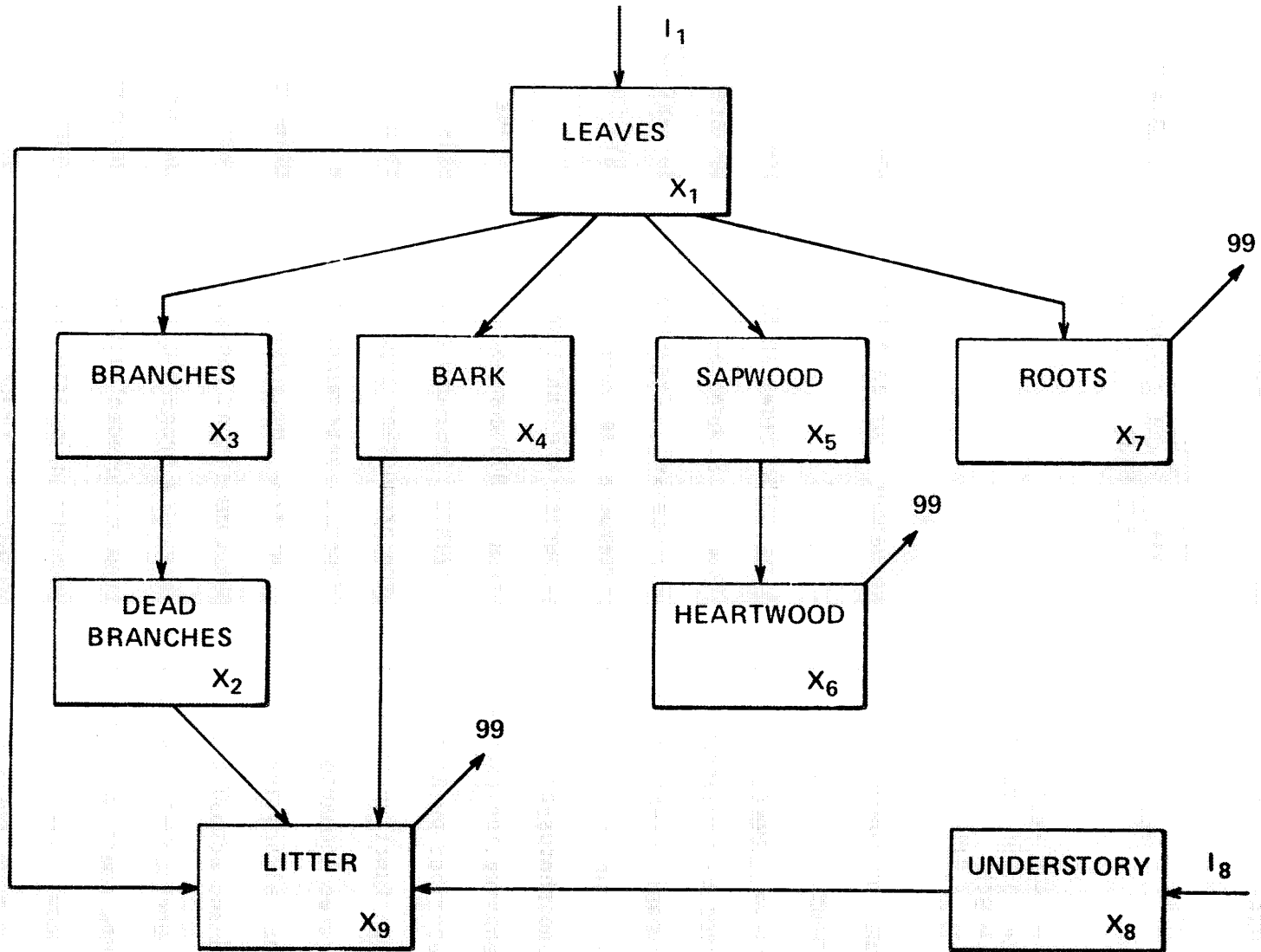


Fig. 2.4.1. Compartmental structure of the temperate broadleaf evergreen forest model. The $F(i,j)$'s indicate the flux of biomass from compartment i to compartment j . The number 99 indicates a compartment external to the system.

Global radiation, $Z_2(t)$, is calculated with the equation:

$$Z_2(t) = \begin{cases} A_0 + B_0 t & \text{if } t \leq 0.5 \\ A_1 + B_1 t & \text{if } 0.5 < t \leq 0.8333 \\ A_0 & \text{if } 0.8333 < t \leq 1.0 \end{cases} \quad (2.4.3)$$

where $A_0 = 1400 \text{ kcal m}^{-2} \text{ d}^{-1}$,
 $A_1 = 13,150 \text{ kcal m}^{-2} \text{ d}^{-1}$,
 $B_0 = 9400$,
 $B_1 = 14,100$.

These equations were fitted to observations for an Australian forest (Attiwill et al. 1973).

2.4.1.3 Flows or rate processes. The flows in the model are represented by the arrows in Fig. 2.4.1. In general, these fluxes are constant coefficient donor control processes. Exceptions include leaf litterfall, which is a function of temperature (see Attiwill et al. 1973), and photosynthesis forcings, which are functions of evapotranspiration (see Attiwill et al. 1973 and Sect. 2.4.1.4). The model described by Attiwill et al. (1973) included a photosynthesis allocation function to partition the production input into growth of various tree compartments. This function determined the average fractional allocation to a particular tree compartment as a function of expected and actual biomass in that compartment (actual biomass was in turn a function of tree bole biomass). A proportional input flux for that compartment was determined from a precedent linear annual version of the model. We have not included this allocation function in our model. A flux representing activation of storage reserves in the roots, $F(7,1)$, is also excluded.

The flows included in our model are defined below. The notation $F(i,j)$ indicates the flow of biomass from compartment i to compartment j . The number 99 represents a carbon or biomass sink, generally the atmosphere.

- I_1 - tree leaves production forcing: see Sect. 2.4.1.4
- I_8 - understory production forcing: see Sect. 2.4.1.4
- $F(1,3)$ - leaf to branch translocation: $a_{13}X_1$
- $F(1,4)$ - leaf to stem bark translocation: $a_{14}X_1$
- $F(1,5)$ - leaf to sapwood translocation: $a_{15}X_1$
- $F(1,7)$ - leaf to root translocation: $a_{17}X_1$
- $F(1,9)$ - leaf litterfall: $FALLX_1$
- $F(2,9)$ - fall of dead branches: $a_{29}X_2$
- $F(3,2)$ - branch mortality: $a_{32}X_3$
- $F(4,9)$ - fall of dead stem bark: $a_{49}X_4$
- $F(5,6)$ - transfer from sapwood to heartwood: $a_{56}X_5$
- $F(6,99)$ - heartwood respiration: r_6X_6
- $F(7,99)$ - root respiration: r_7X_7
- $F(8,9)$ - fall of understory litter: $a_{89}X_8$
- $F(9,99)$ - litter decomposition: r_qX_q

The terms a_{ij} and r_i are flux constants. $FALL$ represents a temperature-dependent function describing the rate of leaf fall (see Attiwill et al. 1973).

2.4.1.4 Photosynthesis and respiration. Photosynthesis is simulated by forcings of monthly net production, I_1 and I_8 , applied to tree leaves, X_1 , and understory vegetation, X_8 , respectively. The forcings are calculated by

$$I_1(t) = 12.0 G(t) \quad (2.4.4)$$

and

$$I_8(t) = p I_1(t) \quad (2.4.5)$$

where p is a constant ratio of understory production to tree leaf production, and $G(t)$ is the growth function, G , evaluated at time t . The value of $G(t)$ is given by:

$$G(t) = g(t)/[1.0 + ag(t)] \quad , \quad (2.4.6)$$

where $g(t)$ is potential growth at time t as a function of evapotranspiration, EV (see Sect. 2.4.1.2), at time t , and a is a growth-altering coefficient. This parameter reflects the reduction in growth associated with reduced leaf area (Attiwill et al. 1973).

The potential growth rate, $g = f(EV)$, is given by

$$g(t) = \begin{cases} bEV(t) & \text{if } 0.0 \leq EV \leq 60 \text{ mm} \\ 60b & \text{if } EV > 60 \text{ mm} \end{cases} \quad , \quad (2.4.7)$$

where b is an empirically derived parameter relating growth and evapotranspiration (EV). For the eucalyptus forest of Attiwill et al. (1973), $b = 6.25$.

Respiration, $F(i,0)$, from living compartments is calculated by:

$$F(i,0) = r_i X_i \quad i = 6, 7 \quad (2.4.8)$$

where r_i is a constant rate coefficient, and X_i is the biomass of compartment i . Live respiration losses are assumed to apply only to heartwood, X_6 , and roots, X_7 .

2.4.1.5 Release of carbon through decomposition. As litter, X_9 , decomposes, CO_2 is evolved according to the relationship

$$F(9,0) = r_9 X_9 \quad , \quad (2.4.9)$$

where r_g is a linear constant rate coefficient, and $F(9,0)$ is the flux of CO_2 as biomass is decomposed.

2.4.2 Seasonal Photosynthesis and Respiration

Rainfall, Z_1 , and global radiation, Z_2 , values were generated using the empirically derived equations of Attiwill et al. (1973) (also see Sect. 2.4.1.2). These input data were used to drive the simulation model and generate total ecosystem photosynthesis and respiration values for an "average" year. A plot of daily fluxes sampled at 5-d intervals is shown in Fig. 2.4.2. Biomass fluxes generated by the model were converted to CO_2 fluxes using the conversion factor of 1 g dry matter = 1.65 g CO_2 (Lieth 1978). Seasonal net CO_2 exchange between the forest stand and the atmosphere is plotted in Fig. 2.4.3. A positive net exchange indicates the stand is acting as a source of atmospheric CO_2 ; a negative value indicates the stand is acting as a sink.

2.5 TROPICAL DECIDUOUS FOREST MODEL

The model of seasonal carbon dynamics in an open tropical deciduous woodland is based on a model of the miombo forest in Zaire presented by Bandhu et al. (1973). Their seasonal model evolved from an annual constant-coefficient model during the International Woodlands Workshop (Reichle et al. 1973). The model simulates biomass dynamics in a compartmented system using first-order linear differential equations. There are actually two models, depending on when fire

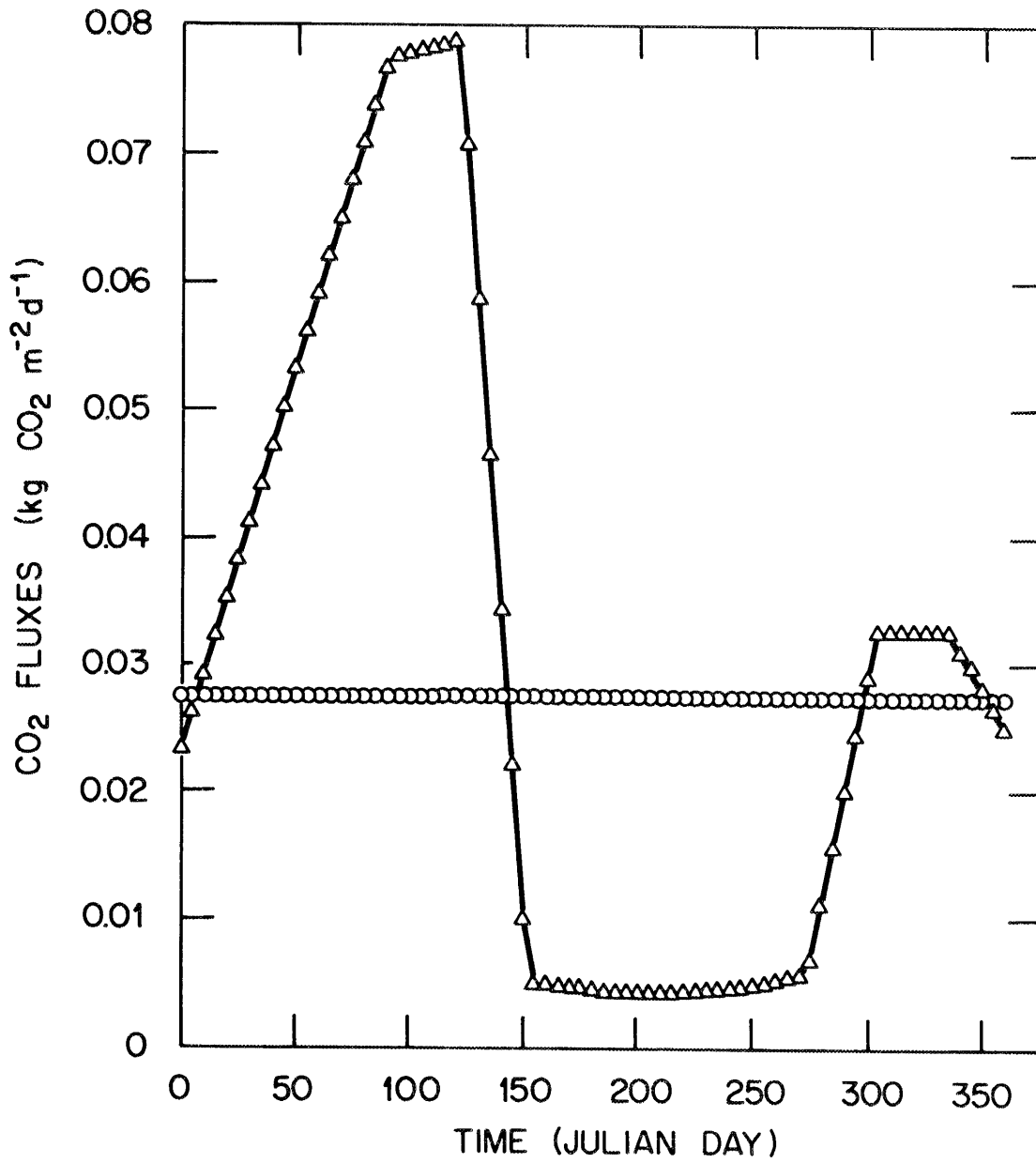


Fig. 2.4.2. Seasonal total ecosystem photosynthesis (Δ) and respiration (o) for a temperate broadleaf evergreen forest stand. Flux units are $\text{kg CO}_2 \text{ m}^{-2} \text{ d}^{-1}$.

ORNL-DWG 85-14327

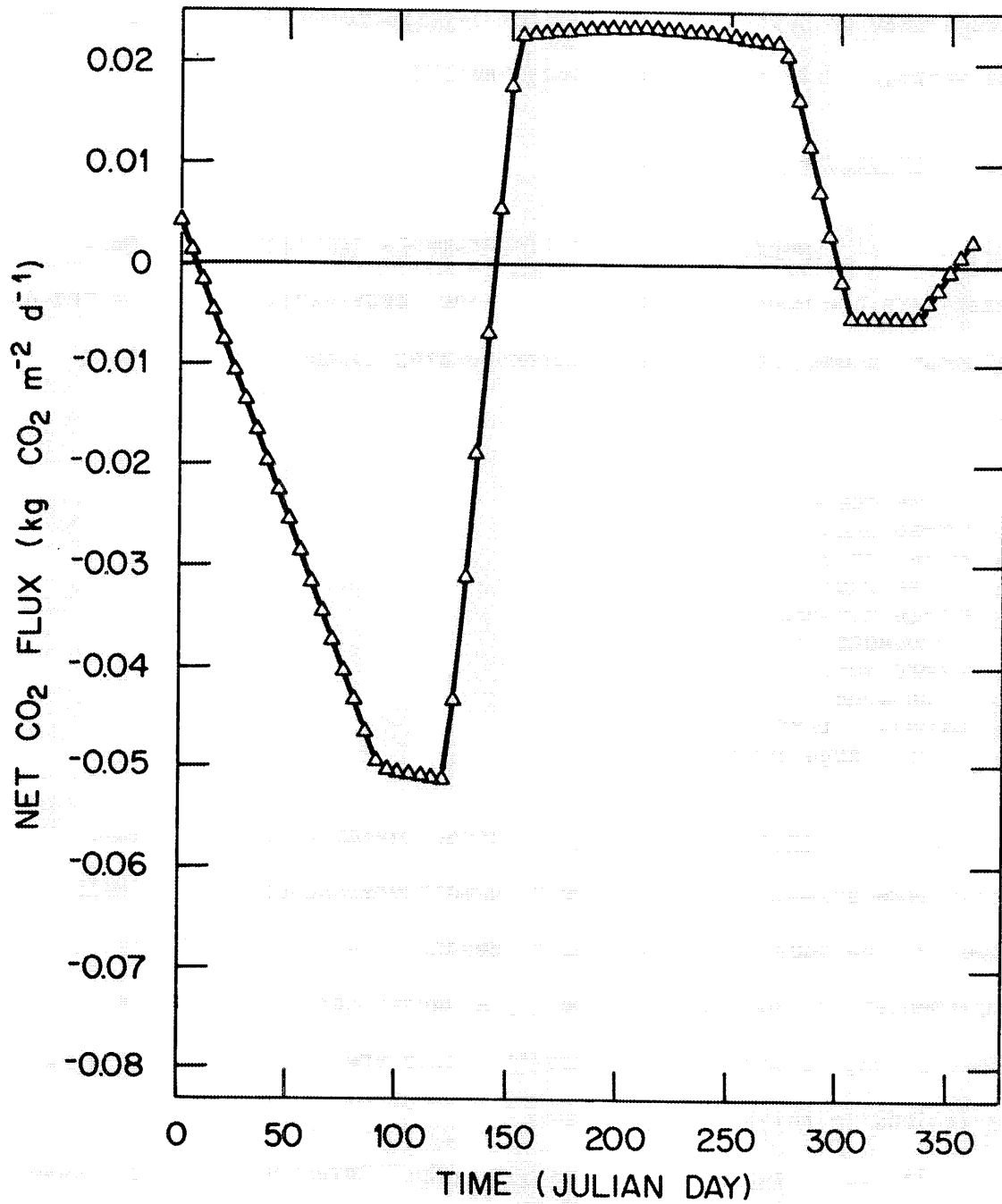


Fig. 2.4.3. Seasonal net CO₂ exchange between the atmosphere and a temperate broadleaf evergreen forest stand. Net flux is respiration minus photosynthesis. Flux units are kg CO₂ m⁻² d⁻¹.

occurs (May or September). The model is structured very similarly to the tropical rain forest model (see Sect. 2.6).

2.5.1 Structure of the Model

2.5.1.1 Compartments. Ten compartments representing biomass reservoirs are modeled (Fig. 2.5.1). The state variables, expressed as kilograms biomass/per hectare, corresponding to the compartments of Fig. 2.5.1 are:

- X₁ - tree leaves
- X₂ - tree branches
- X₃ - tree boles
- X₄ - tree roots
- X₅ - tree flowers and fruits
- X₆ - groundcover vegetation
- X₇ - herbivorous insects
- X₈ - non-woody litter
- X₉ - woody litter
- X₁₀ - soil organic matter.

2.5.1.2 Driving variables. Seasonal dynamics of the miombo forest are assumed to be dependent on moisture (Bandhu et al. 1973). However, the model, as described by Bandhu et al. (1973) and in our implementation, does not involve any exogenous driving variables. Time-varying forcings and rate coefficients are in principle related to variations in rainfall or moisture.

2.5.1.3 Flows or rate processes. Most intercompartmental fluxes are represented as constant donor-controlled processes. A few flows (e.g., photosynthesis, litterfall, and litter to soil transfer) involve time-varying forcings or rate coefficients. The flows indicated by arrows in Fig. 2.5.1 are defined below. The notation $F(i,j)$ indicates

ORNL-DWG 85-14260

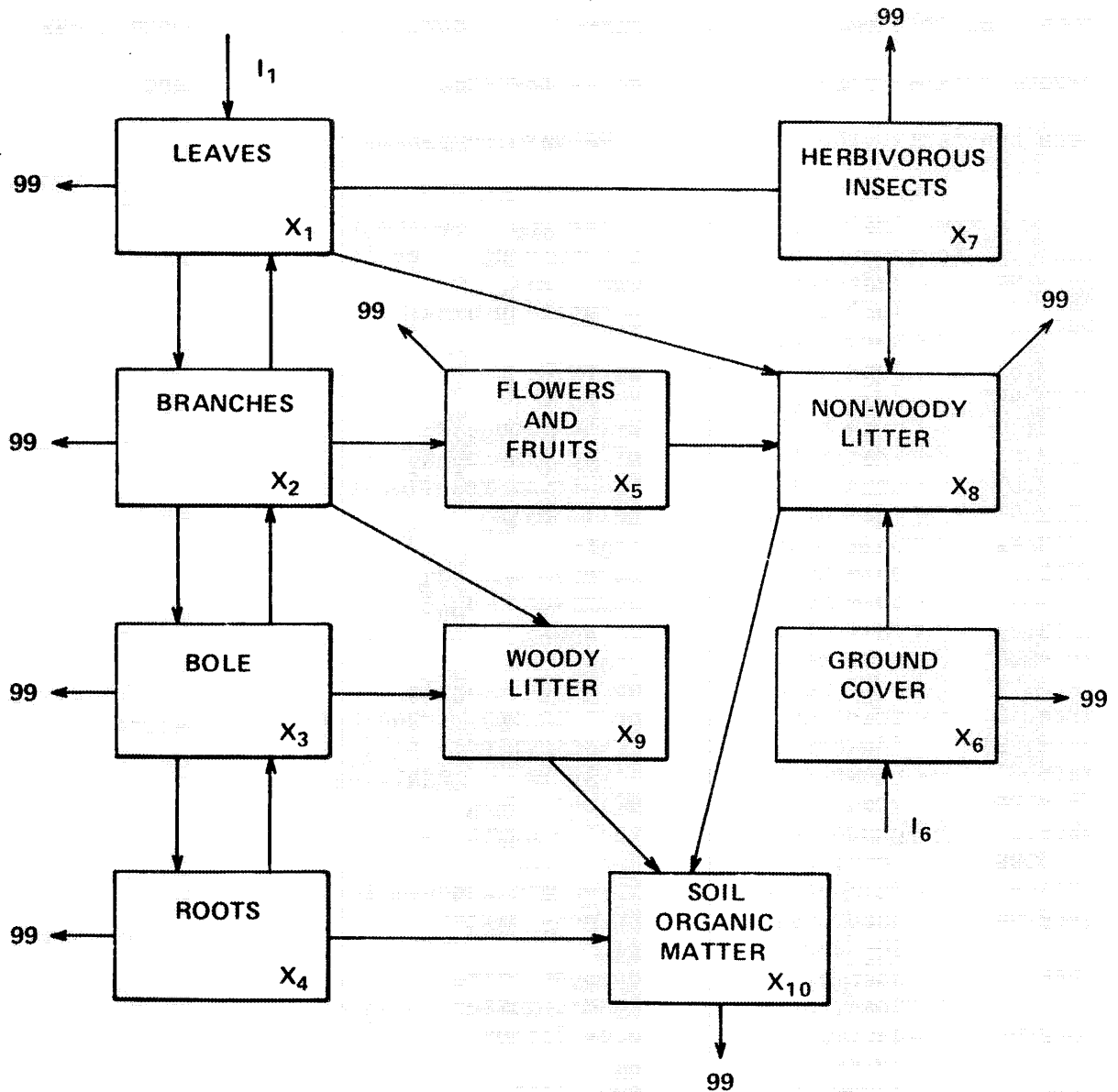


Fig. 2.5.1. Compartmental structure of the tropical deciduous forest model. The $F(i,j)$'s indicate the flux of biomass from compartment i to compartment j . The number 99 indicates a compartment external to the system.

the flow of biomass from compartment i to compartment j . The number 99 represents a carbon sink, generally the atmosphere. The a_{ij} and r_i are constants; the $a_{ij}(t)$ are time-varying parameters.

- I_1 - tree leaf photosynthesis forcing: see Sect. 2.5.1.4
- I_6 - groundcover photosynthesis forcing: see Sect. 2.5.1.4
- $F(1,99)$ - leaf dark respiration: r_1X_1
- $F(1,2)$ - leaf to branch translocation: $a_{12}X_1$
- $F(1,7)$ - herbivory: $a_{17}X_1$
- $F(1,8)$ - leaf litterfall: $a_{18}(t)X_1$
- $F(2,99)$ - branch respiration: r_2X_2
- $F(2,1)$ - branch to leaf translocation: $a_{21}X_2$
- $F(2,3)$ - branch to bole translocation: $a_{23}X_2$
- $F(2,5)$ - branch to flowers and fruit translocation: $a_{25}X_2$
- $F(2,9)$ - fall of dead branches: $a_{29}X_2$
- $F(3,99)$ - bole respiration: r_3X_3
- $F(3,2)$ - bole to branch translocation: $a_{32}X_3$
- $F(3,4)$ - bole to root translocation: $a_{34}X_3$
- $F(3,9)$ - fall of dead boles: $a_{39}X_3$
- $F(4,99)$ - root respiration: r_4X_4
- $F(4,3)$ - root to bole translocation: $a_{43}X_4$
- $F(4,10)$ - transfer of dead roots to soil organic matter: $a_{410}X_4$
- $F(5,99)$ - flowers and fruits respiration: r_5X_5
- $F(5,8)$ - flowers and fruit litterfall: $a_{58}(t)X_5$
- $F(6,99)$ - groundcover respiration: r_6X_6
- $F(6,8)$ - groundcover litterfall: $a_{68}(t)X_6$
- $F(7,99)$ - herbivore respiration: r_7X_7
- $F(7,8)$ - fall of dead herbivores and waste material: $a_{78}X_7$
- $F(8,99)$ - decomposition of nonwoody litter
(CO_2 evolution): r_8X_8
- $F(8,10)$ - decomposition of nonwoody litter
(transfer to soil organic matter): $a_{810}(t)X_8$
- $F(9,99)$ - decomposition of woody litter
(CO_2 evolution): r_9X_9
- $F(9,10)$ - decomposition of woody litter
(transfer to soil organic matter): $a_{910}(t)X_9$
- $F(10,99)$ - decomposition of soil organic matter: $r_{10}X_{10}$

2.5.1.4 Photosynthesis and respiration. Seasonal variations in photosynthesis are incorporated as monthly forcings, $I_1(m)$ and $I_6(m)$ ($m = 1, \dots, 12$), on tree leaves, X_1 , and groundcover, X_6 , respectively. The monthly forcing values, probably best interpreted as gross primary production, are input data to the simulation program.

Respiration from live compartments is given by

$$F(i,0) = r_i X_i \quad i = 1, \dots, 7 \quad (2.5.1)$$

where X_i is the biomass of compartment i , and r_i is a constant rate coefficient specific to that compartment.

2.5.1.5 Release of carbon through decomposition. The evolution of CO_2 during microbial decomposition of dead organic matter is modeled by applying Eq. 2.5.1 to the litter compartments, X_8 and X_9 , and the soil organic matter compartment, X_{10} . The model does not consider seasonal variation in the rate of CO_2 release during decomposition. Decomposition does exhibit seasonality, however, through time-varying rates of transfer from litter to soil organic matter. These variations are assumed to be related to soil and litter moisture (Bandhu et al. 1973), although the model does not include any functional representation of this relationship.

2.5.2 Seasonal Photosynthesis and Respiration

The time-varying coefficients and forcings that drive the seasonal dynamics of the miombo forest model were provided by Bandhu et al. (1973). These were used to derive seasonal total ecosystem photosynthesis and respiration values. Figure 2.5.2 is a plot of daily fluxes sampled at 5-d intervals. Model generated biomass fluxes were converted to CO_2 fluxes (1 g dry weight = 1.65 g CO_2 ; Lieth 1978). Seasonal net CO_2 exchange (respiration minus photosynthesis) between the forest stand and the atmosphere is plotted in Fig. 2.5.3. A positive net exchange indicates the stand is acting as a source of

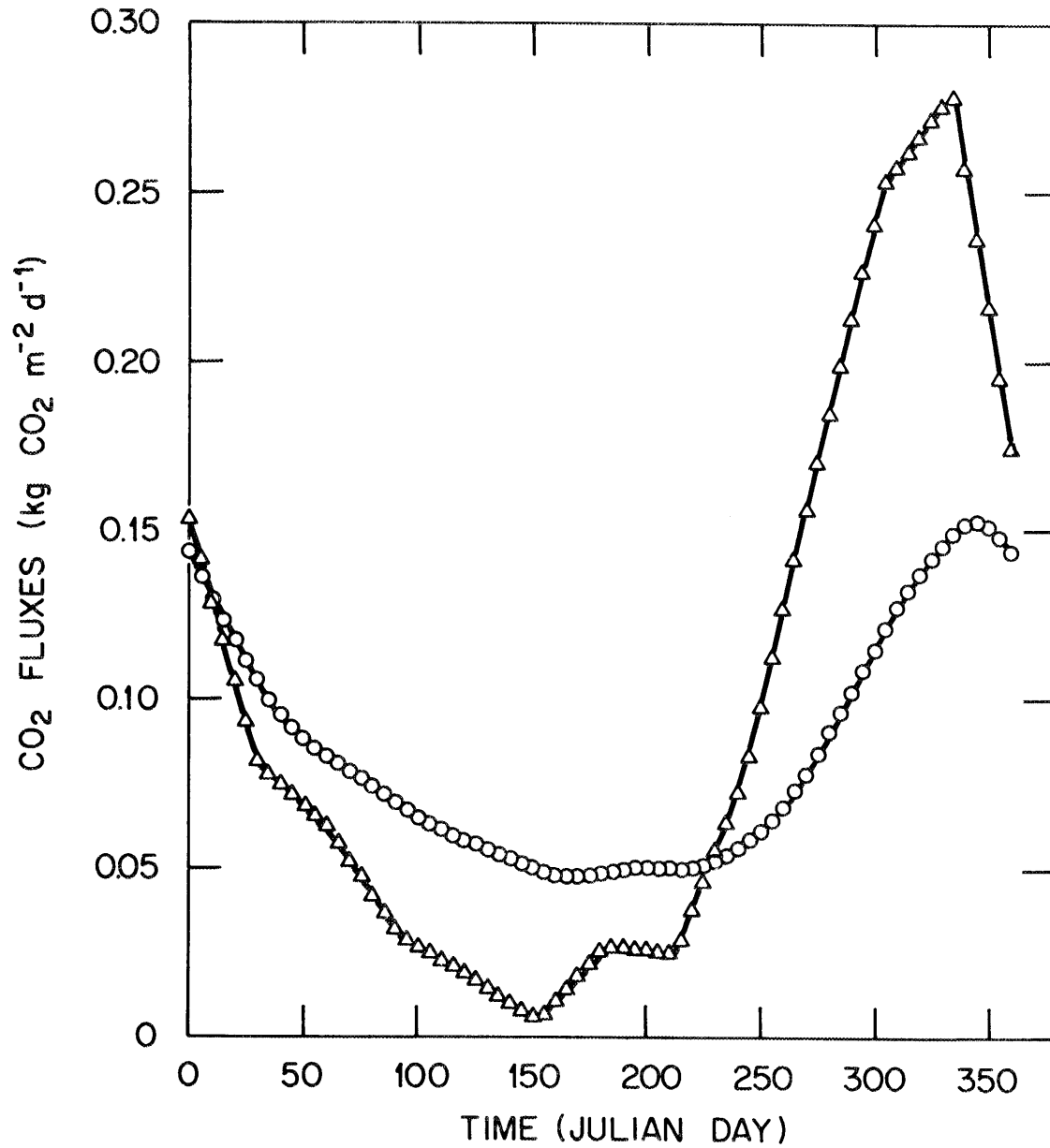


Fig. 2.5.2. Seasonal total ecosystem photosynthesis (Δ) and respiration (o) for a tropical deciduous forest stand. Flux units are $\text{kg CO}_2 \text{ m}^{-2} \text{ d}^{-1}$.

ORNL-DWG 85-14329

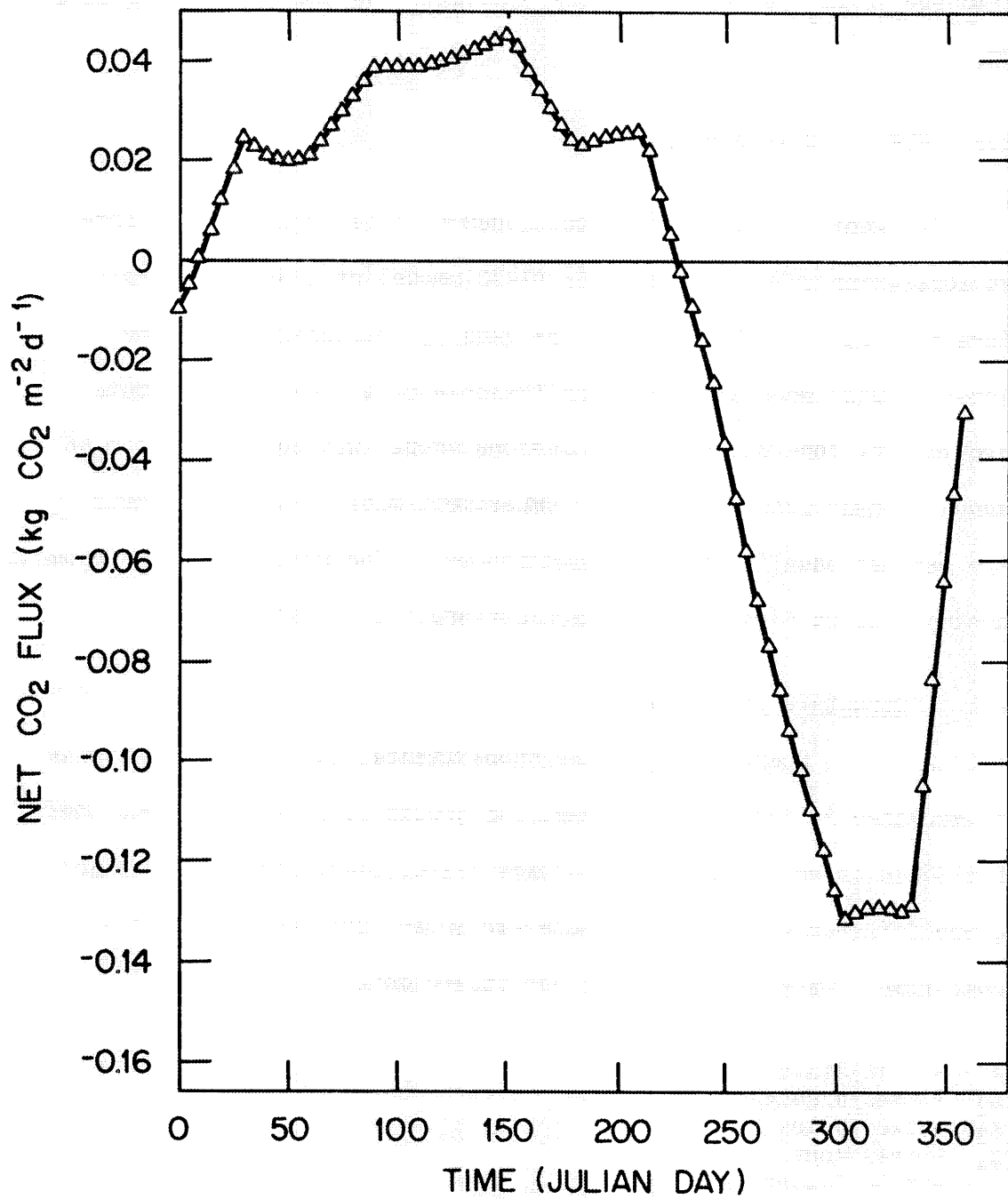


Fig. 2.5.3. Seasonal net CO₂ exchange between the atmosphere and a tropical deciduous forest stand. Net flux is respiration minus photosynthesis. Flux units are kg CO₂ m⁻² d⁻¹.

atmospheric CO₂; a negative value indicates the stand is acting as a CO₂ sink.

2.6 TROPICAL RAIN FOREST MODEL

The model of seasonal carbon dynamics in a tropical rain forest is an adaptation of Bandhu et al.'s (1973) model of a Malaysian rain forest at Pasoh. The model was originally developed during the International Woodlands Workshop (Reichle et al. 1973) using data provided by John Bullock. The seasonal model was developed from an annual linear donor-controlled compartment model and retains much of the earlier model's structure and process. The model simulates biomass dynamics using first-order linear differential equations.

2.6.1 Structure of the Model

2.6.1.1 Compartments. The compartmental structure of the model is depicted in Fig. 2.6.1. Trees and ground cover are distinguished, but there is no consideration of age class, plant species, or plant group differences. The ten state variables corresponding to the compartments are grams biomass per square meter):

- X₁ - tree leaves
- X₂ - tree branches
- X₃ - tree boles
- X₄ - tree roots
- X₅ - tree flowers and fruits
- X₆ - groundcover vegetation
- X₇ - herbivorous insects
- X₈ - non-woody litter
- X₉ - woody litter
- X₁₀ - soil organic matter.

2.6.1.2 Driving variables. The rain forest model includes only one seasonal driving variable. Seasonal phenomena are assumed to be

ORNL-DWG 85-14261

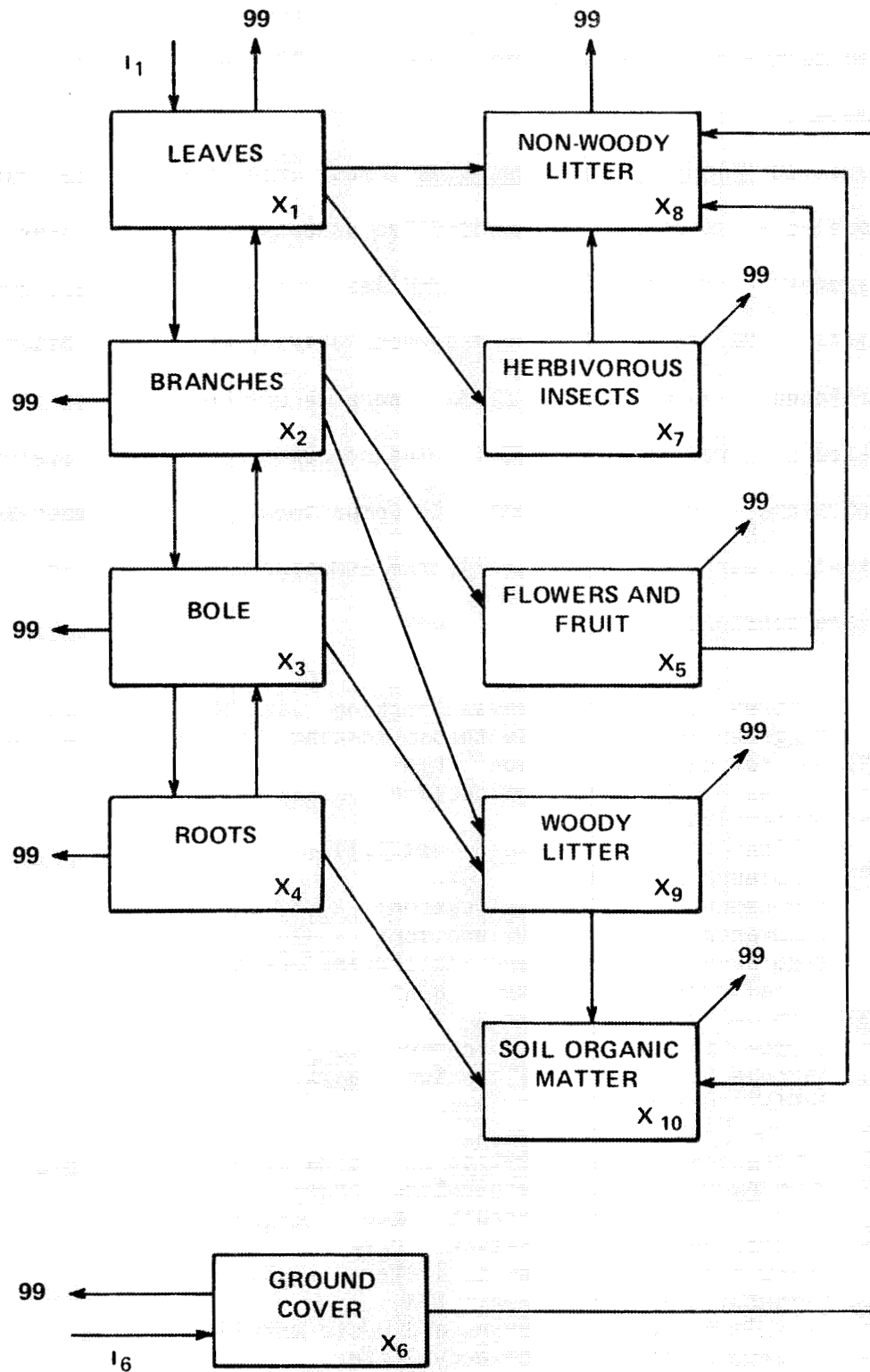


Fig. 2.6.1. Compartmental structure of the tropical rain forest model. the $F(i,j)$'s indicate the flux of biomass from compartment i to compartment j . The number 99 indicates a compartment external to the system.

related to monthly rainfall, $Z(m)$ ($m = 1, \dots, 12$), expressed in millimeters.

2.6.1.3 Flows or rate processes. Most intercompartmental flows are modeled as constant donor-controlled processes. However, the photosynthetic forcings, the I_j 's, and leaf litterfall, $F(1,8)$, are functions of rainfall, the sole exogenous driving variable. Details can be found in Bandhu et al. (1973); here we define the flows indicated by arrows in Fig. 2.6.1. The notation $F(i,j)$ indicates the flux of biomass from compartment i to compartment j . The number 99 represents a carbon sink, generally the atmosphere. The a_{ij} , r_i , and k are constants.

I_1	- tree leaf photosynthesis forcing: see Sect. 2.6.1.4
I_6	- ground-cover photosynthesis forcing: see Sect. 2.6.1.4
$F(1,99)$	- leaf dark respiration: $r_1 X_1$
$F(1,2)$	- leaf to branch translocation: $a_{12} X_1$
$F(1,7)$	- herbivory: $a_{17} X_1$
$F(1,8)$	- leaf litterfall: $(a_{18} + (k/I_1)) X_1$
$F(2,99)$	- branch respiration: $r_2 X_2$
$F(2,1)$	- branch to leaf translocation: $a_{21} X_2$
$F(2,3)$	- branch to bole translocation: $a_{23} X_2$
$F(2,5)$	- branch to flowers and fruit translocation: $a_{25} X_2$
$F(2,9)$	- fall of dead branches: $a_{29} X_2$
$F(3,99)$	- bole respiration: $r_3 X_3$
$F(3,2)$	- bole to branch translocation: $a_{32} X_3$
$F(3,4)$	- bole to roots translocation: $a_{34} X_3$
$F(3,9)$	- fall of dead boles: $a_{39} X_3$
$F(4,99)$	- root respiration: $r_4 X_4$
$F(4,10)$	- transfer of dead root to soil organic matter: $a_{410} X_4$
$F(5,99)$	- flower and fruit respiration: $r_5 X_5$
$F(5,8)$	- fall of flower and fruit litter: $a_{58} X_5$
$F(6,99)$	- ground-cover respiration: $r_6 X_6$
$F(6,8)$	- fall of ground cover to litter: $a_{68} X_6$
$F(7,99)$	- herbivore respiration: $r_7 X_7$
$F(7,8)$	- fall of dead herbivores and waste material: $a_{78} X_7$
$F(8,99)$	- decomposition of nonwoody litter (CO_2 evolution): $r_8 X_8$
$F(8,10)$	- decomposition of nonwoody litter (transfer to soil organic matter): $a_{810} X_8$

$F(9,99)$ - decomposition of woody litter
 (CO_2 evolution): $r_9 X_9$
 $F(9,10)$ - decomposition of woody litter
 (transfer to soil organic matter): $a_{910} X_9$
 $F(10,99)$ - decomposition of soil organic matter: $r_{10} X_{10}$

2.6.1.4 Photosynthesis and respiration. The forcing, I_1 , on the leaf compartment, X_1 , is a function relating leaf primary production to rainfall. The forcing can be interpreted as net daytime photosynthesis or carbon assimilation. The equations used to calculate this forcing are

$$I_1(1) = 12.0[7.51P(1)] \quad (2.6.1)$$

and

$$I_1(m) = 12.0[3.755P(m) + 3.755P(m - 1)] \quad m = 2, \dots, 12. \quad (2.6.2)$$

The term $P(m)$ is given by

$$P(m) = (10/12)Z(m) \quad m = 1, 2, \dots, 12, \quad (2.6.3)$$

where $Z(m)$ is monthly rainfall (in millimeters).

The production forcing, I_6 , on the ground-cover compartment, X_6 , is presumably of the same form (Bandhu et al. 1973). However, in our implementation I_6 is set equal to zero. The Bandhu et al. (1973) paper is ambiguous about the original value used for I_6 .

Respiration from living compartments X_1 through X_7 is modeled using constant rate coefficients in equations of the form

$$F(i,99) = r_i X_i \quad i = 1, 2, \dots, 7, \quad (2.6.4)$$

where $F(i,99)$ is the respiratory flux from compartment i , and r_i is the constant rate coefficient relating respiration to compartment size. The absence of seasonality in respiration, which might be modeled as function of seasonally varying temperature, is a result of Bandhu et al.'s assumption that all seasonal phenomena were related to precipitation. This implies an additional assumption that temperature is relatively constant in the Pasoh, Malaysia rain forest.

2.6.1.5 Release of carbon through decomposition. Respiration losses from nonliving compartments, representing the release of CO_2 during microbial decomposition of organic matter, are modeled by applying Eq. (2.6.4) to compartments X_8 , X_9 , and X_{10} . The constant rate coefficients reflect the implicit assumption that litter/soil moisture and temperature remain relatively constant throughout the year.

2.6.2 Seasonal Photosynthesis and Respiration

Data on seasonal rainfall in a Malaysian rain forest were provided by Bandhu et al. (1973) and were used to drive the production forcing of the simulation model and generate seasonal CO_2 assimilation (photosynthesis) and respiration values for the total ecosystem. Daily fluxes sampled at 5-d intervals are plotted in Fig. 2.6.2. Biomass values generated by the model were converted to CO_2 equivalents using a conversion factor of 1 g dry matter = 1.65 g CO_2 (Lieth 1978). Seasonal net CO_2 exchange between the forest stand and the atmosphere is plotted in Fig. 2.6.3. Net exchange is respiration minus photosynthesis. Hence, a positive value indicates the stand is acting

ORNL-DWG 85-14330

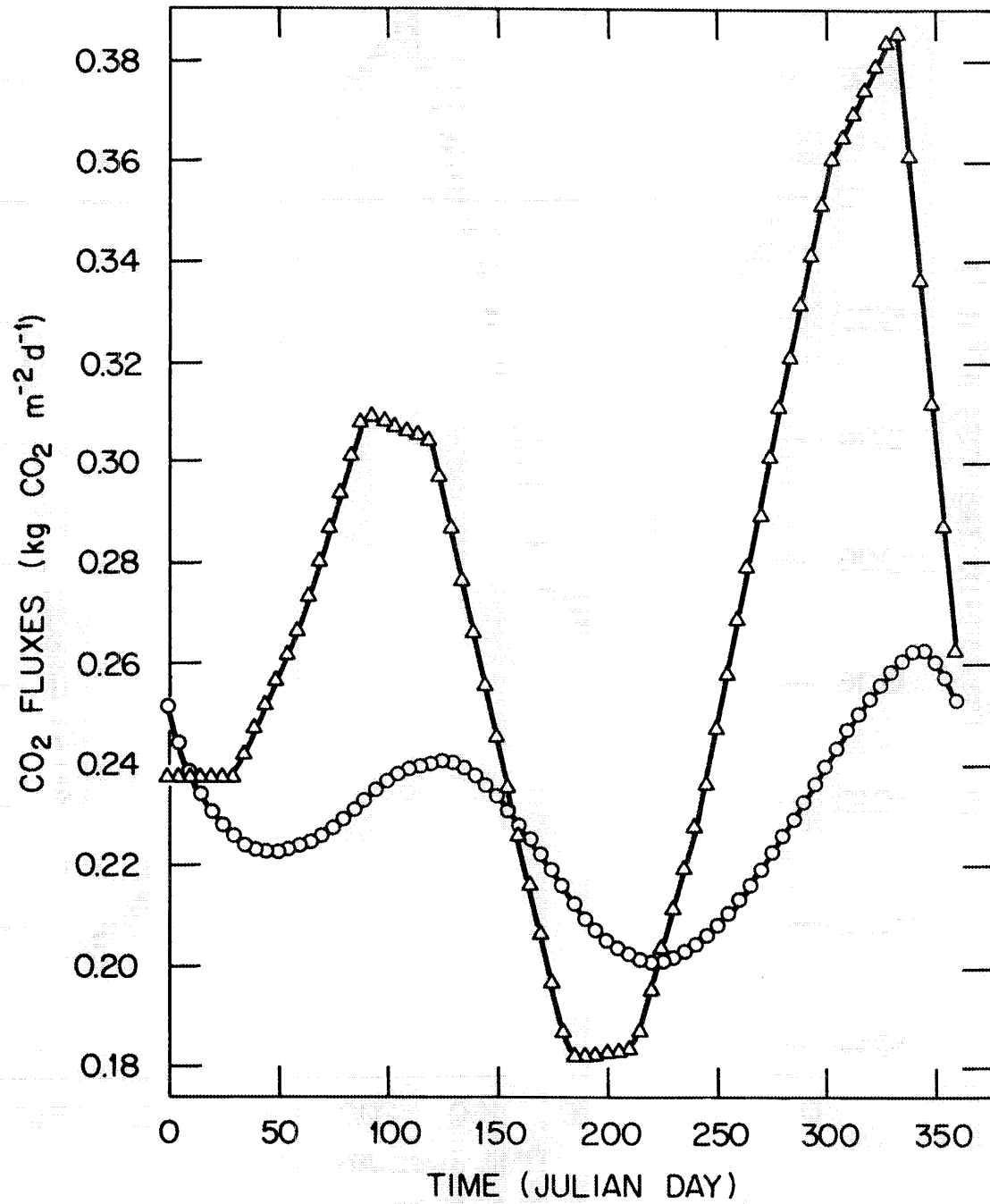


Fig. 2.6.2. Seasonal total ecosystem photosynthesis (Δ) and respiration (o) for a tropical rain forest stand. Flux units are $\text{kg CO}_2 \text{ m}^{-2} \text{ d}^{-1}$.

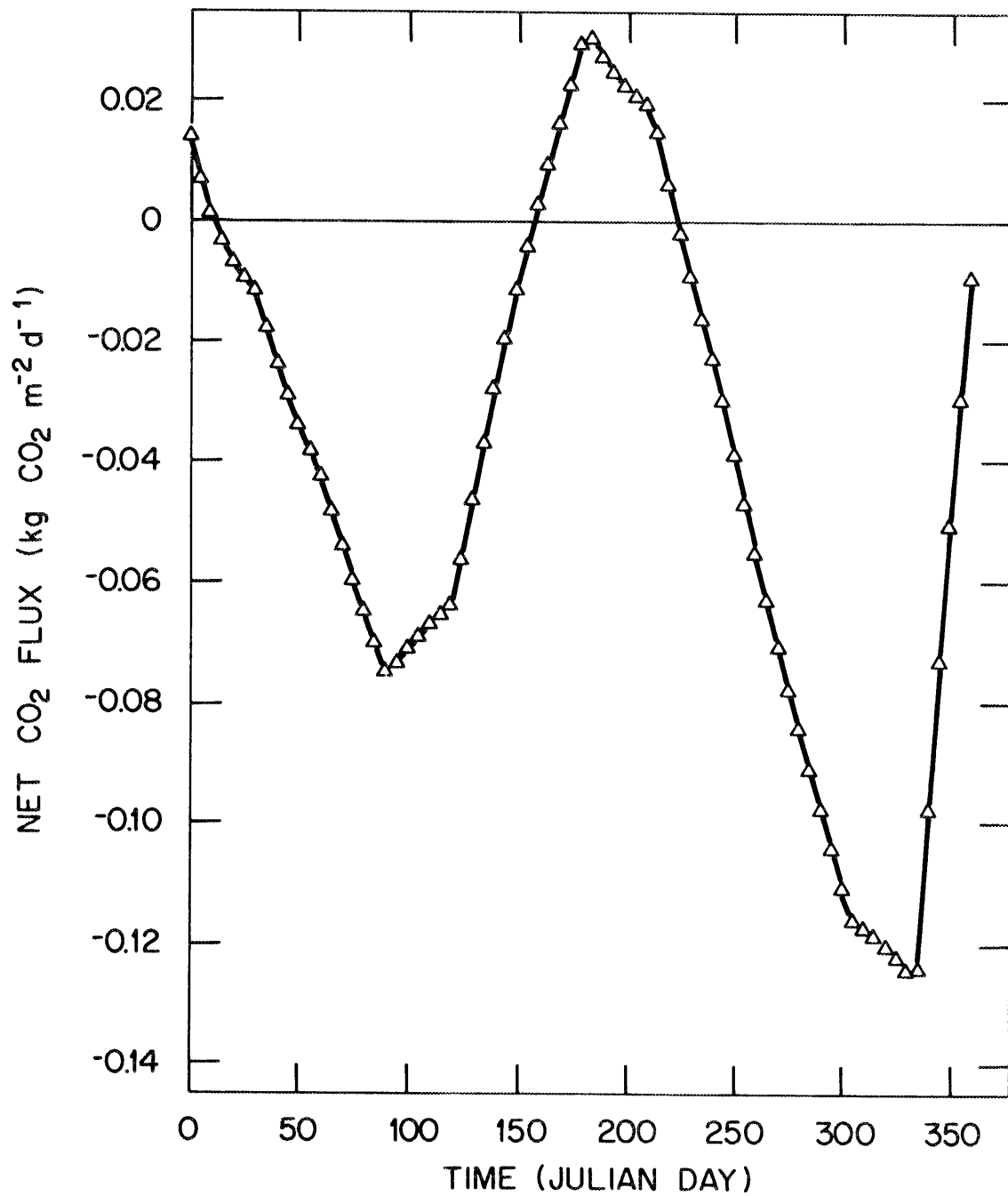


Fig. 2.6.3. Seasonal net CO₂ exchange between the atmosphere and a tropical rain forest stand. Net flux is respiration minus photosynthesis. Flux units are kg CO₂ m⁻² d⁻¹.

as a source of atmospheric CO₂; a negative value indicates the stand is acting as a sink.

2.7 TEMPERATE GRASSLAND MODEL

The temperate grassland model is adapted from the shortgrass prairie producer model described by Parton, Singh, and Coleman (1978) and Parton and Singh (1976). Plant biomass (grams dry weight per square meter), both aboveground and belowground, is described by a compartmental model using difference equations and a time step of one day. The model was originally constructed for the shortgrass prairie at the US/IBP Grassland Biome Pawnee Site, which is dominated by blue grama (*Bouteloua gracilis*) (Parton and Singh 1976; Parton, Singh, and Coleman 1978). The model has also been applied to the tallgrass prairie at the Osage Site, which is dominated by little bluestem (*Andropogon scoparius*), by Parton and Singh (1976). We have used the Pawnee version of the model.

2.7.1 Structure of the Model

2.7.1.1 Compartments. Forty-one compartments or state variables are modeled (Fig. 2.7.1). Conceptually, the model considers a single species of grass and does not consider other grass species, plant types, or age classes (except for three root-age classes). In practice, the model was parameterized with data for the dominant species at the site (i.e., blue grama at Pawnee). All state variables are expressed in grams dry weight biomass per square meter. The state variables corresponding to the compartments of Fig. 2.7.1 are defined as:

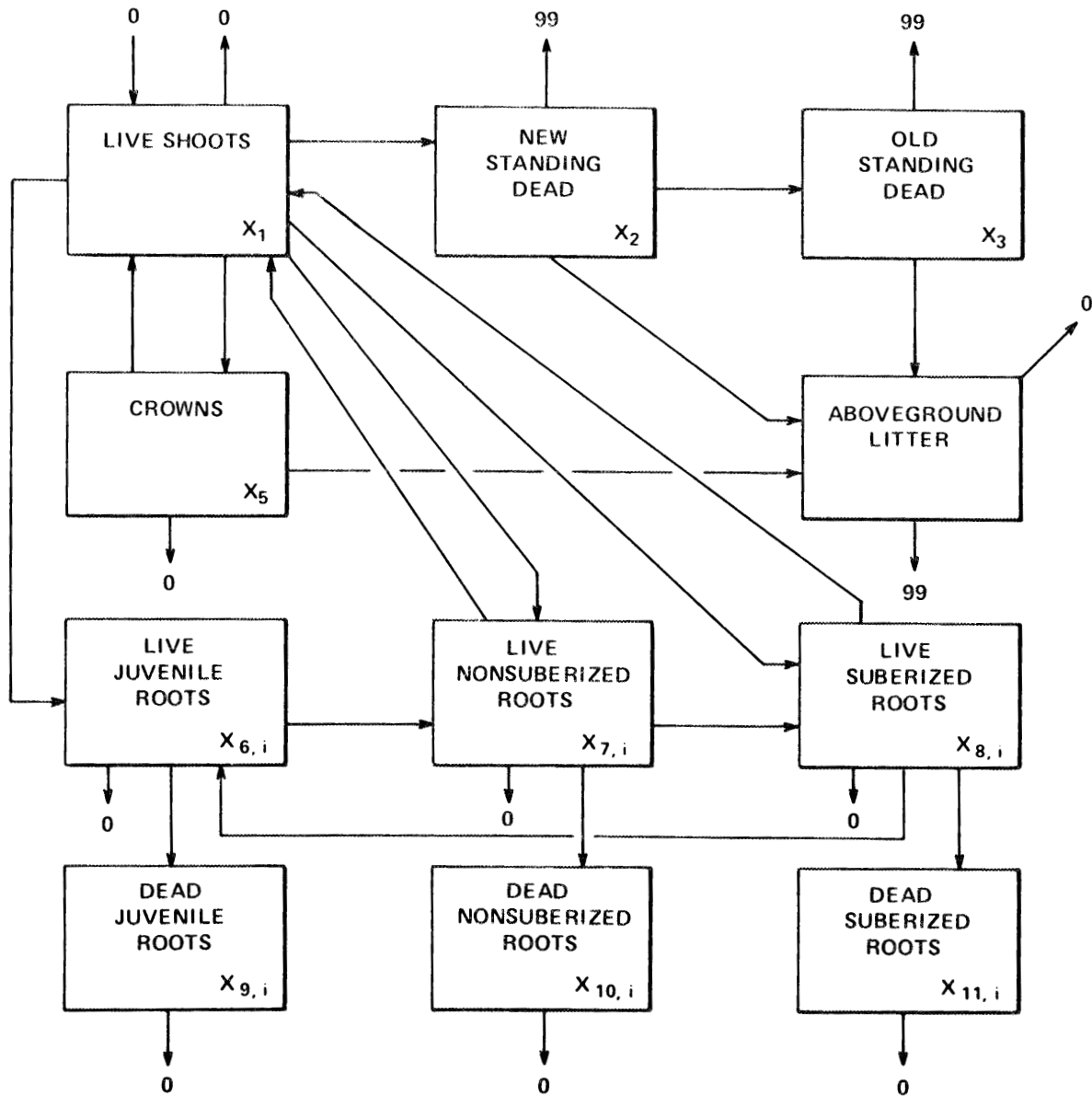


Fig. 2.7.1. Compartmental structure of the temperate grassland model. The $F(i,j)$'s indicate the flux of biomass from compartment i to compartment j . The numbers 99 and 0 indicate compartments external to the system.

- X_1 - live shoots
- X_2 - new standing dead (standing dead of current year)
- X_3 - old standing dead
- X_4 - aboveground litter
- X_5 - crowns
- $X_{6,i}$ - live juvenile roots in the i th soil layer
six soil layers considered (0-5, 5-15, 15-30,
30-45, 45-60, and 60-75 cm)
- $X_{7,i}$ - live nonsuberized roots in the i th soil layer
- $X_{8,i}$ - live suberized roots in the i th soil layer
- $X_{9,i}$ - dead juvenile roots in the i th soil layer
- $X_{10,i}$ - dead nonsuberized roots in the i th soil layer
- $X_{11,i}$ - dead suberized roots in the i th soil layer

2.7.1.2 Driving variables. The model involves a number of driving variables. The original model was coupled with an abiotic submodel (Parton 1976) that calculated most of these variables, many of which responded to changes in the state variables (i.e., there was feedback between the biota and the abiotic environment). Other variables were strictly exogenous driving variables. The submodel we used to derive and incorporate the driving variables is a minor modification of Parton (1976). Following is a list of the driving variables used in the model.

- $Z_1(i)$ - soil water potential (-bars) in the i th soil layer
- Z_2 - weighted average soil water potential (-bars)
- $Z_3(i)$ - soil temperature ($^{\circ}\text{C}$) in the i th soil layer
- Z_4 - soil surface temperature ($^{\circ}\text{C}$)
- Z_5 - 14-d running average soil temperature ($^{\circ}\text{C}$) in the top two soil layers
- Z_6 - solar irradiance (W/m^2)
- $Z_7(j)$ - daytime air temperature ($^{\circ}\text{C}$) for the j th ($j = 1, \dots, 4$) daytime interval
- $Z_8(j)$ - nighttime air temperature ($^{\circ}\text{C}$) for the j th ($j = 1, \dots, 4$) nighttime interval
- Z_9 - minimum daily air temperature ($^{\circ}\text{C}$)
- Z_{10} - maximum daily air temperature ($^{\circ}\text{C}$)
- Z_{11} - average daily air temperature ($^{\circ}\text{C}$)
- Z_{12} - daily rainfall (cm)
- Z_{13} - wind speed (km/h)
- Z_{14} - phenological stage (dimensionless)

2.7.1.3 Flows or rate processes. Fluxes between compartments are modeled mechanistically, and the equations describing them can be quite complex. Details of the functional forms can be found in Parton and Singh (1976), Parton, Singh, and Coleman (1978), and Detling, Parton, and Hunt (1978). Here we simply define the fluxes indicated by arrows in Fig. 2.7.1. The notation $F(i,j)$ indicates the flow of biomass from compartment i to compartment j . The number 0 represents the atmosphere; the number 99 represents a carbon/biomass sink external to the modeled system. Unless otherwise indicated, all flows are given as grams dry weight biomass per square meter per day.

$F(0,1)$	- net daytime photosynthesis
$F(1,0)$	- night respiration
$F(1,2)$	- shoot mortality
$F(1,5)$	- shoot to crown translocation
$F(1,6_i)$	- shoot to juvenile roots translocation
$F(1,7_i)$	- shoot to non-suberized roots translocation
$F(1,8_i)$	- shoot to suberized roots translocation
$F(2,3)$	- transfer of recent standing dead to old standing dead (g dw biomass $m^{-2}year^{-1}$)
$F(2,4)$	- fall of new standing dead
$F(2,99)$	- leaching of recent standing dead
$F(3,4)$	- fall of old standing dead
$F(3,99)$	- leaching of old standing dead
$F(4,0)$	- litter decomposition
$F(4,99)$	- leaching and mechanical mixing of litter
$F(5,0)$	- crown respiration
$F(5,1)$	- transfer of stored carbohydrates to shoots
$F(5,4)$	- crown death
$F(6_i,0)$	- juvenile root respiration in the i th soil layer
$F(6_i,7_i)$	- aging of juvenile roots in the i th soil layer
$F(6_i,9_i)$	- death of juvenile roots in the i th soil layer
$F(7_i,0)$	- nonsuberized root respiration in the i th soil layer
$F(7,1)$	- transfer of carbohydrates stored in nonsuberized roots
$F(7_i,8_i)$	- aging of nonsuberized roots in the i th soil layer
$F(7_i,10_i)$	- death of nonsuberized roots in the i th soil layer
$F(8_i,0)$	- suberized root respiration in the i th soil layer
$F(8,1)$	- transfer of carbohydrates stored in suberized roots

- $F(8_i,6_i)$ - spring initiation of juvenile root growth in the i th soil layer
 $F(8_i,11_i)$ - death of suberized roots in the i th soil layer
 $F(9_i,0)$ - decomposition of dead juvenile roots in the i th soil layer
 $F(10_i,0)$ - decomposition of dead nonsuberized roots in the i th soil layer
 $F(11_i,0)$ - decomposition of dead suberized roots in the i th soil layer

2.7.1.4 Photosynthesis and respiration. Net photosynthesis (grams dry weight biomass per square meter per day) is the difference between net daytime photosynthesis, $F(0,1)$, and night respiration $F(1,0)$. Net daytime photosynthesis is calculated as a function of canopy air temperature, $Z_7(j)$, soil water potential, Z_2 , total shortwave solar radiation, Z_6 , and phenology, Z_{14} , using the equation

$$F(0,1) = \sum_{j=1}^4 C_j L M_x P \Delta t_d / 4 \quad , \quad (2.7.1)$$

where

- C_j = the combined effect of daily weighted average soil water potential and air temperature (dimensionless on (0,1)),
 L = leaf area index (dimensionless),
 M_x = net photosynthesis rate (g m^{-2} leaf area h^{-1}) for a given irradiance under conditions of optimal temperature and soil water potential,
 P = phenology control parameter, $P = f(Z_{14})$, (dimensionless on (0,1)),
 $\Delta t_d / 4$ = length of daytime period j (h).

The term M_x is given by a piecewise linear approximation of the functional relationship presented by Parton, Singh, and Coleman (1978). The leaf area index and phenology control parameter are calculated according to Parton, Singh, and Coleman (1978). The term C_j is determined for each j th daylight time period using the equation presented by Detling, Parton, and Hunt (1978).

Shoot dark respiration, $F(1,0)$, is a function of nighttime air temperature, $Z_8(j)$, and the weighted average soil water potential. The flux is described by

$$F(1,0) = \sum_{j=1}^4 C_j^R L \Delta t_n / 4 , \quad (2.7.2)$$

where C_j^R is dark respiration (grams per square meter leaf area per hour) as a function of nighttime air temperature and soil water potential; L is leaf area index, and $\Delta t_n / 4$ is the length of nighttime period j (hours). The equation used to obtain C_j^R is described by Detling, Parton, and Hunt (1978).

Root respiration in the i th soil layer is calculated as a function of soil water potential, $Z_7(i)$, and temperature, $Z_3(i)$, using the equations

$$F(6_i,0) = M_r T_r R_1 X_{6,i} , \quad (2.7.3a)$$

$$F(7_i,0) = M_r T_r R_2 X_{7,i} , \quad (2.7.3b)$$

$$F(8_i,0) = M_r T_r R_3 X_{8,i} , \quad (2.7.3c)$$

where

M_r = control parameter for the effect of soil water potential
 T_r = control parameter for the effect of soil temperature
 R_j = maximum fraction of root biomass of type j
 respired per day at 0 bars soil water potential
 $X_{j,i}$ = live root biomass of type j in the i th soil layer

The control parameters M_r and T_r are given by equations described in Parton, Singh, and Coleman (1978).

Crown respiration is calculated using Eq. 2.7.3b with the following modifications: crown biomass, X_5 , replaces root biomass;

soil surface temperature, Z_4 , is used to determine T ;
 and soil water potential in the top 5 cm, $Z_1(1)$, is used to determine M_r . Also, the maximum respiration rate for nonsuberized roots, R_2 , is assumed to approximate that for crowns.

2.7.1.5 Release of carbon through decomposition. The release of CO_2 during the decomposition of dead roots is described by

$$F(9_i, 0) = D_1^D \min(M_i^D, T_i^D) X_{9,i} d_i \quad , \quad (2.7.4a)$$

$$F(10_i, 0) = D_2^D \min(M_i^D, T_i^D) X_{10,i} d_i \quad , \quad (2.7.4b)$$

$$F(11_i, 0) = D_3^D \min(M_i^D, T_i^D) X_{11,i} d_i \quad , \quad (2.7.4c)$$

where

D_j^D = maximum turnover rate for dead roots of type j ,
 $X_{j,i}$ = dead root biomass of type j in the i th layer,
 d_i = depth control parameter for decomposition in the i th soil layer,
 M_i^D = soil water control parameter for decomposition in the i th soil layer,
 T_i^D = soil temperature control parameter for decomposition in the i th soil layer.

The control parameters M_i^D and T_i^D are implemented as piecewise linear approximations of the functional relationships presented by Parton, Singh, and Coleman (1978). The formulation $\min(M_i^D, T_i^D)$ indicates that only the most limiting factor, the minimum control parameter, is used to depress the maximum root turnover rate, D_j^D .

The release of CO_2 in the decomposition of aboveground litter, $F(4,0)$, is a function of litter biomass, X_4 , soil water potential in

the top soil layer, $Z_1(1)$, and soil surface temperature, Z_4 . Equation 2.7.4b is used with the assumption that maximum litter turnover resulting from decomposition is 75% of that for nonsuberized roots. We decompose dead crowns and litter mixed into the top soil layer with the same equation used for aboveground litter, with the appropriate biomass substitutions. This may be a slight deviation from Parton, Singh, and Coleman (1978), who did not explicitly describe the fate of these components.

2.7.2 Seasonal Photosynthesis and Respiration

An only slightly modified version of Parton's (1976) abiotic model was used to generate driving variables for the simulation model. Parameters for the abiotic model were taken from Parton (1976), Parton and Singh (1976), and Parton (1978). Input data for the abiotic model were extracted from various US/IBP Grassland Biome Technical Reports and a climatic atlas of the United States (U.S. Department of Commerce 1968). When daily input values were called for, they were interpolated from monthly means using a piecewise-linear spline function. Daily rainfall was an exception and was obtained by dividing the appropriate mean monthly rainfall by the number of days in the month. The input data were generally long-term averages, and they permitted simulation of seasonal total stand photosynthesis and respiration values for an "average" year. A plot of daily fluxes sampled at weekly intervals is shown in Fig. 2.7.2. Biomass fluxes generated by the model were converted to CO_2 fluxes using a conversion factor of 1 g dry matter = 1.467 g CO_2 (Brown and Trlica 1974). Seasonal net CO_2

ORNL-DWG 85-14332

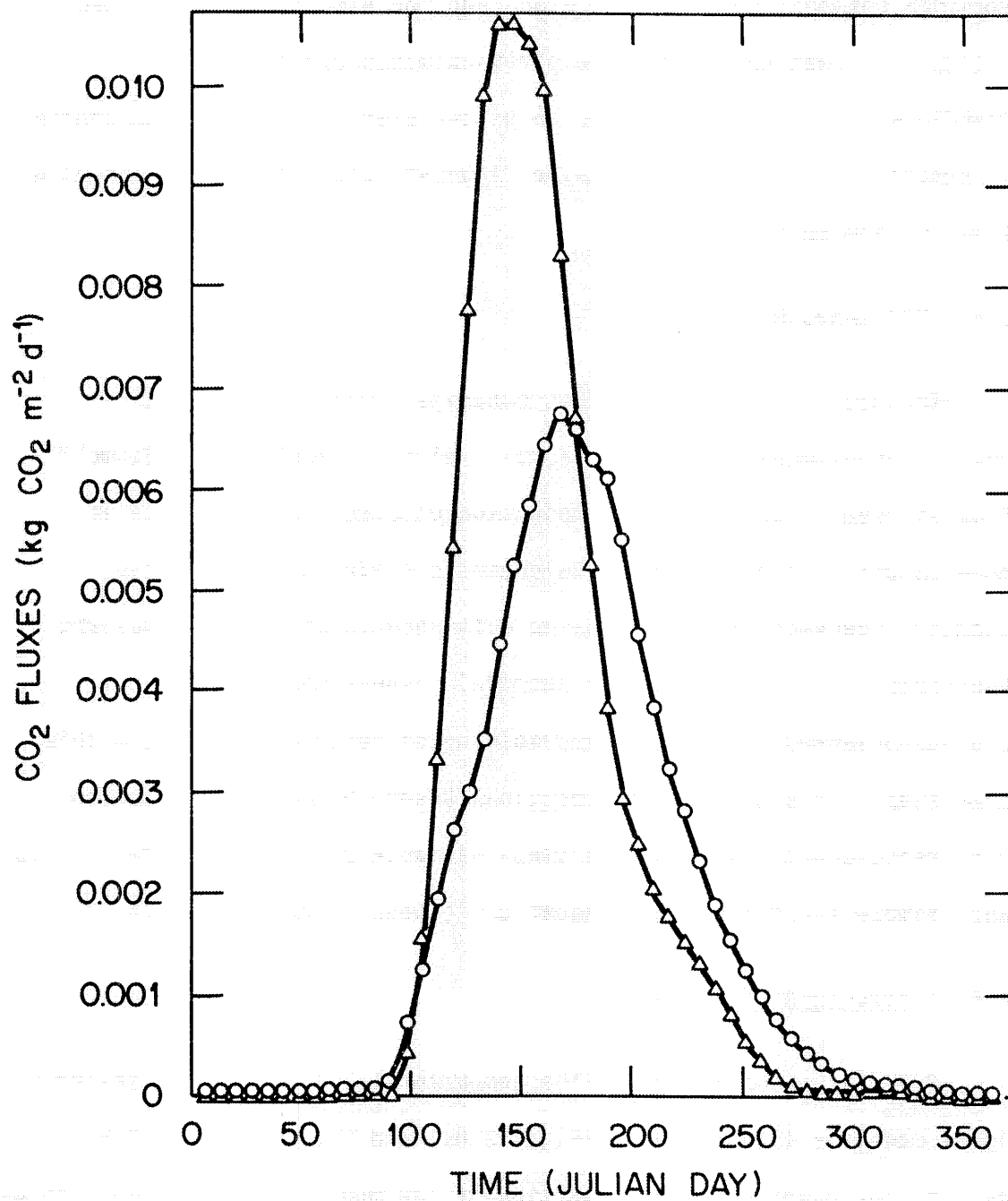


Fig. 2.7.2. Seasonal total ecosystem photosynthesis (Δ) and respiration (o) for a temperate grassland plot. Flux units are kg CO₂ m⁻² d⁻¹.

exchange between the grassland stand and the atmosphere is plotted in Fig. 2.7.3. Net exchange is respiration minus photosynthesis.

Therefore, a positive value indicates the stand is acting as a source of atmospheric CO₂; negative values indicate the stand is acting as a sink for atmospheric CO₂.

2.8 ARID LANDS MODEL

The model of seasonal carbon dynamics in arid lands is an adaptation of models developed as part of the US/IBP Desert Biome Program (see Goodall 1981). Production or carbon assimilation is modeled with an adaptation of Valentine's (1974) plant processes submodel; decomposition is modeled with an adaptation of Parnas and Radford's (1974) decomposition submodel. These mechanistic process-oriented models are described by difference equations with a time step of one day. In the original Desert Biome implementation, difference equations with time steps variable by submodel were used to approximate the differential equations (Goodall and Gist 1973).

2.8.1 Structure of the Model

2.8.1.1. Compartments. The compartmental structure of the arid lands model is illustrated in Figs. 2.8.1 and 2.8.2. Figure 2.8.1 depicts the plant production portion of the model, and Fig. 2.8.2 shows the structure of the decomposition submodel. The compartments of Fig. 2.8.1 are repeated for three functional plant groups (i.e., annuals, perennial herbs, and woody shrubs), and dry matter within each compartment is divided into nitrogen, ash, protein carbon, reserve

ORNL-DWG 85-14333

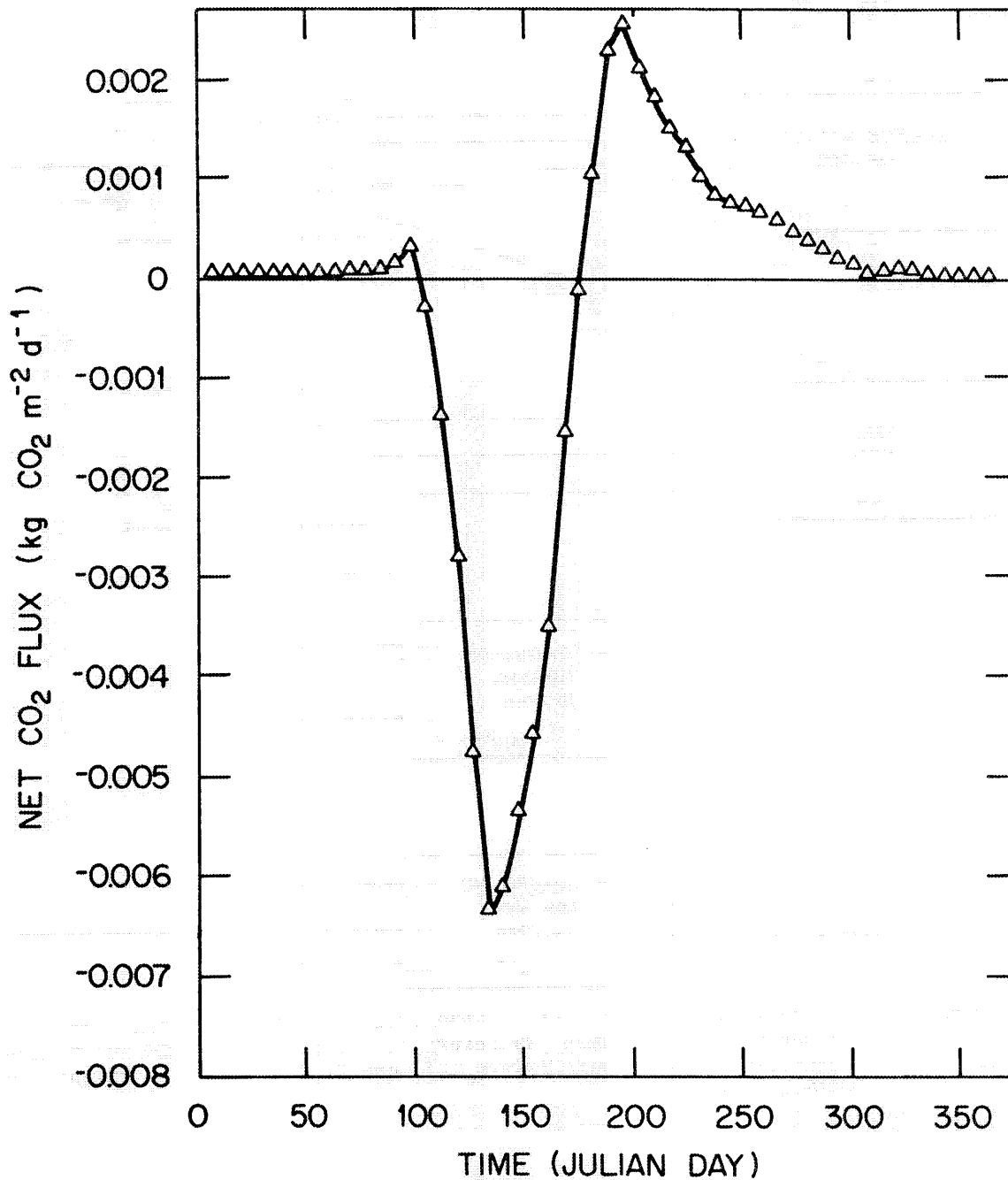


Fig. 2.7.3. Seasonal net CO₂ exchange between the atmosphere and a temperate grassland plot. Net flux is respiration minus photosynthesis. Flux units are kg CO₂ m⁻² d⁻¹.

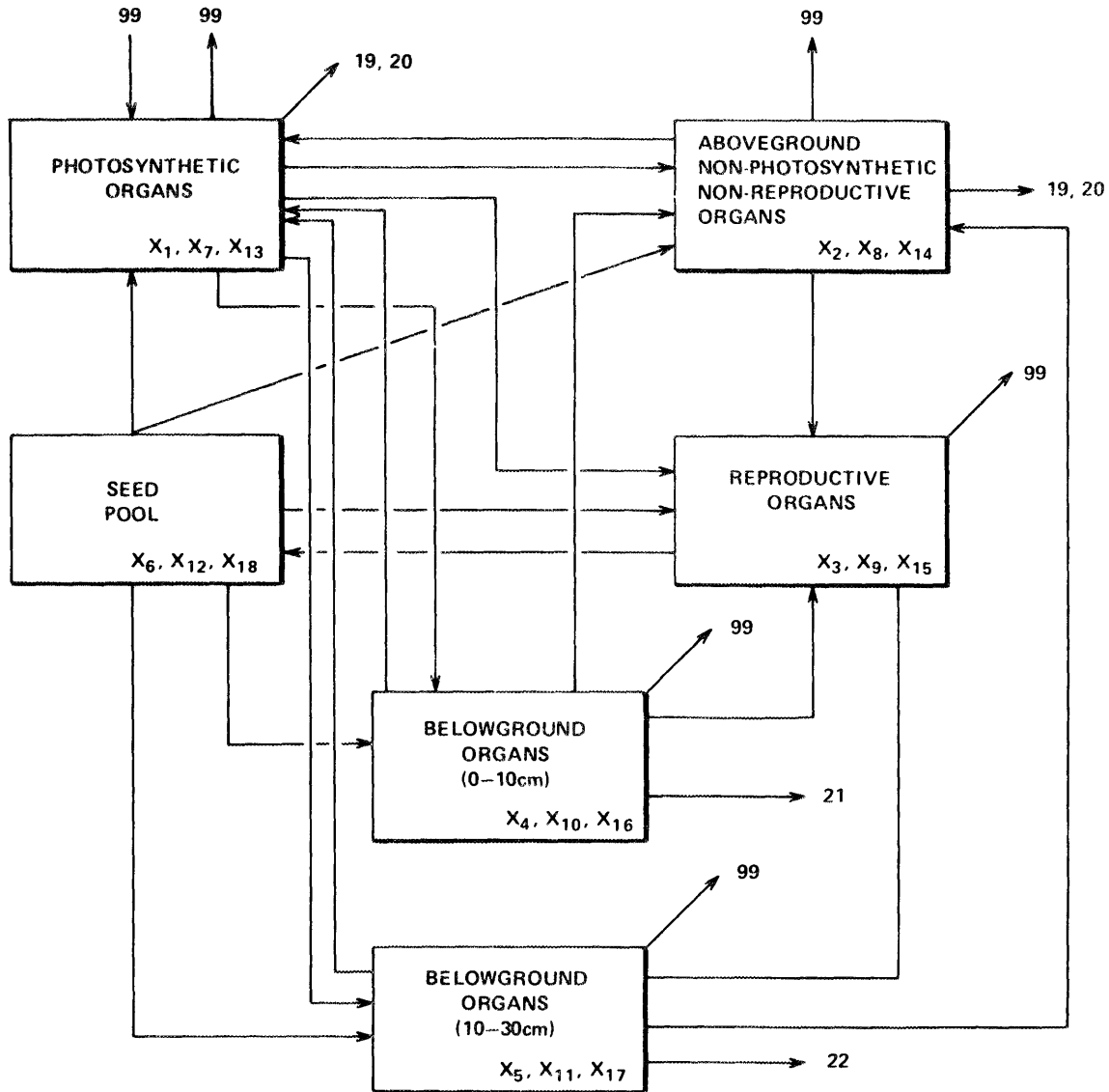


Fig. 2.8.1. Compartmental structure of the arid lands model - production submodel. The number 99 refers to a compartment external to the system. The numbers 19, 20, 21, and 22 refer to compartments in Fig. 2.8.2.

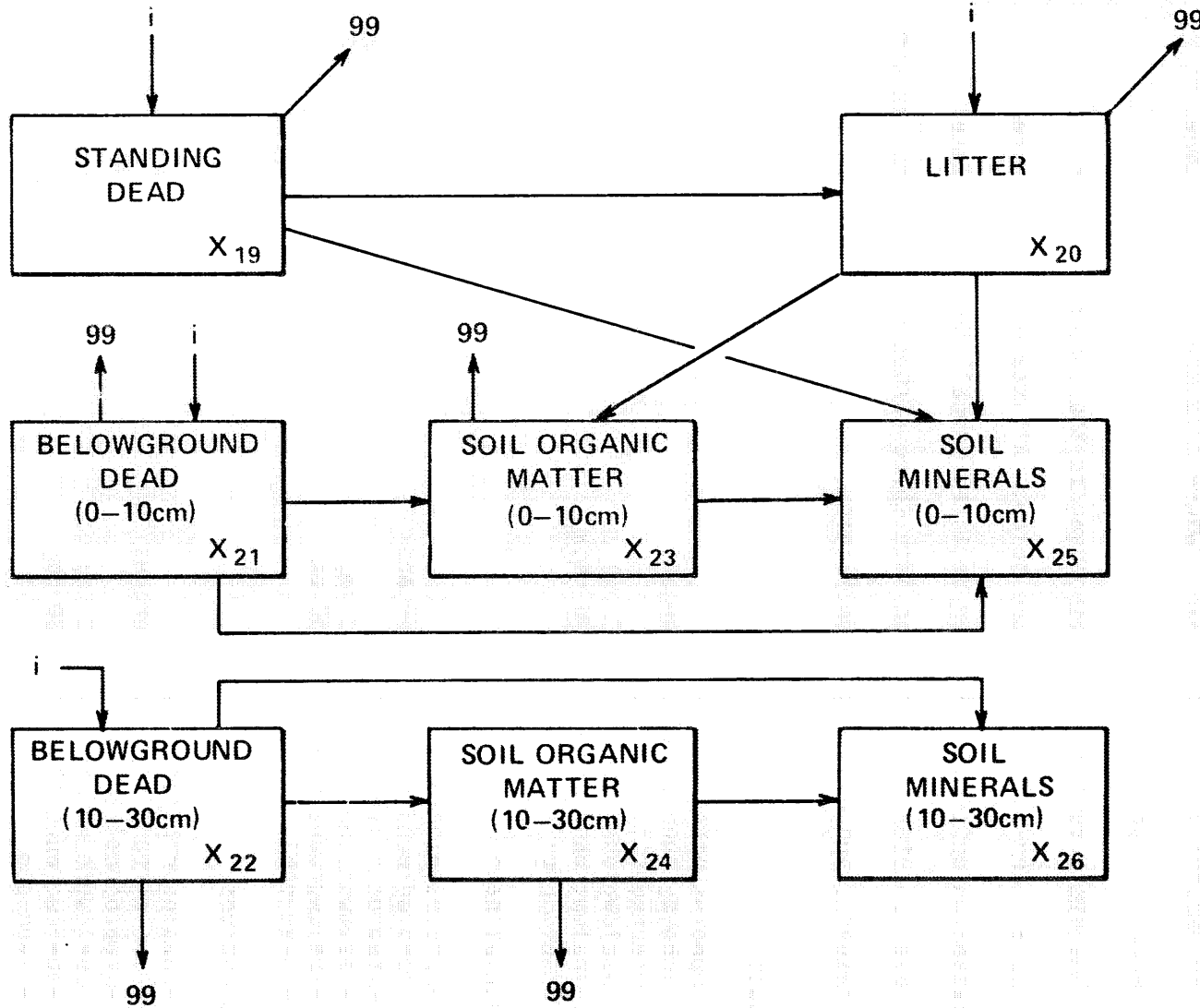


Fig. 2.8.2. Compartmental structure of the arid lands model - decomposition submodel. The $F(i,j)$'s indicate the flux of biomass from compartment i to compartment j . The number 99 indicates a compartment external to the system; the letter i refers to source compartments in Fig. 2.8.1.

carbon, and structural carbon. Similarly, the dead organic material of Fig. 2.8.2 is also divided into these five constituents. The biomass of n decomposer groups is modeled, where n is equal to the number of dead material types.

The state variables corresponding to the compartments of Figs. 2.8.1 and 2.8.2 are listed below. All state variables are expressed in units of grams per hectare. Recall that each state variable is actually subdivided into three carbon constituents, an ash constituent, and a nitrogen constituent.

annuals

- X_1 - photosynthetic organs
- X_2 - aboveground structural organs
- X_3 - reproductive organs
- X_4 - belowground organs (0-10 cm)
- X_5 - belowground organs (10-30 cm)
- X_6 - seed pool

perennial herbs

- X_7 - photosynthetic organs
- X_8 - aboveground structural organs
- X_9 - reproductive organs
- X_{10} - belowground organs (0-10 cm)
- X_{11} - belowground organs (10-30 cm)
- X_{12} - seed pool

Woody shrubs

- X_{13} - photosynthetic organs
- X_{14} - aboveground structural organs
- X_{15} - reproductive organs
- X_{16} - belowground organs (0-10 cm)
- X_{17} - belowground organs (10-30 cm)
- X_{18} - seed pool

The state variables (measured in grams per hectare) corresponding to the litter and belowground compartments of Fig. 2.8.2 are listed below. Again, each organic matter state variable is subdivided into

five constituents: protein carbon, reserve carbon, structural carbon, nitrogen, and ash. The soil mineral compartments contain nitrogen and ash.

- X₁₉ - standing dead
- X₂₀ - litter
- X₂₁ - belowground dead (0-10 cm)
- X₂₂ - belowground dead (10-30 cm)
- X₂₃ - soil organic matter (0-10 cm)
- X₂₄ - soil organic matter (10-30 cm)
- X₂₅ - soil minerals (0-10 cm)
- X₂₆ - soil minerals (10-30 cm)

Not shown in Fig. 2.8.2, for the sake of clarity, are compartments or state variables representing decomposer biomass. There is a specific decomposer group associated with each soil horizon, the standing dead, and the litter. These state variables (grams per hectare) are:

- X₂₇ - decomposers of standing dead
- X₂₈ - decomposers of litter
- X₂₉ - decomposers of the upper (0-10 cm) soil horizon
- X₃₀ - decomposers of the lower (10-30 cm) soil horizon

2.8.1.2 Driving variables. Most processes in the model are described mechanistically and involve a number of exogenous driving variables:

- Z₁(i) - soil temperature in the ith soil horizon (°C)
- Z₂(i) - soil water potential in the ith soil horizon (bars)
- Z₃ - mean daytime air temperature (°C)
- Z₄ - mean nighttime air temperature (°C)
- Z₅ - photoperiod (h)
- Z₆ - precipitation (mm)
- Z₇ - solar radiation (cal cm⁻²-d⁻¹)

Driving variables calculated within the model include:

Z_8 - current phenological stage (nondimensional)
 $Z_9(i)$ - soil nitrogen concentration in the i th soil horizon
($\text{g/ha}^{-1}/\text{mm}^{-1}$)

Driving variables Z_3 to Z_7 are incorporated as daily inputs to the simulation program. Variables $Z_1(i)$ and $Z_2(i)$ are determined by a soils subroutine.

2.8.1.3 Flows or rate processes. The arrows in Figs. 2.8.1 and 2.8.2 represent the flux of chemical constituents between components of the model. Many of these fluxes are described by equations relating a flux rate to various combinations of driving variables and carbon concentrations. These functions are generally too complex to be adequately described in the limited scope of this report. We only define the model fluxes; full details can be found in Valentine (1974) and Parnas and Radford (1974). The notation $F(i,j)$ indicates the flow of constituent material from compartment i to compartment j . The number 99 indicates a source/sink external to the system. All flows into the system are labeled $F(99,j)$; all flows out of the system are labeled $F(i,99)$. Some flows involve all four of the motile constituents (storage carbon is not transferred), others involve only CO_2 carbon or reserve carbon. The fluxes labeled $F(i,j)^*$ involve only CO_2 carbon; those labeled $F(i,j)^{**}$ involve only reserve carbon. The flows without asterisks involve all four motile constituents (i.e., nitrogen, ash, protein carbon, and reserve carbon).

Production Subsystem (Fig. 2.8.1)

Annuals

- F(99,1)* - net daytime photosynthesis
- F(1,2)** - translocation from leaves to structural organs
- F(1,3)** - translocation from leaves to reproductive organs
- F(1,4)** - translocation from leaves to belowground organs in the upper soil horizon
- F(1,5)** - translocation from leaves to belowground organs in the lower soil horizon
- F(1,19) - transfer of dead leaves to standing dead
- F(1,20) - transfer of dead leaves to litter
- F(1,99)* - leaf respiration
- F(2,19) - transfer of dead structural parts to standing dead
- F(2,20) - transfer of dead structural parts to litter
- F(2,99)* - structural organ respiration
- F(3,6) - seed shedding
- F(3,99)* - reproductive organ respiration
- F(4,21) - root mortality in the upper soil horizon
- F(4,99)* - root respiration from the upper soil horizon
- F(5,22) - root mortality in the lower soil horizon
- F(5,99)* - root respiration from the lower soil horizon
- F(6,1) - seed germination
- F(6,2) - seed germination
- F(6,3) - seed germination
- F(6,4) - seed germination
- F(6,5) - seed germination

Perennial herbs

- F(99,7)* - net daytime photosynthesis
- F(7,8)** - translocation from leaves to structural organs
- F(7,9)** - translocation from leaves to reproductive organs
- F(7,10)** - translocation from leaves to belowground organs in the upper soil horizon
- F(7,11)** - translocation from leaves to belowground organs in the lower soil horizon
- F(7,19) - transfer of dead leaves to standing dead
- F(7,20) - transfer of dead leaves to litter
- F(7,99)* - leaf respiration
- F(8,19) - transfer of dead structural parts to standing dead
- F(8,20) - transfer of dead structural parts to litter
- F(8,99)* - structural organ respiration
- F(9,12) - seed shedding
- F(9,99)* - reproductive organ respiration

F(10,7) - translocation during leafing out
 F(10,8) - translocation during leafing out
 F(10,9) - translocation during leafing out
 F(10,21) - root mortality in the upper soil horizon
 F(10,99)* - root respiration from the upper soil horizon
 F(11,7) - translocation during leafing out
 F(11,8) - translocation during leafing out
 F(11,9) - translocation during leafing out
 F(11,22) - root mortality in the lower soil horizon
 F(11,99)* - root respiration from the lower soil horizon
 F(12,7) - seed germination
 F(12,8) - seed germination
 F(12,9) - seed germination
 F(12,10) - seed germination
 F(12,11) - seed germination

Woody shrubs

F(99,13)* - net daytime photosynthesis
 F(13,14)** - translocation from leaves to structural organs
 F(13,15)** - translocation from leaves to reproductive organs
 F(13,16)** - translocation from leaves to belowground organs in the upper soil horizon
 F(13,17)** - translocation from leaves to belowground organs in the lower soil horizon
 F(13,19)** - transfer of dead leaves to standing dead
 F(13,20) - transfer of dead leaves to litter
 F(13,99) - leaf respiration
 F(14,13) - translocation during leafing out
 F(14,15) - translocation during leafing out
 F(14,19) - transfer of dead structural parts to standing dead
 F(14,20) - transfer of dead structural parts to litter
 F(14,99)* - structural organ respiration
 F(15,18) - seed shedding
 F(15,99)* - reproductive organ respiration
 F(16,13) - translocation during leafing out
 F(16,15) - translocation during leafing out
 F(16,21) - root mortality in the upper soil horizon
 F(16,99)* - root respiration from the upper soil horizon
 F(17,13) - translocation during leafing out
 F(17,15) - translocation during leafing out
 F(17,22) - root mortality in the lower soil horizon
 F(17,99)* - root respiration from the lower soil horizon
 F(18,13) - seed germination
 F(18,14) - seed germination
 F(18,15) - seed germination
 F(18,16) - seed germination
 F(18,17) - seed germination

Within each plant organ compartment there are three carbon subcompartments. The subcompartments are illustrated in Fig. 2.8.3. The possible fluxes between carbon fractions are indicated by labeled arrows in Fig. 2.8.3 and are defined as.

- $f(p,r)$ - allocation of carbon to reserve pool after protein synthesis is provided for
- $f(r,p)$ - allocation of reserve carbon to protein carbon for protein synthesis
- $f(r,s)$ - allocation of reserve carbon to structural carbon

Decomposition Subsystem (Fig. 2.8.2)

- $F(i,19)$ - input of dead organic matter to standing dead
- $F(19,25)$ - mineralization of nitrogen from standing dead
- $F(19,25)$ - mineralization of ash from standing dead
- $F(19,99)^*$ - decomposer respiration from standing dead
- $F(i,20)$ - input of dead organic matter to litter
- $F(20,23)$ - external breakdown of litter
- $F(20,25)$ - mineralization of nitrogen from litter
- $F(20,25)$ - mineralization of ash from litter
- $F(20,99)^*$ - decomposer respiration from litter
- $F(i,21)$ - input of dead organic matter to belowground dead in the upper soil horizon
- $F(21,23)$ - external breakdown of belowground dead in the upper soil horizon
- $F(21,25)$ - mineralization of nitrogen from belowground dead in the upper soil horizon
- $F(21,25)$ - mineralization of ash from belowground dead in the upper soil horizon
- $F(21,99)^*$ - decomposer respiration from belowground dead in the upper soil horizon
- $F(i,22)$ - input of dead organic matter to belowground dead in the lower soil horizon
- $F(22,24)$ - external breakdown of belowground dead in the lower soil horizon
- $F(22,26)$ - mineralization of nitrogen from belowground in the lower soil horizon
- $F(22,26)$ - mineralization of ash from belowground dead in the lower soil horizon
- $F(22,99)^*$ - decomposer respiration from belowground dead in the lower soil horizon
- $F(23,25)$ - mineralization of nitrogen from the soil organic matter of the upper soil horizon
- $F(23,25)$ - mineralization of ash from the soil organic matter of the upper soil horizon

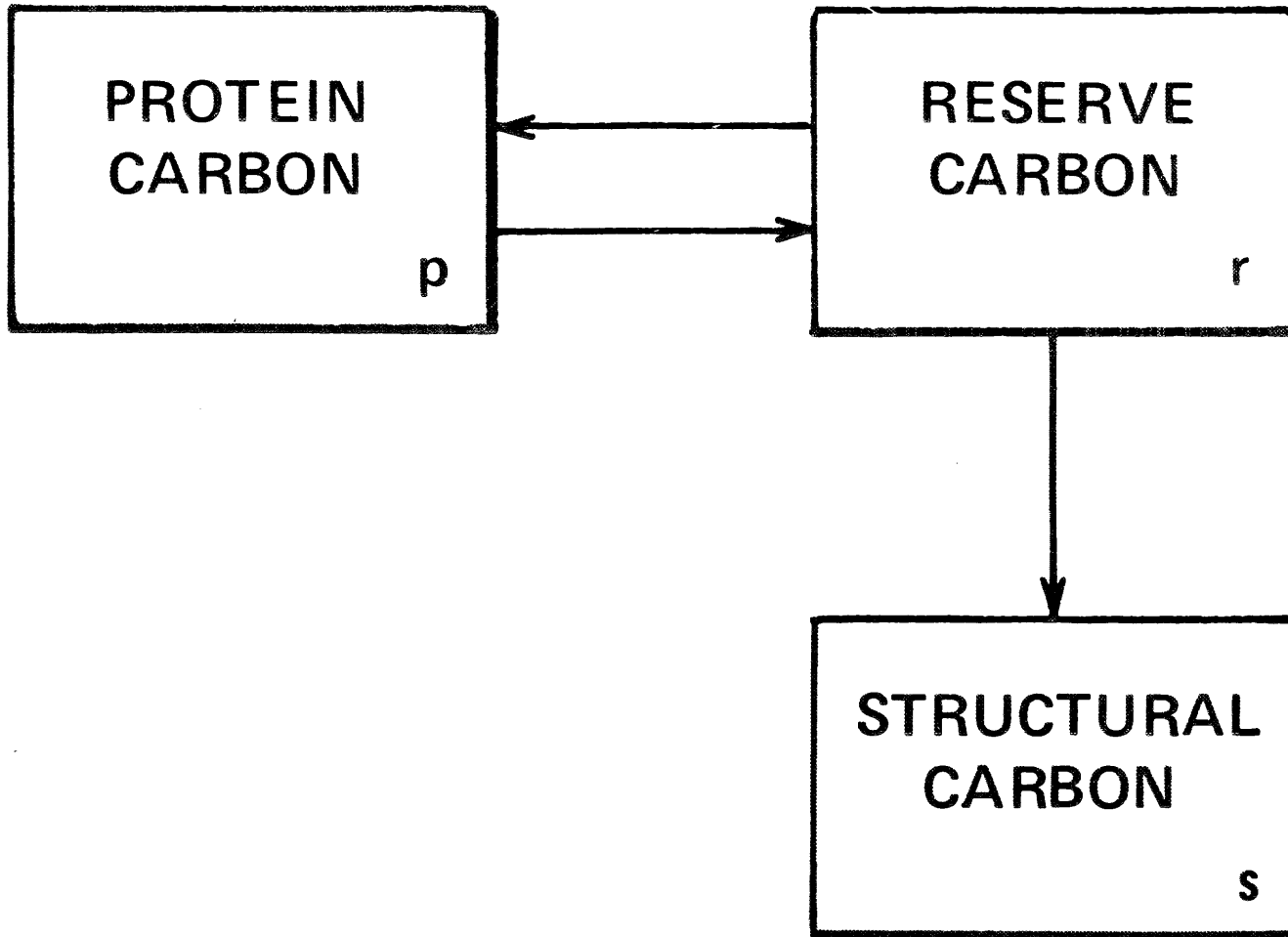


Fig. 2.8.3. Compartmental representation of carbon components in living plant compartments of the arid lands model. The arrows represent the transformation of carbon from one form to another.

- F(23,99) - decomposer respiration from the soil organic matter of the upper soil horizon
- F(24,26) - mineralization of nitrogen from the soil organic matter of the lower soil horizon
- F(24,26) - mineralization of ash from the soil organic matter of the lower soil horizon
- F(24,99)* - decomposer respiration from the soil organic matter of the lower soil horizon

Decomposers are associated with the standing dead, litter, belowground dead, and soil organic matter compartments of Fig. 2.8.2. These are not depicted in the figure for the sake of clarity. The flows between decomposers, substrate, and material sink not included in Fig. 2.8.2 are defined as:

- F(19,27) - assimilation of standing dead material by the standing dead decomposers
- F(20,28) - assimilation of litter material by litter decomposers
- F(21,29) - assimilation of upper soil horizon belowground dead by decomposers of the upper soil horizon
- F(22,23) - assimilation of lower soil horizon belowground dead by decomposers of the lower soil horizon
- F(23,29) - assimilation of upper soil horizon soil organic matter by decomposers of the upper soil horizon
- F(24,30) - assimilation of lower soil horizon soil organic matter by decomposers of the lower soil horizon
- F(25,28) - nitrogen immobilization by litter decomposers
- F(25,29) - nitrogen immobilization by decomposers of the upper soil horizon
- F(26,30) - nitrogen immobilization by decomposers of the lower soil horizon
- F(27,19) - death of standing dead decomposers
- F(28,20) - death of litter decomposers
- F(29,23) - death of upper soil horizon decomposers
- F(30,24) - death of lower soil horizon decomposers

2.8.1.4 Photosynthesis and respiration. The model computes a mean hourly rate of net daytime carbon fixation. This net daytime photosynthesis is a function of mean daytime air temperature (Z_3),

mean hourly irradiance for the day (Z_7'), and mean weighted soil water potential (Z_2'), or

$$P_H = P_{HMAX} \times f_1(Z_3) \times f_2(Z_7') \times f_3(Z_2') \quad , \quad (2.8.1)$$

where

P_H = realized hourly rate of net photosynthesis
(g C g⁻¹ protein C h⁻¹),
 P_{HMAX} = optimal hourly rate of net photosynthesis
(g C g⁻¹ protein C h⁻¹),
 $f_1(Z_3)$ = effect of air temperature (dimensionless),
 $f_2(Z_7')$ = effect of irradiance (dimensionless),
 $f_3(Z_2')$ = effect of soil water (dimensionless).

The functional forms for f_1 , f_2 , and f_3 can be found in Valentine (1974) and Goodall (1981). The model allows for changes in P_{HMAX} and optimal temperature (Z_3 where $f_1(Z_3) = 1.0$) as a result of acclimatization (see Valentine 1974).

The daily net photosynthesis rate (g C g⁻¹ protein C d⁻¹) is given by

$$P_D = P_H Z_5 \quad , \quad (2.8.2)$$

where Z_5 is the photoperiod. The amount of carbon actually fixed per day (PN) is

$$PN = P_D X_{Ip} \quad , \quad (2.8.3)$$

where X_{Ip} is the amount of protein carbon (grams per hectare) in the photosynthetic organs. Equations (2.8.1), (2.8.2), and (2.8.3) are applied to annuals, perennial herbs, and woody shrubs. Constants such as P_{HMAX} may vary with plant type, and X_{Ip} is replaced by X_{1p} , X_{7p} , and X_{13p} .

Hourly rates of respiration for photosynthetic organs are averages over dark hours. Hourly rates of respiration for nonphotosynthetic organs are averages over a 24-h period. Respiration rates for the organs of each plant type are calculated as functions of air temperature (soil temperature for roots) and soil water potential using equations of the form

$$R_H(j) = [a_1(j) + a_2(j)\exp(a_3(j)T)]f_4(W) \quad , \quad (2.8.4)$$

where

- $R_H(j)$ = hourly respiration rate of the j th organ
 (g C g⁻¹ reserve C h⁻¹),
 $a_1(j)$ - $a_3(j)$ = rate parameters,
 T = temperature (°C; air temperature for
 aboveground organs, soil temperature for
 belowground organs adjusted for acclimation,
 $f_4(W)$ = the effect of soil water potential
 (dimensionless)
 W = soil water potential (bars) of the horizon
 appropriate for organ j .

The functional form of $f_4(W)$ is described in Valentine (1974) and Goodall (1981). Daily rates and amounts of carbon respired are obtained by the appropriate transformations.

2.8.1.5 Release of carbon through decomposition. Carbon dioxide is released during decomposition through decomposer respiration. The rate of carbon release via microbial decomposition is

$$R_m = \sum_C (\sum_T r_{ic}) \quad , \quad (2.8.5)$$

where

- R_m = rate of carbon release (g C ha⁻¹d⁻¹),
 \sum_C = summation over all carbon types,

\sum = summation over all dead organic matter compartments,
 r_{ic} = rate of respiration of carbon type c from decomposition
of dead organic matter type i ($\text{g C ha}^{-1} \text{d}^{-1}$).

The rate r_{ic} is given by

$$r_{ic} = (1 - e)D_{ic} \quad , \quad (2.8.6)$$

where e is the efficiency of microbial assimilation (dimensionless), and D_{ic} is the rate of decomposition of carbon type c in dead organic matter type i.

2.8.2 Seasonal Photosynthesis and Respiration

Input data for the forcing functions were generated by a subroutine provided by Valentine (1974) as a temporary means of generating exogenous values. A more detailed, empirical subroutine is provided by Goodall and Gist (1973). The driving variables permitted simulation of seasonal total ecosystem (less live plant consumers) photosynthesis and respiration. A plot of daily fluxes, sampled weekly, is shown in Fig. 2.8.4. Carbon fluxes were converted to CO_2 fluxes using a conversion factor of $1 \text{ g C} = 3.66 \text{ g CO}_2$ (Brown and Trlica 1974). Seasonal net CO_2 exchange (respiration minus photosynthesis) between the vegetation and the atmosphere is plotted in Fig. 2.8.5. Positive net exchange values indicate the vegetation is acting as a source of atmospheric CO_2 ; negative values indicate the vegetation is acting as a sink.

2.9 TUNDRA MODEL

A general model of biomass decomposition, ABISCO, was developed by Bunnell and Dowding (1974) to compare tundra sites. Later, the model

ORNL-DWG 85-17014

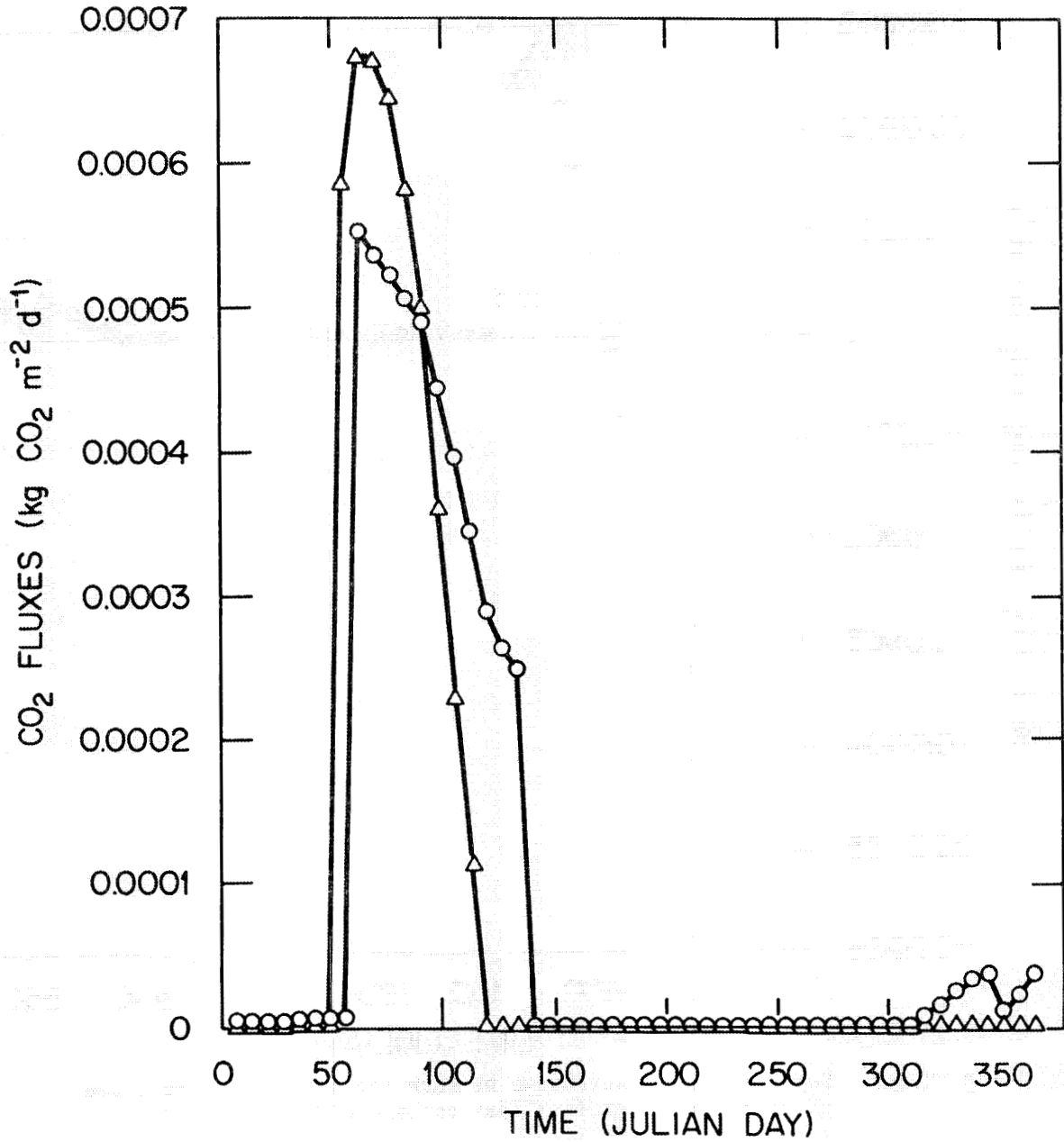


Fig. 2.8.4. Seasonal total ecosystem photosynthesis (Δ) and respiration (o) for a stand of arid land vegetation. Flux units are $\text{kg CO}_2 \text{ m}^{-2} \text{ d}^{-1}$.

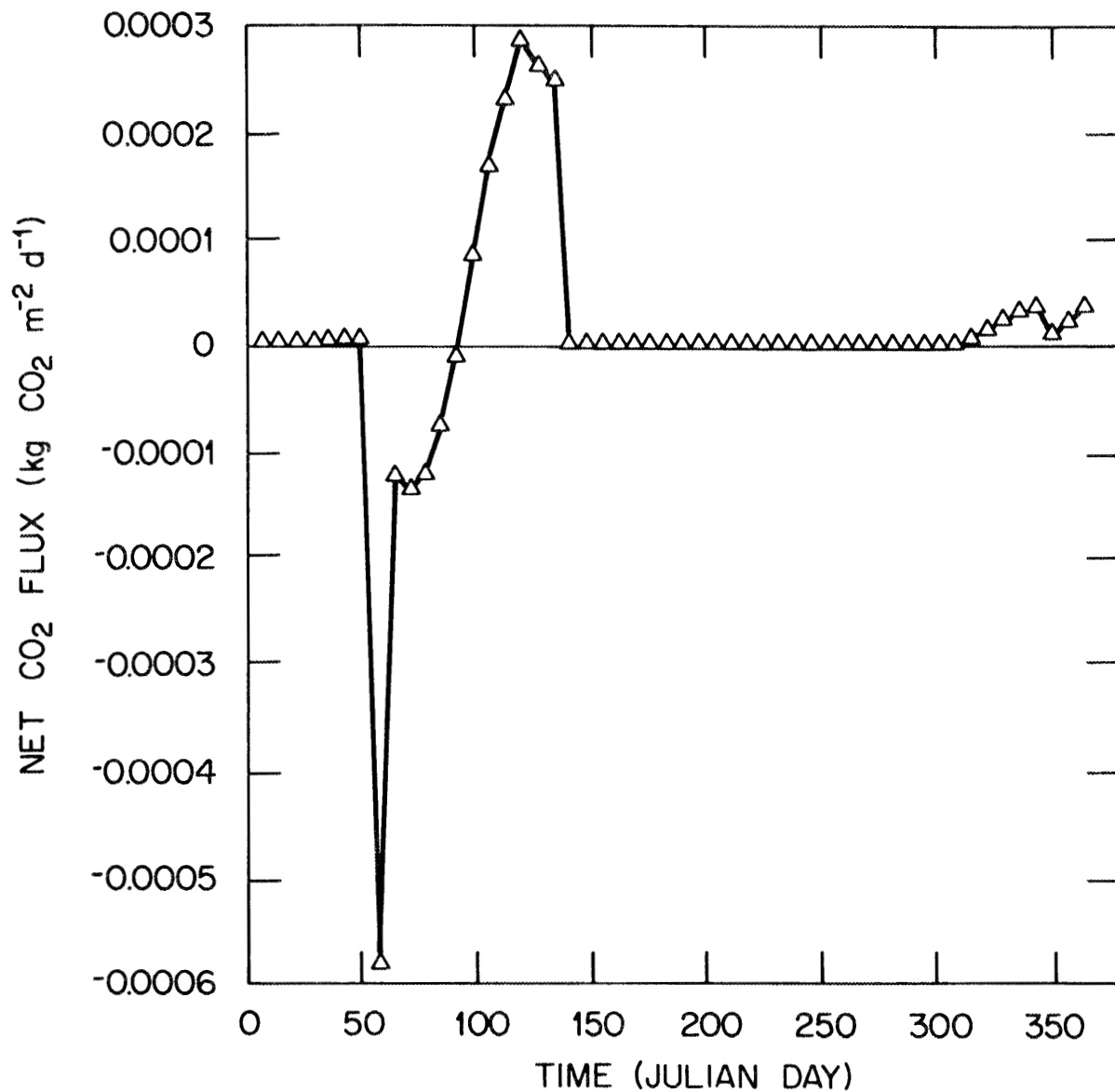


Fig. 2.8.5. Seasonal net CO₂ exchange between the atmosphere and a stand of arid land vegetation flux units are kg CO₂ m⁻² d⁻¹.

was extended by Bunnell and Scoullar (1975) to provide a fairly complete description of tundra biomass dynamics, and was renamed ABISCO II. The model is oriented towards a detailed description of microbial respiration and photosynthesis.

2.9.1 Structure of the Model

2.9.1.1 Compartments. The compartmental structure of the model is shown in Fig. 2.9.1. The state variables corresponding to the compartments are defined as (values are in units of g biomass/m²):

- X₁ - aboveground live biomass
- X₂ - green litter
- X₃ - old standing dead biomass
- X₄ - litter
- X₅ - soil organic matter
- X₆ - live rhizomes and stem bases
- X₇ - dead roots and rhizomes
- X₈ - soil humus
- X₉ - herbivores
- X₁₀ - feces
- X₁₁ - new standing dead biomass
- X₁₂ - leachate
- X₁₃ - live roots

2.9.1.2 Driving variables. There are three exogenous driving variables in the model:

- Z₁ - temperature (°C)
- Z₂ - relative sunlight intensity (langleys)
- Z₃ - percent moisture level of the substrate

The values of Z₁, Z₂, and Z₃ in the model can be specified on a daily basis in the model.

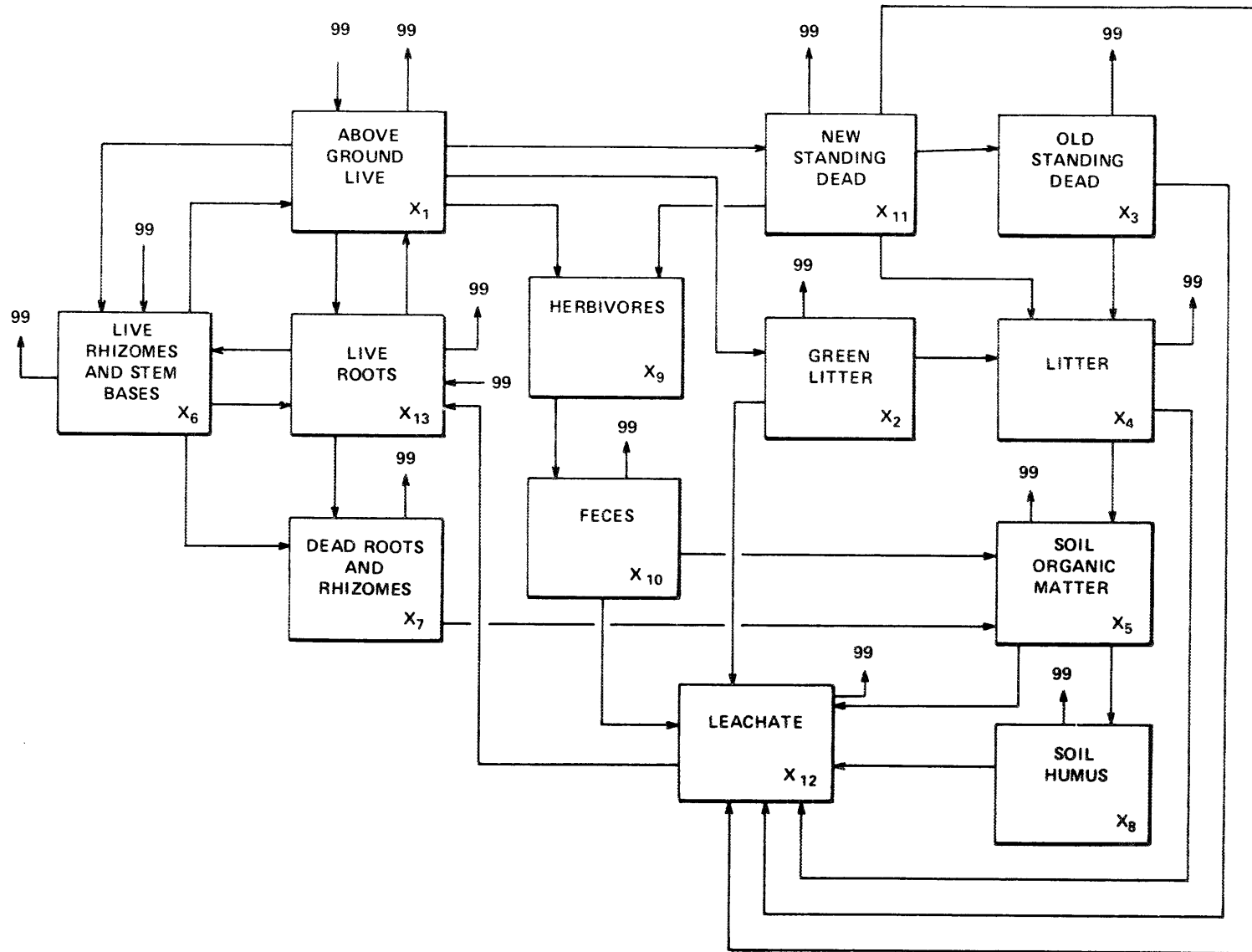


Fig. 2.9.1. Compartmental structure of the tundra model (ABISCO II). Modified from Bunnell and Scoullar (1975).

2.9.1.3. Flows or rate processes. The flows of organic matter correspond to the arrows between compartments in Fig. 2.9.1. The detailed functional representations of these flows and the assumptions involved are described in Bunnell and Scoullar (1975). The notation $F(i,j)$ indicates the flow of material from compartment i to compartment j . The number 99 refers to a compartment external to the system. All flows into the system are labeled $F(99,j)$, and all flows out of the system are labeled $F(i,99)$. In the list that follows, we present the functional forms of the fluxes, excepting photosynthesis and respiration, which are discussed in the next section. The units of the fluxes are grams biomass per square meter per day.

- $F(99,1)$ - photosynthetic input to aboveground live biomass :
 $0.7(2.8/4.3)PHOTOS$
- $F(99,6)$ - photosynthetic input to live rhizomes: $0.7(0.8/4.3)PHOTOS$
- $F(99,13)$ - photosynthetic input to live roots: $0.7(0.7/4.3)PHOTOS$
- $F(i,99)$ - respiration of compartment i , $RES_i X_i$ ($i = 1,2,\dots,13$)
- $F(6,7)$ - death rate of rhizomes: $CDR_6 X_6$
- $F(1,6)$ - translocation rate from aboveground living biomass to rhizomes: $DTH_1 CRHZ_1 X_1$
- $F(1,2)$ - transfer rates from aboveground living biomass to green litter: $DTH_1(1.0 - CRHZ_1)X_1(0.5)$
- $F(13,6)$ - translocation rate from live root to rhizomes:
 $DTH_{13} CRHZ_{13} X_{13}$
- $F(13,7)$ - transfer rate of live root to dead root biomass:
 $DTH_{13}(1.0 - CRHZ_{13})X_{13}$
- $F(1,11)$ - transfer rate from above ground living biomass to new standing dead biomass: $DTH_1(1.0 - CRHZ_1)X_1(0.5)$
- $F(5,12)$ - leaching rate of soil organic matter: $CLCH_5 X_5$
- $F(8,12)$ - leaching rate of soil humus: $CLCH_8 X_8$
- $F(2,12)$ - leaching rate of green litter: $RGLE_2 TLMOD_2 X_2$
- $F(3,12)$ - leaching rates of old standing dead biomass:
 $RGLE_3 TLMOD_3 X_3$
- $F(4,12)$ - leaching rate of litter: $RGLE_4 TLMOD_4 X_4$
- $F(11,12)$ - leaching rate of new standing dead biomass:
 $RGLE_{11} TLMOD_{11} X_{11}$
- $F(2,4)$ - transfer rate of green litter to litter:
 $[(1.0 - PGWTL)/PGWTL][RES_2 + F(2,12)]X_2$
- $F(11,3)$ - transfer rate of new standing dead to old standing dead:
 $[(1.0 - PNSDWL)/PNSDWL][RES_{11} + F(11,12)]X_{11}$

- F(6,13) - transfer rate from rhizomes to roots: $CROT_6 X_6$
- F(4,5) - transfer rate from litter to soil organic matter:
 $[(1.0 - PSDWL)/PSDWL][RES_1 + F(4,12)]X_4$
- F(5,8) - transfer rate from soil organic matter to soil biomass:
 $[(1.0 - PBGDL)/PBGDL][RES_5 + F(5,12)]X_5$

In the fluxes above,

$$RGLE_1 = \begin{cases} CLCH_i & Z_3 \geq CMXM_i \\ [(Z_3 - CMNT_i) / (CMXM_i - CMNM_i)] CLCH_i & CMXM_i < Z_3 < CMNM_i \\ 0.0 & Z_3 \leq CMNM_i \end{cases} , \quad (2.9.1)$$

$$TLMOD_i = \begin{cases} 1.0 & Z_1 \geq CMXT_i \\ (Z_1 - CMNT_i) / (CMXT_i - CMNT_i) & CMNT_i < Z_1 < CMXT_i \\ 0.0 & Z_1 \leq CMNT_i \end{cases} , \quad (2.9.2)$$

$$DTH_i = \begin{cases} 0.0 & BIOINC \geq CXAR_i \\ CDXR_i (CXAR_i - BIOINC) / (CXAR_i - CMAR_i) & CMAR_i < BIOINC < CXAR_i \\ CDXR_i & BIOINC \leq CMAR_i \end{cases} , \quad (2.9.3)$$

where BIOINC is the increment of biomass to compartment i on a given day. Also,

- RES_i = respiration per unit biomass of compartment i (see Section 2.9.1.4),
- PHOTOS = total photosynthetic production (see Section 2.9.1.4),
- and CDR_i, CRHZ_i, CLCH_i, PGWTL, PNSDWL, CROT_i, PSDWL, and PBGDL are constants.

2.9.1.4 Photosynthesis and respiration. Photosynthetic growth is expressed as

$$\text{PHOTOS} = (\text{CO1HPT})(Z_2)(\text{TEMPO})(\text{SUNLIT})X_1, \quad (2.9.4)$$

where CO1HPT is a constant (i.e., maximum photosynthetic rate); Z_2 is irradiance (langleys), and TEMPO represents the temperature effect on photosynthesis. TEMPO is given by the equation

$$\text{TEMPO} = \begin{cases} 0.0 & Z_1 \leq \text{TPMIN} \\ & \text{or } Z_1 \geq \text{TPMAX} \\ \frac{(\text{CO1HPT} - \text{TPMIN} + \text{TPOPT})(Z_1 - \text{TPMIN})}{(\text{CO1HPT} - \text{TPMIN} + \text{TPMAX} - Z_1)\text{TPOPT}} & \text{TPMIN} \leq Z_1 \leq \text{TPOPT} \\ \frac{(\text{CO1HPT} - \text{TPMIN} + \text{TPOPT})(\text{TPMAX} - Z_1)}{(\text{CO1HPT} - \text{TPMIN} + \text{TPMAX} - Z_1)\text{TPOPT}} & \text{TPOPT} < Z_1 < \text{TPMAX} \end{cases}, \quad (2.9.5)$$

where TDMIN = -2.0°C, TDMAX = 30.0°C, TDOPT = 15.0°C, and CO1HPT is constant. In Eq. (2.9.4), SUNLIT is the proportion of green biomass capable of photosynthesis, or,

$$\text{SUNLIT} = 1.0 - \left(1.0 - \frac{X_1}{\text{BTOT}}\right) \frac{X_1}{\text{BMX}}, \quad (2.9.6)$$

where

$$\text{BTOT} = X_1 + X_2 + X_3,$$

BMX = live biomass necessary for 100% interception of incoming radiation.

Respiration from live plant compartments is modeled as a temperature-dependent process. Respiration per unit live biomass, RES_i , is given by

$$RES_i = a_{3i} a_{4i}^{[(T - 10)/10]} \quad i = 1, 6, 13, \quad (2.9.7)$$

where a_{3i} is the respiration rate at 10°C; a_{4i} is the Q_{10} coefficient, and T is temperature.

2.9.1.5 Release of carbon through decomposition. Respiratory losses of CO_2 from dead plant, litter, and soil organic matter compartments, generated by microbial decomposers using the substrate as an energy source, is simulated with an explicit model of microbial respiration (Bunnell and Tait 1974). The respiration rate per unit biomass of the dead organic matter compartments, RES_i , is a function of both temperature, T , and substrate moisture, M , and is given by

$$R(T, M) = \frac{M}{a_1 + M} \left(\frac{a_2}{a_2 + M} \right) a_3 a_4^{\left(\frac{T-10}{10} \right)}, \quad (2.9.8)$$

where

- a_1 = % moisture content at which the substrate is half-saturated with water,
- a_2 = % moisture content at which half the channels are saturated and blocked with water,
- a_3 = the respiration rate that occurs at 10°C when neither oxygen nor moisture are limiting,
- a_4 = the Q_{10} coefficient.

Equation (2.9.8) is applied to compartments X_2 to X_5 , X_7 , X_8 , and X_{10} to X_{12} . The parameters a_1 , a_2 , a_3 , and a_4 are compartment specific.

2.9.2 Seasonal Photosynthesis and Respiration

Parameter values supplied by Bunnell and Scoullar (1975) were inserted in the model. Trial seasonal driving functions for radiation, Z_2 , and temperature, Z_1 , were supplied;

$$Z_1 = -3.0 + 18.0 \sin\{2\pi(t-51)/365\} \quad , \quad (2.9.9)$$

$$Z_2 = 0.5 + 0.5 \sin\{2\pi(t-80)/365\} \quad , \quad (2.9.10)$$

where t is time. The radiation level, Z_1 , has been normalized so that it reaches a maximum, 1.0 (corresponding to 665 langleys at Barrow, Alaska). A constant value of soil moisture, Z_3 , is assumed here.

A plot of total ecosystem photosynthesis and respiration values over a year is shown in Fig. 2.9.2. Biomass fluxes generated by the model ($\text{g biomass m}^{-2}\text{d}^{-1}$) were corrected to CO_2 fluxes ($\text{kg CO}_2 \text{ m}^{-2}\text{d}^{-1}$) by multiplication by $(1.65)(0.001)$. Seasonal net CO_2 exchange (respiration minus photosynthesis) between the tundra ecosystem and the atmosphere is shown in Fig. 2.9.3.

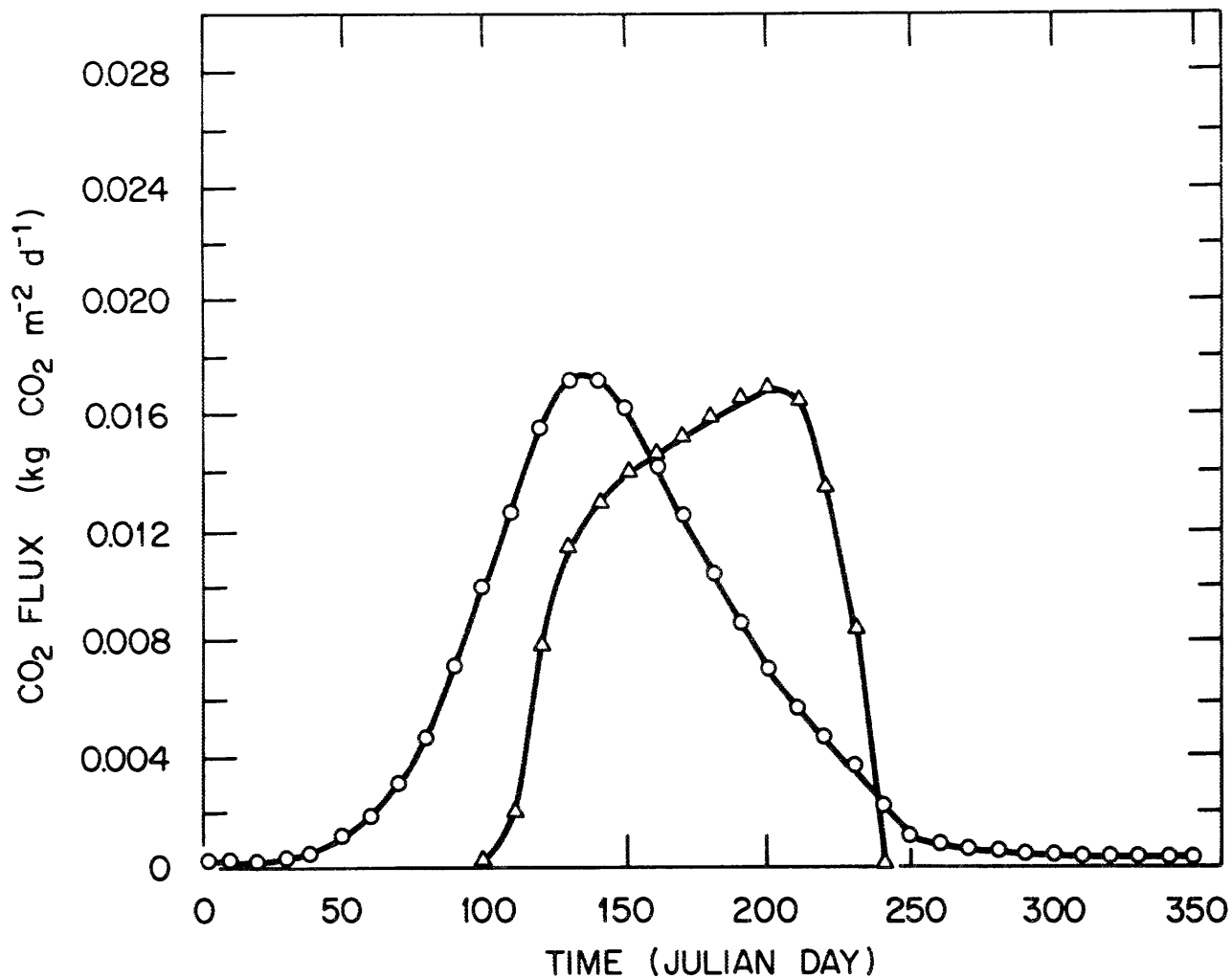


Fig. 2.9.2. Seasonal total ecosystem photosynthesis and respiration for a tundra ecosystem modeled by ABISCO II. Flux units are kg CO₂ m⁻²d⁻¹.

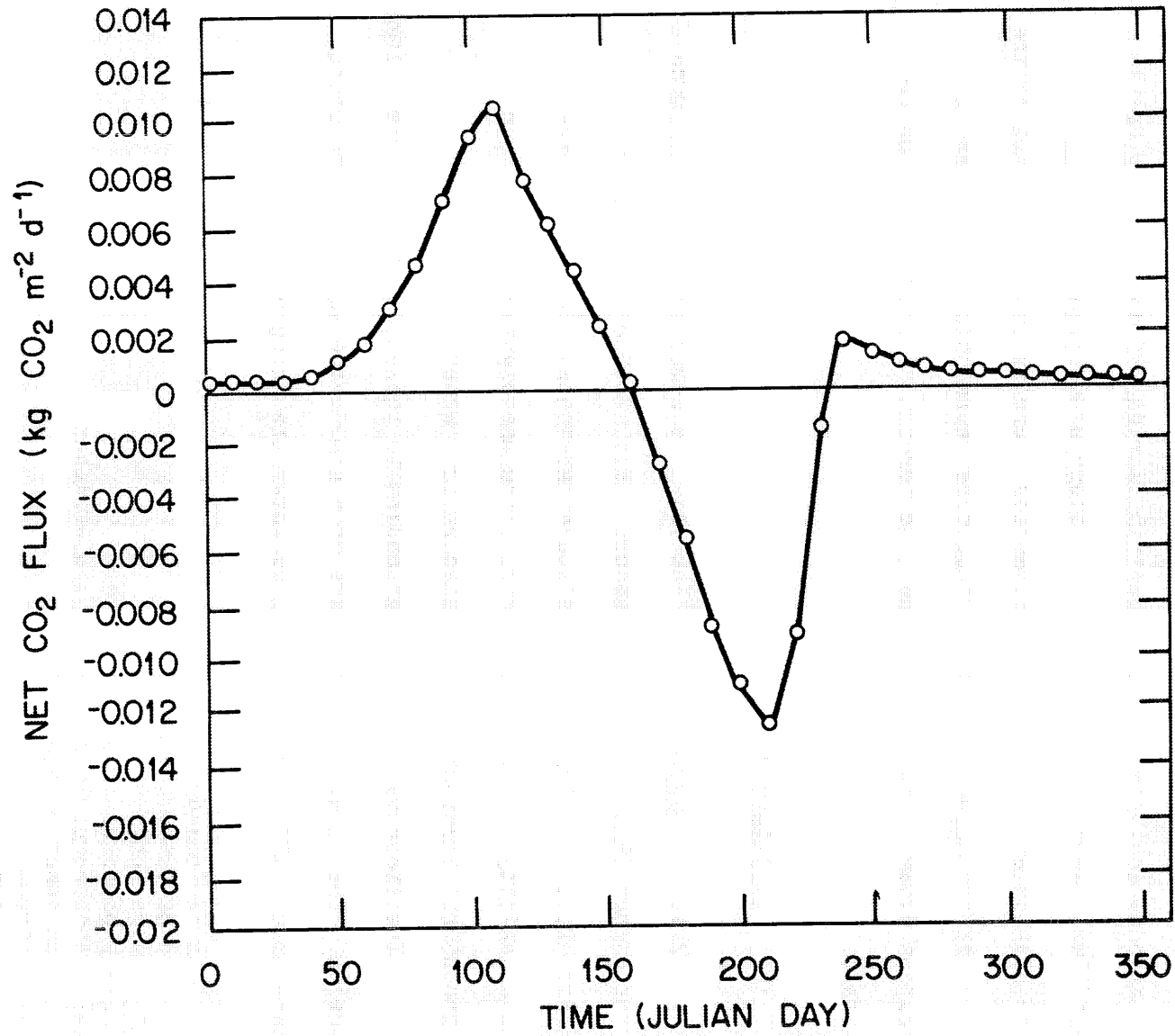


Fig. 2.9.3. Seasonal net CO₂ exchange between the atmosphere and a tundra ecosystem. Net flux is respiration minus photosynthesis. Flux units are kg CO₂ m⁻²d⁻¹.

2.10 PINE FLATWOODS MODEL

A model for carbon, phosphorus, and water cycles in a pine flatwoods ecosystem in north central florida was developed by Golkin and Ewel (1984). This system is a slash pine (*Pinus elliotii*) plantation and is typical of commercial forests that occupy 46% of the Florida landscape. The model should be representative of seasonal carbon dynamics for much of the pine forests of southeastern United States.

2.10.1 Structure of the Model

2.10.1.1 Compartments. The model is composed of three submodels for carbon (Fig. 2.10.1), phosphorus (Fig. 2.10.2), and water (Fig. 2.10.3). The three models are intricately coupled, as the availability of phosphorus controls the photosynthetic rates and phosphorus transport is regulated by soil water.

The state variables corresponding to these compartments are listed below. The values of carbon are in g C m^{-2} , the values of phosphorus are in g P m^{-2} , and the values of water are in $\text{kg H}_2\text{O m}^{-2}$.

- X₁ - pine foliage
- X₂ - pine stems and branches
- X₃ - pine roots
- X₄ - phosphorus in pine foliage
- X₅ - phosphorus in pine stems and branches
- X₆ - phosphorus in pine roots
- X₇ - shrubs
- X₈ - phosphorus in shrubs
- X₉ - herbs
- X₁₀ - phosphorus in herbs
- X₁₁ - carbon in litter and upper soil horizons

ORNL-DWG 85-14422

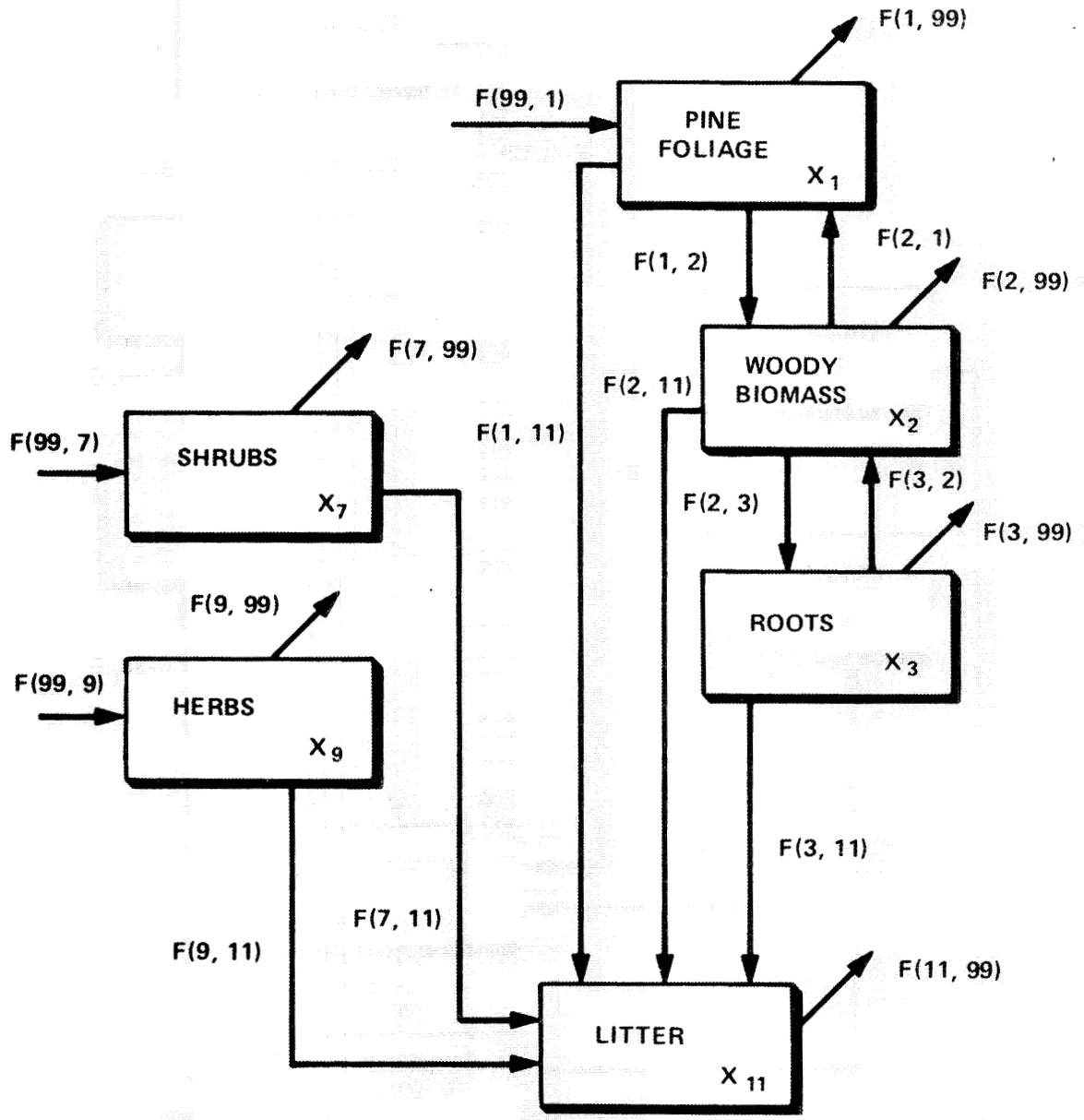


Fig. 2.10.1. Compartmental structure of pine flatwoods carbon flow submodel. Modified from Golkin and Ewel (1984).

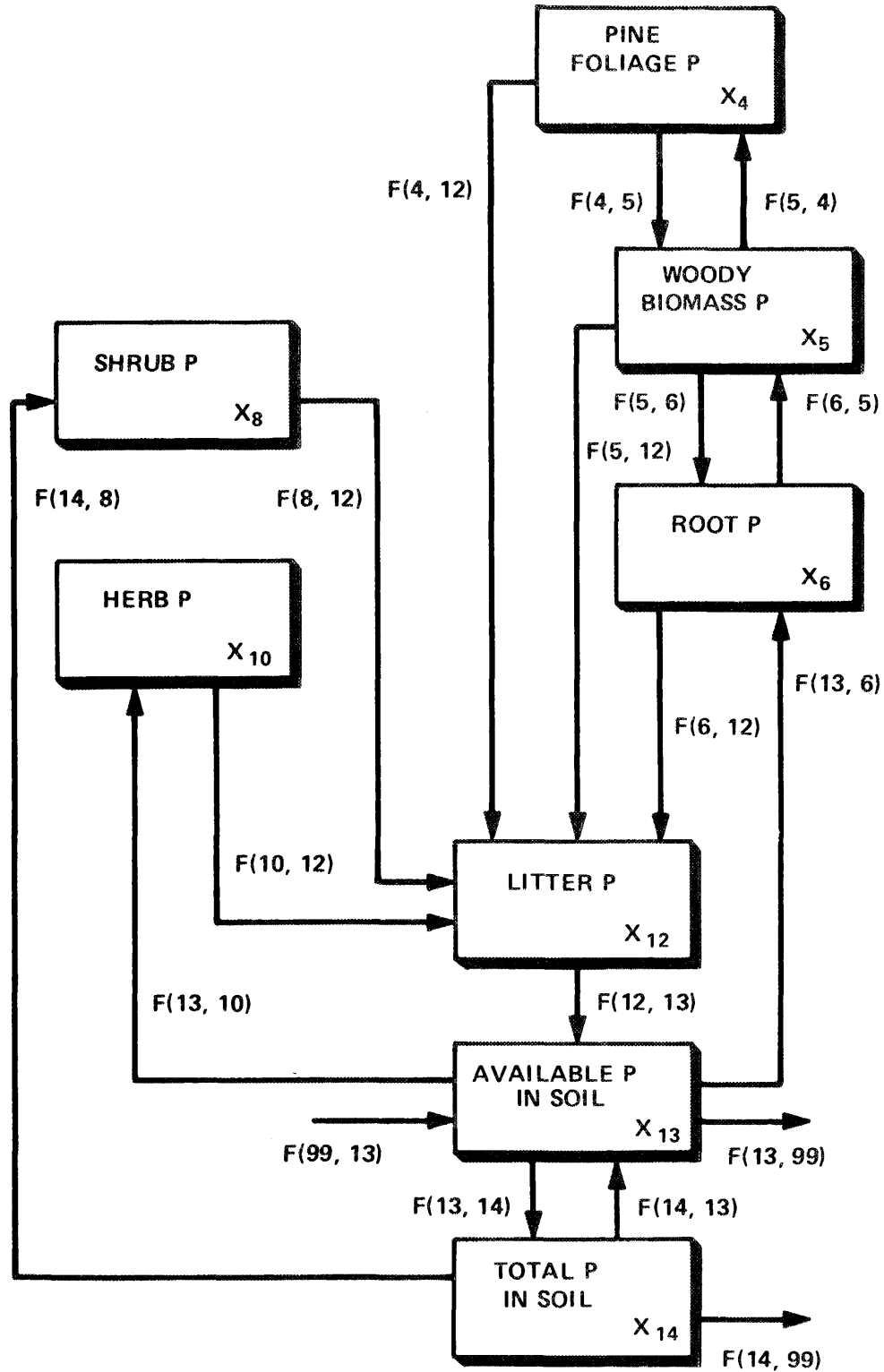


Fig. 2.10.2. Compartmental structure of pine flatwoods phosphorus cycling submodel. Modified from Golkin and Ewel (1984).

ORNL-DWG 85-14424

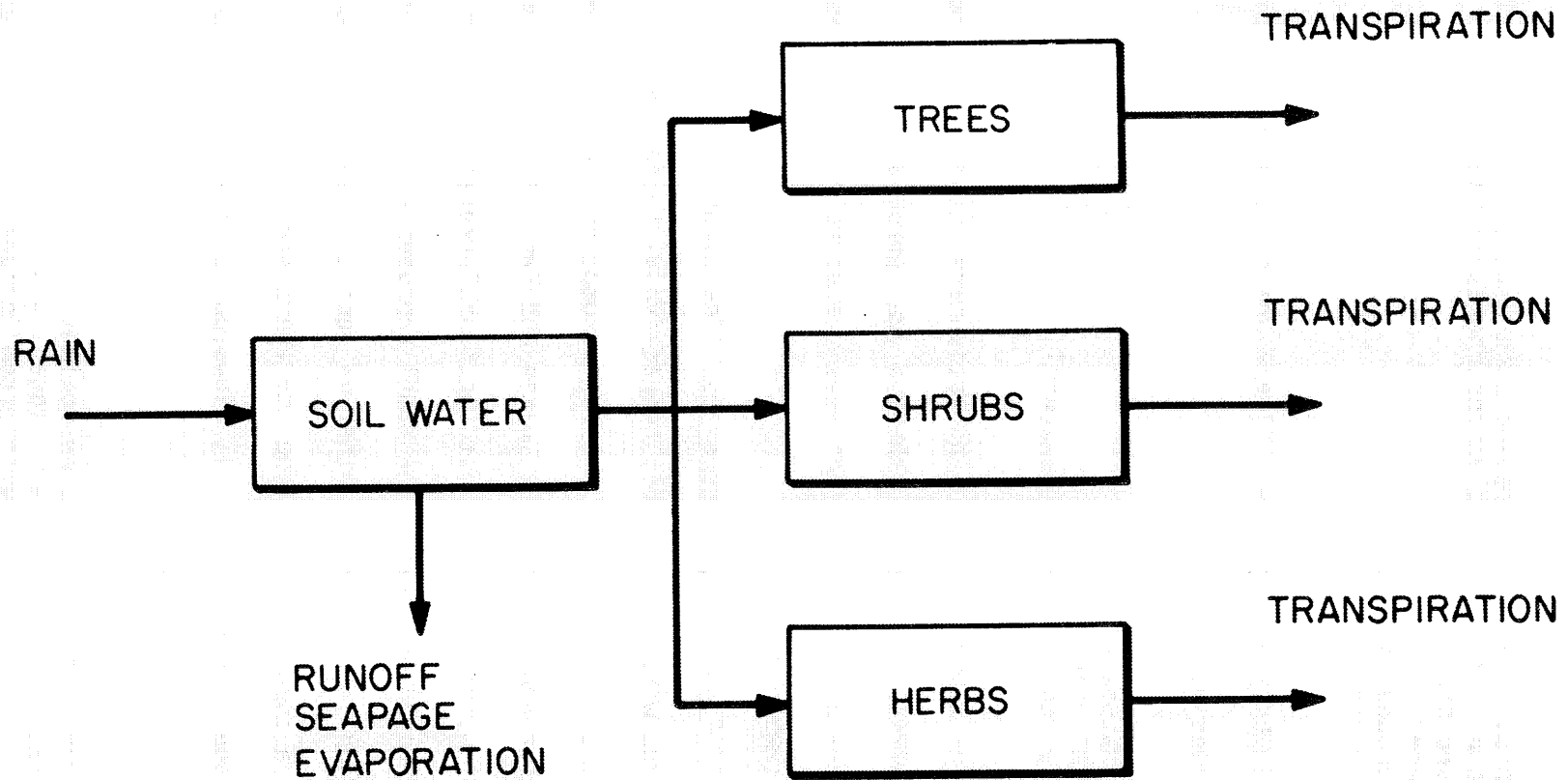


Fig. 2.10.3. Compartmental structure of pine flatwoods water flow submodel. Modified from Golkin and Ewel (1984).

X_{12} - phosphorus in litter and associated with soil organic matter
 X_{13} - available (acid-extractable) phosphorus in the soil
 X_{14} - total phosphorus in the soil
 X_{15} - soil water
 X_{16} - water in deep aquifer
 X_{17} - phosphorus in fertilizer

2.10.1.2 Driving variables. There are three exogenous driving variables in the model:

$Z_1(t)$ - temperature ($^{\circ}\text{C}$)
 $Z_2(t)$ - rainfall (inches)
 $Z_3(t)$ - insolation ($1000 \text{ langleys week}^{-1}$)

Daily values of temperature and insolation are interpreted from a series of empirical values throughout a year (from Golkin 1981). Rainfall values are taken from daily values of rain from September 1, 1977, to September, 1980.

2.10.1.3 Flows or rate processes. The flows of carbon, phosphorus, and water correspond, respectively, to the arrows in Figs. 2.10.1, 2.10.2, and 2.10.3. The assumptions underlying these flows are described in detail by Golkin and Ewel (1984). Here we only define the flows and provide their functional representation of the carbon and phosphorus flows. The model representation of photosynthesis and respiration is discussed further in Section 2.10.1.4. The number 99 refers to a compartment external to the system. All flows into the system are labeled $F(99,j)$ and all flows out of the system are labeled $F(i,99)$. The K_j 's are constants.

$F(99,1)$ - photosynthesis of pine foliage: $A_1 X_1$
 $F(1,99)$ - respiration of pine foliage: $C_1 X_1$
 $F(1,2)$ - translocation of carbon from foliage to stem + branches: 0
 if $(A_1 \leq C_1)$ and $C_2 X_1$ if $(A_1 > C_1)$
 $F(1,11)$ - litterfall of pine foliage: $C_4 X_1$

- F(3,1) - translocation of carbon from roots to foliage: C_3X_3
 F(2,3) - respiration of stem and branches: C_7X_2
 F(2,11) - stem and branch litterfall: C_6X_2
 F(3,11) - root sloughing: C_9X_3
 F(5,4) - phosphorus translocation from stem and branches to foliage: P_2X_6
 F(4,5) - phosphorus translocated from foliage to stem and branches: P_3X_1
 F(4,12) - phosphorus in litterfall: P_6X_4
 F(6,5) - phosphorus translocation from roots to stem and branches: P_1X_6
 F(5,6) - phosphorus translocation from stem and branches to roots: P_4X_1
 F(5,12) - phosphorus in stem and branch litterfall: P_7X_5
 F(13,6) - phosphorus uptake by roots: U_1
 F(6,12) - phosphorus in sloughed roots: P_5X_6
 F(99,7) - shrub respiration: A_2X_7
 F(7,99) - shrub litterfall: $C_{10}X_7$
 F(7,11) - shrub litterfall: $C_{11}X_7$
 F(13,8) - phosphorus uptake by shrubs: U_2
 F(8,12) - phosphorus in shrub litterfall: P_8X_8
 F(99,9) - photosynthesis of herbs: $C_{12}X_9$
 F(9,11) - herb litterfall: $C_{13}X_9$
 F(13,10) - phosphorus uptake by herbs: U_3
 F(10,12) - phosphorus in herb litter: P_9X_{10}
 F(11,99)₁ - litter respiration: $C_{14}X_{11}$
 F(11,99)₂ - carbon lost in runoff: $C_{14}X_{11}$
 F(12,99)₁ - phosphorus mobilized from litter: $P_{10}X_{12}$
 F(12,99)₂ - litter phosphorus lost in runoff: $P_{11}X_{12}$
 F(14,13) - transfer of unavailable to available phosphorus: $P_{13}X_{14}$
 F(99,13) - phosphorus in rainfall: P_{14}
 F(13,14) - transfer of available to unavailable phosphorus: $P_{12}X_{13}$
 F(13,99)₁ - available phosphorus lost in lateral flow: $P_{15}X_{13}$
 F(13,99)₂ - available phosphorus lost in overland flow: $P_{16}X_{13}$
 F(13,99)₃ - available phosphorus lost in deep percolation: $P_{17}X_{13}$
 F(17,13) - transfer of fertilizer to available phosphorus: $P_{19}X_{17}$

 (14,99) - unavailable phosphorus lost overland flow: $P_{16}X_{14}$
 F(99,15) - rainfall input: $Z_2(t)$
 F(17,99) - fertilizer lost in runoff

where

- C_1 = See Section 2.10.1.4
 C_2 = $F_2(t)(A_1 - C_1)$
 C_3 = $K_{16}F_3(t)$
 C_4 = $K_8F_9(t)$
 C_5 = $K_{12}C_2F_4(t)W_2$
 C_6 = K_{13}
 C_7 = See Section 2.10.1.4
 C_8 = See Section 2.10.1.4
 C_9 = $K_{15}F_8(t)$

C_{10} = See Section 2.10.1.4
 C_{11} = $K_{21}F_9(t)$
 C_{12} = See Section 2.10.1.4
 C_{13} = K_{80}
 C_{14} = See Section 2.10.1.5
 C_{15} = $K_{78}(W_3 - W_4)$

P_1 = $K_{28}F_5(t)$
 P_2 = $K_{29}P_1$
 P_3 = $K_{30}F_6(t)C_2$
 P_4 = $K_{31}F_7(t)C_5$
 P_5 = $K_{32}C_9X_6$
 P_6 = $K_{38}C_4$
 P_7 = $K_{37}C_6$
 P_8 = C_{11}
 P_9 = $K_{46}C_{13}$
 P_{10} = C_{14}
 P_{11} = $K_{64}W_4$
 P_{12} = K_{72}
 P_{13} = K_{73}
 P_{14} = $K_{71}Z_2(t)$
 P_{15} = $K_{63}W_3$
 P_{16} = $K_{67}W_4$
 P_{17} = $K_{63}W_5$
 P_{18} = $L_{66}W_5$
 P_{19} = K_{74}
 P_{20} = $K_{66}W_4$

W_2 = effect of soil water conditions on root growth

W_3 = lateral percolation through the soil

W_4 = overland runoff

W_5 = flow from surface to deep aquifer

$F_i(t)$ = functions controlling the timing of carbon and phosphorus flows within a tree

U_1 = $K_{35}C_5X_1X_{13}\{1 - \exp(K_{35}X_6/X_{13})\}/(K_{33} + X_{13})$

U_2 = $K_{42}A_3X_9X_{13}\{1 - \exp(K_{45}X_{10}/X_9)\}/(K_{43} + X_{13})$

U_3 = $K_{32}A_2X_7X_{13}\{1 - \exp(K_{41}X_8/X_7)\}/(K_{40} + X_{13})$

A_1, A_2, A_3 - see Section 2.10.1.4

2.10.1.4 Photosynthesis and Respiration. There are three photosynthesis functions; (1) pine foliage A_1 , (2) shrubs A_2 , and (3) herbs A_3 . These all have the same form, so we show only the photosynthesis of pine foliage:

$$A_1 = K_4L_1W_1X_4/(K_9X_1 + X_4) , \quad (2.10.1)$$

where

$$L_1 = K_1Z_3(t)/(1 + K_1X_1) , \quad (2.10.2)$$

where

K_1 = light extinction coefficient for pine

K_2 = pine productivity coefficient

K_9 = phosphorus photosynthetic activity

There are functions for respiration for the following live plant compartments; (1) pine foliage C_7 , (2) stem and branch respiration C_f (3) root respiration C_8 , (4) shrubs C_{10} , (5) herbs. These are as follows;

$$C_7 = K_5 Z_1(t) + K_6 A_1 - K_7 \quad (2.10.3)$$

$$C_f = K_{10} Z_1(t) - K_{11} \quad (2.10.4)$$

$$C_8 = K_{14} X_8 \quad (2.10.5)$$

$$C_{10} = K_{18} Z_1(t) + K_{19} A_2 - K_{20} \quad (2.10.6)$$

where K_5 , K_6 , K_7 , K_{10} , K_{11} , K_{14} , K_{18} , K_{19} and K_{20} are constants.

2.10.1.5 Release of carbon through decomposition. Respiratory losses of CO_2 from litter is represented by the function.

$$C_{14} = K_{26} Z_1(t) + K_{27}.$$

2.10.2 SEASONAL PHOTOSYNTHESIS AND RESPIRATION

Data on the forcing functions, temperature, rainfall, and insolation, were provided in Golkin (1981). Values of the forcing functions, $F_1(t)$ through $F_9(t)$, as well as the initial values of the state variables, were obtained from the same source. These values were used to simulate CO_2 fluxes over the course of a year. Daily fluxes at 5-day intervals are plotted in Fig. 2.10.4. Carbon values generated by the model were converted to CO_2 equivalents using a

conversion factor of $1 \text{ gC} = 3.67 \text{ g CO}_2$. Seasonal net CO_2 exchange between the forest stand and the atmosphere is plotted in Fig. 2.10.5. Net exchange is respiration minus photosynthesis. Hence, a positive value indicates the stand is acting as a source of atmospheric CO_2 ; a negative value indicates the stand is acting as a sink.

ORNL - DWG 85-14425

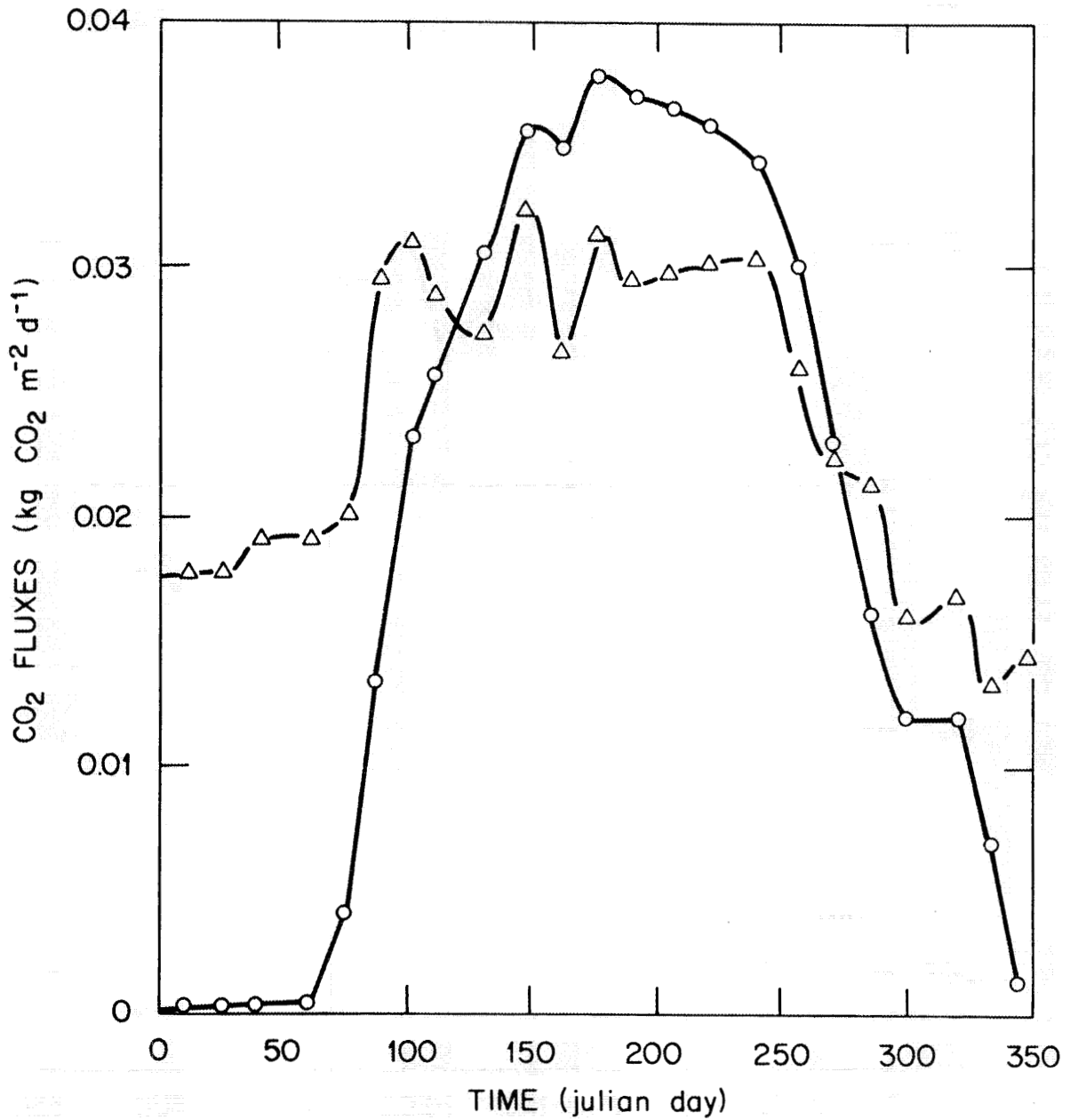


Fig. 2.10.4. Seasonal total ecosystem photosynthesis (Δ) and respiration (o) for a pine flatwoods ecosystem. Flux units are kg CO₂ m⁻² d⁻¹.

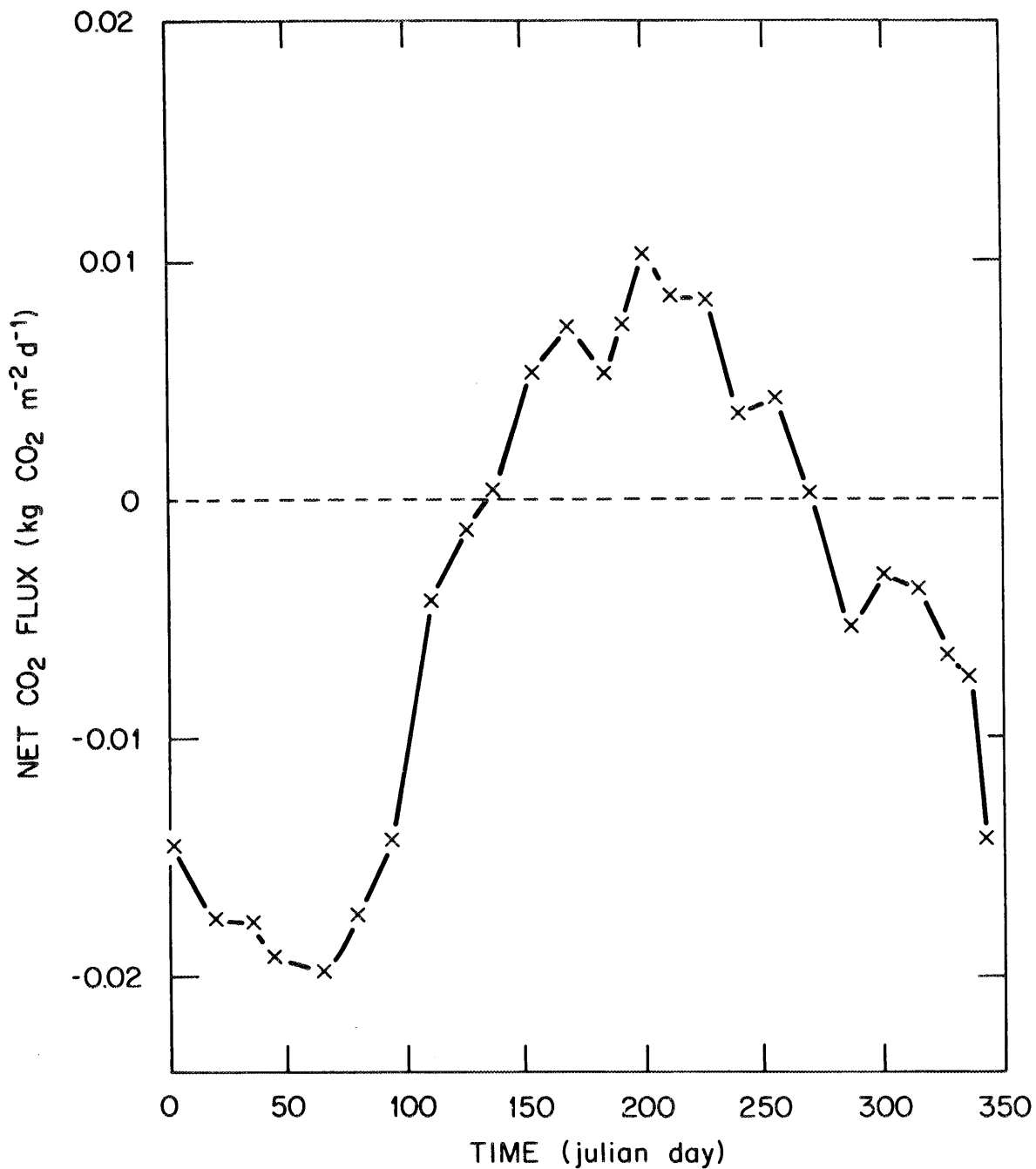


Fig. 2.10.5. Seasonal net CO₂ exchange between the atmosphere and a pine flatwoods ecosystem. Flux units are kg CO₂ m⁻² d⁻¹.

3. EXTRAPOLATION OF SITE-SPECIFIC MODELS TO BIOME-LEVEL MODELS

A goal of future research will be to extend site-specific models so that they represent the seasonal carbon fluxes of whole biomes. The process of extrapolating site-specific models to biome-level models will involve two phases. Phase one of the process will be to identify the geographical extent of the biomes or ecosystem types over which the site-specific models can be taken as representative. Any classification of ecosystems or plant formations is to some degree subjective (Lieth 1975). The classification scheme, and mapping of geographical distribution, is dependent on the criteria for similarity (e.g., biotic or climatic) and the purpose behind the classification. No matter how classified, a biome will have a considerable amount of internal heterogeneity in vegetative, climatic, and edaphic characteristics, as well as land use and successional stage. We propose to deal with this problem of biome identification and heterogeneity in the following way.

On the first level of resolution, biomes will be defined by a combination of the availability of site-specific models and the classification and mapping of major world ecosystems described by Olson, Watts, and Allison (1983). Initially, at least, we will allow the models to define the biomes. The Olson, Watts, and Allison classification is hierarchical, and the largest ecosystem class for which a given site-specific model is the sole representative will be defined as a Level One Biome. Table 3.1 describes the representative site-specific models that have been collected to date. From our model

Table 3.1. List of available seasonal terrestrial carbon flux models that have been collected up to the present time

Authors	Site	General biome type
Bandhu et al. (1973)	Pasoh, Malaysia	Tropical rainforest
Bandhu et al. (1973)	Lubumbashi, Zaire	Tropical dry deciduous Woodland
Andersson et al. (1973)	Virelles, Belgium	Temperate deciduous forest
Sollins, Reichle, and Olson (1973)	Oak Ridge, Tennessee	Temperate deciduous forest
Attiwill et al. (1973)	Victoria, Australia	Temperate broad-leaved evergreen forest
Coniferous Forest Modeling Group (1977)	Cascade Mts., Oregon	North temperate coniferous forest
Kanninen, Hari, and Kellomaki (1982)	Central Finland	Boreal coniferous forest
Bosatta (1980)	Ivantjarnsheden, Sweden	Boreal coniferous forest
Golkin and Ewel (1984)	Northcentral Florida	Pine flatwoods
Singh (1973)	Northern India	Tropical grassland
Krishnamurthy (1978)	Rajkot, India	Tropical grassland
Morris et al. (1978) Furniss et al. (1982)	Nylsvley Savanna, North Transvaal	Tropical savanna
Parton and Singh (1984)	Delhi, India	Tropical grassland
Detling, Parton, and Hunt (1979) Parton, Singh, and Coleman (1978)	Northeastern Colorado	Temperate grassland (shortgrass)
Parton and Singh (1976)	Osage, Oklahoma	Temperate grassland, (tallgrass)
Pendleton et al. (1983)	Fresno County, California	Temperate grassland, (annual)
Heasley, Lauenroth, and Yorks (1984)	Southeastern Montana	Temperate grassland (mixed)

Table 3.1. (continued)

Authors	Site	General biome type
Gilmanov (1977)	Karachi, Western Siberia	Temperate grassland
Bunnell and Scoullar (1975)	Point Barrow, Alaska	Boreal tundra
Bunnell and Scoullar (1975)	Devon Island, Canada	Boreal tundra
Bunnell and Scoullar (1975)	Moore House, United Kingdom	Heath and moorland
Valentine (1974) Parnas and Radford (1974)	Desert Southwest, United States	Arid land/desert

descriptions in Sect. 2, it is obvious that all of these models have not yet been fully implemented. Figure 3.1 illustrates the world distribution of site-specific models. Table 3.2 describes the regional classification of the model sites according to the Olson, Watts, and Allison (1983) classification scheme. Table 3.3 provides descriptive information for these regional types.

The next step in defining the appropriate biogeographical region over which a site-specific model may be extrapolated will be to use our compilation of data on seasonal terrestrial carbon fluxes (King and DeAngelis 1985). The sites of these empirical data sources will be assigned to an ecosystem type according to vegetation characteristics, geographical location, and the ecosystem mapping of Olson, Watts, and Allison (1983). Some of the empirical sites will represent sufficiently unique ecosystem types that they can be defined as subtypes (i.e., Level Two Ecosystem Complexes) within a Level One Biome. These ecosystem types will then be traced upwards through the hierarchical classification until a Level One Biome is reached. Hence, we will have defined a large-scale biome with heterogeneity described by the number, type, and geographical distribution of empirical data sources on seasonal terrestrial carbon fluxes. It is not clear whether the intensive sites described by the site-specific models are representative of the wider region whose structure they represent, or whether the input or turnover rates should be adjusted to make them more representative. Our proposed extrapolation will aid in clarifying this point.

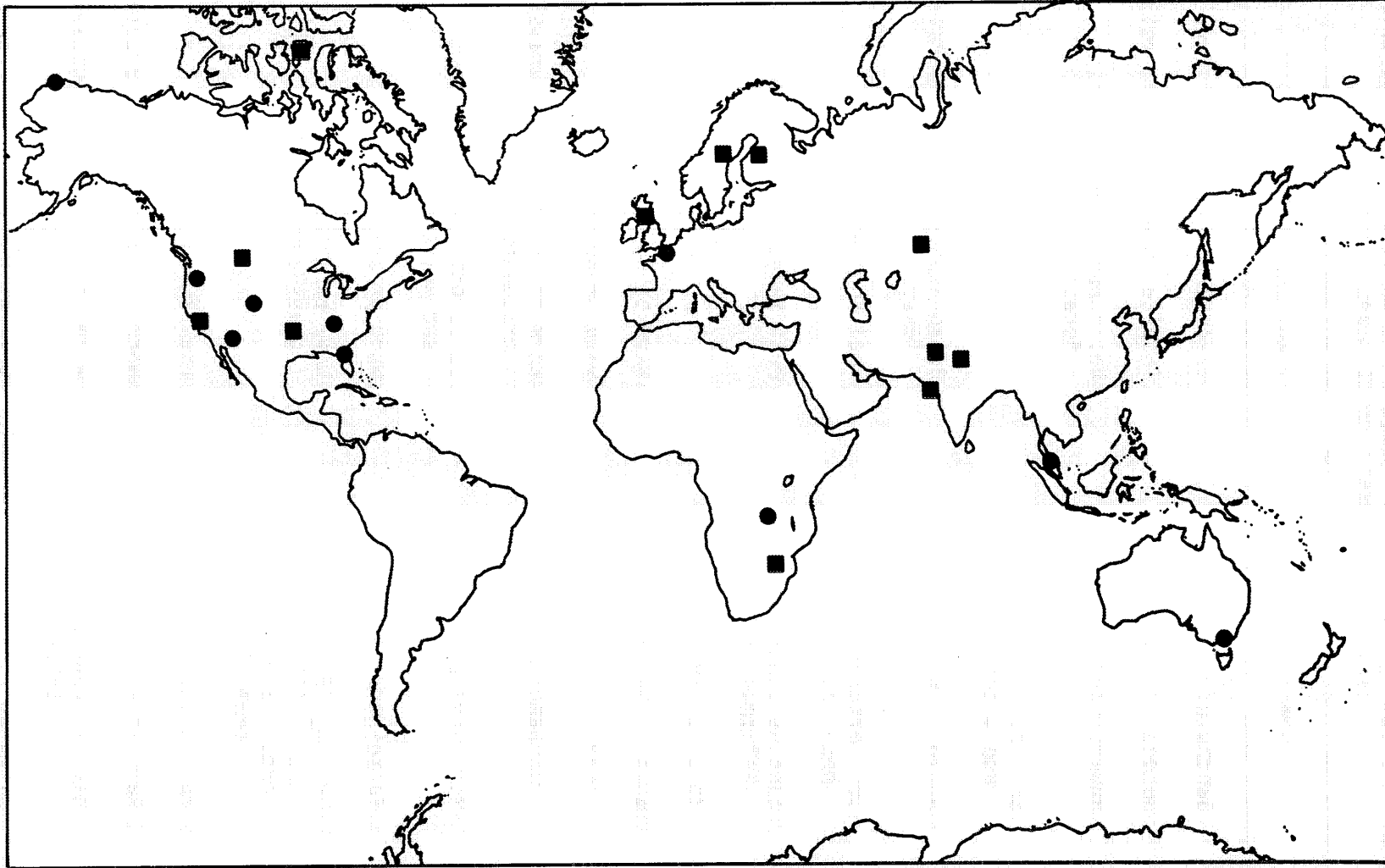


Fig. 3.1. World distribution of the site-specific models collected to date (● - implemented models; □ - models not yet implemented).

Table 3.2. Regional classification of the site-specific models according to Olson, Watts, and Allison (1983)

Models	Regional classification
Bandhu et al. (1973) - a	Evergreen equatorial forest
Bandhu et al. (1973) - b	Tropical dry forest and woodland
Andersson et al. (1973)	Deciduous (summergreen) forest
Sollins, Reichle, and Olson (1973)	"
Attiwill et al. (1973)	Broad-leaved south temperate forest
Coniferous Forest Modeling Group (1977)	Cool conifer
Kanninen, Hari, and Kellomaki (1982)	Main taiga
Bosatta (1980)	"
Golkin and Ewel (1984)	Warm or hot conifer
Singh (1973)	Warm or hot farms, etc.
Krishnamurthy (1978)	Warm or hot shrub and grassland grassland
Morris et al. (1978)	Succulent and thorn woods and scrub
Parton and Singh (1984)	Warm or hot farms, etc.
Detling, Parton, and Hunt (1979) Parton, Singh, and Coleman (1978)	Warm or hot shrub and grassland
Parton and Singh (1976)	Field/woods complex
Pendleton et al. (1983)	Warm or hot shrub and grassland
Heasley, Lauenroth, and Yorks (1984)	Warm or hot shrub and grassland
Gilmanov (1977)	Warm or hot shrub and grassland

Table 3.2. (continued)

Models	Regional classification
Bunnell and Scoullar (1975) - a	Tundra
Bunnell and Scoullar (1975) - b	Tundra
Bunnell and Scoullar (1975) - c	Heath and moorland
Valentine (1974) Parnas and Radford (1974)	Desert and semidesert

Table 3.3. Descriptions of the Olson, Watts, and Allison (1983) regional classifications represented by the site-specific models

Regional classification	Area (10 km ²)	Total Plant carbon (Gt)	Net Primary Prod. (Gt/yr)
Evergreen equatorial forest	10.38	155.7	8.3
Tropical dry forest and woodland	4.72	33	2.7
Deciduous (summergreen) forest	1.49 ^a	15.0 ^a	0.9 ^a
Broad-leaved south temperate forest	a	a	a
Cool conifer	3.5 ^b	59 ^b	2.1 ^b
Warm or hot conifer	b	b	b
Main taiga	7.16 ^c	62 ^c	3 ^c
Warm or hot towns, etc.	d	d	d
Warm or hot shrub and grassland	17.3	22.6	7.0
Succulent and thorn woods and scrub	4.0	16	1.6
Field/woods complex	d	d	d
Tundra	11.0	9.0	1.4
Heath and moorland	0.15	0.22	0.04
Desert and semidesert	18.2 ^e	5.0 ^e	1.4 ^e

^aEstimate for Olson, Watts, and Allison's (1983) temperate broad-leaved forest.

^bEstimate for Olson, Watts, and Allison's (1983) other conifer

^cEstimate for Olson, Watts, and Allison's (1983) main and southern taiga.

^dOlson, Watts, and Allison's (1983) Plate 1, map of carbon distribution, distinguishes areas of human habitation and cultivation or old fields or bush fallow that is partly recovering from recent cycles of cropping. However, the model sites are not of sufficient scale to encompass these influences and cannot be considered representative of the regional type indicated. Possibly the immature recovery phases of native vegetation could approximate the regional average pools, but the dynamics of the system would preferably take into account the existence of a mosaic of different cover types.

^eEstimate for Olson, Watts, and Allison's (1983) nonpolar desert or semidesert, including sandy desert that may be bare over wide areas.

The previously discussed method of describing and defining biomes is dependent on the availability of appropriate site-specific models and data on seasonal carbon fluxes. Consequently, the process may be data-limited. This problem is not, however, unique to the methodology we propose. We believe that our process of biome identification is appropriate to the project goals and is capable of defining credible biomes with sufficient resolution to permit the development of biome-scale models of seasonal carbon dynamics. These points are amplified in the following discussion of gaps in our present coverage of the terrestrial biosphere.

The most notable absences in our present representation (see Tables 3.1 to 3.3) of the terrestrial biosphere, as portrayed by Olson, Watts, and Allison (1983), are their Mixed Woods; Second Growth Woods and Field Mosaics; Crops, Settlements, and Marginal Lands; Northern or Maritime Taiga; and Tropical Savanna and Woodland categories. We expect to represent seasonal production in croplands with models appropriate to simulate carbon fluxes in crop systems [e.g., the CANOPY model of Terjung and O'Rourke (1980) and Band et al. (1981), and the SPAM model of Stewart and Lemon (1969)]. There also exist published empirical data on seasonal carbon fluxes in a variety of agricultural systems. These models and empirical sources are reviewed by King and DeAngelis (in preparation).

By combining our representation of agricultural systems with the appropriate forest or woodland models, and given estimates of the relative areal extent of the two system types for a given biome, we should be able to characterize seasonal carbon flux in a variety of

woods and field mosaics. Similarly, it may be possible to estimate carbon flux in open wooded areas such as the Northern Taiga and Tropical Savanna (see below) by using the appropriate combination of ecosystem-type models. If such exercises provide unreasonable or suspicious results, we have the option of reducing the scale of biome- or ecosystem-type resolution. That is, we will not initially consider the open Northern Taiga to be distinct from the rest of the Boreal Forest (Taiga in the broad Russian sense of this word). We are aware that such lumping of ecosystem types may reduce the accuracy of our estimates of biome-scale carbon fluxes; a regionally extended model of this more coarsely aggregated region may require a different weighted average of pools and fluxes than found in the site-specific research areas from which the original calibrations were derived. However, such simplifications and approximations are a real, if unfortunate, part of ecological investigations of this scale; they are also a necessary compromise between data availability and project goals. Furthermore, they draw attention to some of the gap-filling research requirements of the future.

The Mixed Woods category of Olson, Watts, and Allison (1983) presents a similar problem but at a different scale. Instead of heterogeneity on a scale of hectares, as in the forest-field mosaics, heterogeneity occurs on a scale of tens of square meters. Part of this problem is alleviated by models, such as that of Sollins, Reichle, and Olson (1973), that may explicitly consider mixed stands. Some of this heterogeneity may also be simulated by considering the proportional representation of pure stands (and simulating those stands), provided

models of the pure stands are available. This heterogeneity may be dealt with by ignoring it in a first approximation of regional carbon flux.

The treatment of Tropical Savanna and Woodland is problematic. Faced with an absence of tropical savanna ecosystem models that represent both grasses and trees, we may be forced to construct our own compartment model of seasonal carbon fluxes. Data sets exist that make construction of a seasonal donor-controlled compartment model possible [see King and DeAngelis (1985) and Huntley and Walker (1982)].

With these considerations, we believe that we can expand our representation of Olson, Watts, and Allison's (1983) biosphere to accurately encompass at least 86% of the land area, 91% of the total plant carbon, and 82% of the annual net primary production.

Whittaker and Likens (1975) presented another classification of ecosystem types and associated net primary production. They pooled some of the stand types in mixed regional mosaics that were distinguished by Olson, Watts, and Allison (1983). Whittaker and Likens did not, however, describe how such pooling might affect the representative coverage of the larger heterogeneous assemblages to which their area values apply. The most notable gaps in our present representation of the terrestrial biosphere portrayed by Whittaker and Likens (1975) are their Woodland and Shrubland and Cultivated Land categories. Using the same strategies outlined for representing croplands and woodland mosaics in the Olson, Watts, and Allison (1983)

scheme, we expect to be able to encompass nearly 100% of the land area, total plant carbon, and annual net primary production estimated by Whittaker and Likens (1975). In short, we expect our methodology to be capable of adequately representing the extent of the terrestrial biosphere.

Phase two of the extrapolation process will involve the simulation of biome-level seasonal carbon dynamics. The site-specific models are, in almost all cases, driven by seasonally variable climatic or other abiotic factors (see Sect. 2). First, we will determine the geographic distribution (across the Level One Biome) of the driving variable data associated with the site-specific model which represents that region. Many of the sources of seasonal carbon flux data include data on climatic variables (King and DeAngelis 1985). Where the driving variables needed for a site-specific model are not included in a seasonal carbon flux data source, or where additional heterogeneity within a defined vegetation association is desirable, independent sources of climatic data (e.g., other ecological studies, climatic atlases, and climatic data bases), general climate functions (e.g., solar radiation as a function of latitude and time of year), interpolations, and reasonable assumptions will be used to provide the needed driving variables. We will then run the site-specific simulation models using the geographically distributed driving variable data. These data will probably be long-term averages not specific to any given year.

At a minimum, we will run each model using the driving variable data associated with the centroid of the appropriate Level One Biome.

To provide greater resolution, we will run the model for the centroid of each of the cells of a geographical grid. The spatial resolution of this grid will be determined in part by the resolution of existing three-dimensional general circulation models (GCM's; see Sect. 4). We also plan to simulate carbon dynamics for at least the most fully described empirical data sites, using the appropriate models and the driving variable data associated with those sites. Decisions on additional simulations will be based partly on recognized vegetational heterogeneity and the heterogeneity across the Level One Biomes of the driving variable data sets.

The extrapolation process we have outlined is an expression of the working hypothesis that the dynamics imposed by the regionally distributed seasonal driving variables (e.g., climate) will capture most of the geographic and temporal variability in biome carbon dynamics. This hypothesis involves the assumption that the intrinsic, qualitative, and structural aspects of the carbon fluxes of a biome or regional ecosystem complex, in particular CO_2 exchange with the atmosphere, are geographically homogeneous. We also assume that these homogeneous biome-level characteristics are adequately represented by those properties of the site-specific models not dependent on the driving variables. Incorporation of the driving variables will introduce heterogeneity. Consequently, the extrapolation will transform the site-specific models for each biome into an array of models (differing in the dynamics introduced by the driving variables) that address some of the variability across a Level One Biome. How well the internal heterogeneity in biome-level carbon dynamics is

expressed will be dictated by our ability to obtain independent driving variable data, the geographic heterogeneity of those data, the distribution of seasonal carbon flux data sites, decisions on the relative importance of a vegetation association (e.g., areal extent, relative carbon storage, and relative net primary productivity), and determinations of a geographic grid resolution compatible with GCM's.

The seasonal carbon flux data sources will not only provide climatic data but will also serve as points of model evaluation (Cale, O'Neill, and Shugart 1983). Unfortunately, very few empirical data are available on the model predictions of greatest interest to our investigation, that is, the seasonal exchange of CO_2 between the atmosphere and an entire vegetation stand. However, the sources of empirical data on seasonal carbon fluxes (King and DeAngelis 1985) do contain data on seasonal standing crop and within-stand carbon fluxes (e.g., litterfall). In our simulations of a particular ecosystem type or vegetation association, we will attempt to approximate those empirical data. As stated earlier, we are proceeding on the assumption that the dynamics imposed by seasonal driving variables will capture most of the seasonal variability in the empirical data, for example, in standing crop. However, this process will probably require some iterative tuning of rate parameters or site-specific parameters (e.g., soil-type factors). We hope to keep changes in the site-specific models to a minimum. Any changes will be documented, and their implications explored. Given the assumption that an accurate prediction of stand-atmosphere CO_2 exchange accompanies an accurate prediction of standing crop, our ability to simulate standing crop with

acceptable accuracy will reinforce the acceptability of the simulated CO_2 exchanges. This model evaluation procedure will inject a degree of objectivity into our simulation of regional carbon fluxes and should increase the reliability of our results. Where data on stand-atmosphere CO_2 exchanges exist, we will, of course, compare these observations with our model predictions and work towards a reasonable fit between prediction and observation. The former procedure, comparing model predictions with observations of standing crops and within-stand carbon dynamics, will also provide an assessment of the generality of the site-specific models.

The development of a method to extrapolate site-specific models to biome-level models, as part of the problem of scaling local phenomena up to regional and global scales, is an evolving process. The method described here is a working outline. As the extrapolation proceeds, the method will be refined and modified in response to theoretical and practical considerations. Each change will be evaluated according to its contribution towards a useful method of systematically relating local and large-scale processes and phenomena.

4. CONCLUDING REMARKS

The objective of this report has been to document a number of site models currently in use at ORNL to describe seasonal carbon fluxes in a variety of terrestrial ecosystems. We have not yet used all available models, or analyzed in detail the seasonal patterns described by the models discussed here. This will be done in a subsequent report.

Completion of the extrapolation process discussed in Sect. 3 will provide a suite of models describing the seasonal carbon dynamics of the earth's main terrestrial biomes. These models will guide decisions on how many transitional or strongly disturbed system models are desirable. Present cases probably simulate the seasonal exchange of CO_2 between the atmosphere and the main land areas of the terrestrial biota (see Sect. 2). Together with the geographical distribution of the biomes and climate, they will provide time-varying boundary conditions, or a biospheric CO_2 exchange model, for an atmospheric CO_2 tracer model (see Pearman and Hyson 1981; Hansen et al. 1982; Fung et al. 1983; Heimann, Keeling, and Fung 1985).

The integration of our biospheric exchange model into an atmospheric CO_2 tracer model might consist of two parts:

1. Time series climatic data can be used to drive our biospheric exchange model. These data can come from two or more possible sources (as described in Sect. 3). First, many of the site studies described by King and DeAngelis (1985) contain climatic data for specific years. Second, one can use actual climatic data on a global basis for a period of years. These data can be used as input for a biospheric exchange model. The results could include the seasonally varying net CO_2 fluxes at the centroids of the principal biomes of the earth over one or more years. More refined spatial resolution is also possible, but this will probably require additional years of evaluation.

2. The spatially distributed time-series fluxes of CO₂ from part one can be used as the boundary conditions for a tracer GCM.

A more detailed discussion of the integration of biome-level models into a global CO₂ model would be premature. The specifics of the process will depend on a number of variables, including such things as the spatial and temporal resolution of the tracer GCM. Discussion of these factors must be postponed until the process of site-specific to biome-level model extrapolation is more advanced. However, a couple of general comments are germane.

The coupling of ecosystem models and GCM's at the interface between regional components of the biosphere and the atmosphere involves problems of scale and hierarchical organization (Allen and Starr 1982, O'Neill et al. in press). Ecosystem models generally represent stands covering at most a few hectares, and results are presented in spatial units of square meters or hectares. A three-dimensional atmospheric model (e.g., a tracer GCM) generally has a ground-level resolution no smaller than 10^4 km². Convergence to a common scale requires crossing a number of spatial scales and possibly an equal number of hierarchical levels. This problem has not been well investigated. It is not at all clear, even reasonably suspect (O'Neill 1979), that averages, assumptions of homogeneity, and simple unit transformations will produce the correct, even a useful, convergence. Any attempt to couple ecosystem models and GCM's, to integrate ecosystem and atmospheric dynamics should include a recognition of these problems and attempt their resolution. Our evolving extrapolation from stand to biome will involve explicit consideration

of those principles now emerging from considerations of scale and hierarchy in ecological systems (Allen and Starr 1982; Allen, O'Neill, and Hoelstra 1984; O'Neill et al. in press; Urban, O'Neill, and Shugart in review). These principles also have an important role in understanding the biosphere-atmosphere interface.

The method we have outlined in this report for developing a biospheric CO₂ source function is of course not the only approach. Other source functions have been built and utilized (Junge and Czeplak 1968; Pearman and Hyson 1981; Fung et al. 1983), although we are uncomfortable with the ecology of some of them. Further development of alternative source functions is likely. The relatively rapid meteorological smoothing of climatic and CO₂ data in the atmosphere may mean that the geophysical purposes can be served to fair approximation by even broader pooling than that currently suggested by Tables 3.2 and 3.3, and by a smaller number of pools than were suggested for various purposes of local ecosystem dynamics and incorporated in the site-specific models. Ecologically sound models that depart considerably from the compartmental approach of ecosystem models are also possible. A variety of large-scale carbon dynamic models that can be used as biospheric CO₂ source functions will likely be available in the near future. Understanding gained in their development will almost certainly benefit the modeling of biosphere-atmosphere-geosphere interfaces in other biogeochemical cycles.

REFERENCES

- Allen, T. F. H. and T. B. Starr. 1982. Hierarchy: Perspectives for Ecological Complexity. University of Chicago Press, Chicago.
- Allen, T. F. H., R. V. O'Neill, and T. W. Hoekstra. 1984. Interlevel relations in ecological research and management: Some working principles from hierarchy theory. General Technical Report, U.S. Dept. of Agriculture, Rocky Mountain Forest and Range Exp. Stat., Fort Collins, Colo.
- Andersson, F., S. Denaeyer, P. Duvigneaud, N. T. Edwards, J. E. Satchell, P. Sollins, N. Tarsia, H. M. Thandrup, W. Van Winkle, J. B. Waide, and J. R. Webster. 1973. Seasonal model of a temperate deciduous forest. pp. 296-305. IN L. Kern (ed.), Modeling Forest Ecosystems. EDFB-IBP-73-7, Oak Ridge National Laboratory, Oak Ridge, Tenn.
- Attiwill, P., R. S. Booth, F. Eckardt, P. Lossaint, J. B. Mankin, T. Shidei, H. H. Shugart, and B. Ulrich. 1973. Seasonal model of the broadleaved evergreen forest. pp. 313-319. IN L. Kern (ed.), Modeling Forest Ecosystems, EDFB-IBP-73-7. Oak Ridge National Laboratory, Oak Ridge, Tenn.
- Bacastow, R. B., and C. D. Keeling. 1981. Atmospheric carbon dioxide concentration and the observed airborne fraction. pp. 103-112. IN B. Bolin (ed.), Carbon Cycle Modelling - SCOPE 16. John Wiley and Sons, New York.

- Bacastow, R. B., C. D. Keeling, T. P. Whorf, and C. S. Wong. 1981. Seasonal amplitude in atmospheric CO₂ concentration at weather station P, 1970-1980. Paper presented at the Bern Conference on Interpretation of Atmospheric CO₂ Data, Bern, Switzerland, September 14-18, 1981.
- Band, L. E., O. B. Elfes, J. T. Hayes, L. O. Means, P. A. O'Rourke, B. J. Stevenson, W. H. Terjung, and P. E. Todhunter. 1981. Application of a photosynthesis model to an agricultural region of varied climates: California. *Agric. Meteor.* 24:201-217.
- Bandhu, D., J. Bullock, C. S. Gist, F. Malaisse, H. Ogawa, B. Rust, and M. A. Strand. 1973. Seasonal model of the tropical forests. pp. 285-295. IN L. Kern (ed.), *Modeling Forest Ecosystems*, EDFB-73-7. Oak Ridge National Laboratory, Oak Ridge, Tenn.
- Bosatta, E. 1980. Modelling of soil processes--an introduction. pp. 553-564. IN T. Persson (ed.), *Structure and Function of Northern Coniferous Forests--An Ecosystem Study*, *Ecol. Bull.* 32. Swedish Natural Science Research Council, Stockholm.
- Bremeyer, A. I., and G. M. Van Dyne. 1980. *Grasslands, Systems Analysis, and Man*. Cambridge University Press, Cambridge, U.K.
- Brown, L. F., and M. J. Trlica. 1974. Photosynthesis of two important grasses of the shortgrass prairie as affected by several ecological variables. US/IBP Grassland Biome Tech. Rep. No. 244. Colorado State University, Fort Collins.

- Bunnell, F. L., and D. E. Tait. 1974. Mathematical simulation models of decomposition processes. pp. 207-225. IN: A. J. Holding, O. W. Heal, S. F. McLean, Jr., and P. W. Flanagan (eds.), Soil Organisms and Decomposition in Tundra. Tundra Biome Steering Committee, Stockholm.
- Bunnell, F. L., and P. Dowding. 1974. ABISKO - A generalized decomposition model for comparisons between tundra sites. pp. 227-247. IN A. J. Holding, O. W. Heal, S. F. MacLean, Jr., and P. W. Flanagan (eds.), Soil Organisms and Decomposition in Tundra. Tundra Biome Steering Committee, Stockholm.
- Bunnell, F. L., and K. A. Scoullar. 1975. ABISKO II: A computer simulation model of carbon flux in tundra ecosystems. pp. 425-448. IN T. Rosswall and O. W. Heal (eds.), Structure and Function of Tundra Ecosystems. Ecol. Bull. 20. Swedish Natural Science Research Council, Stockholm.
- Cale, W. G. Jr., , R. V. O'Neill, and H. H. Shugart. 1983. Development and application of desirable ecological models. Ecol. Modelling 18:171-186.
- Coniferous Forest Biome Modeling Group. 1977. CONIFER: A model of carbon and water flow through a coniferous forest. Documentation. Coniferous Forest Biome Bull. 8. University of Washington, Seattle.
- DeAngelis, D. L., R. L. Gardner, and H. H. Shugart. 1981. Productivity of forest ecosystems studied during the IBP: The woodlands data set. pp. 567-672. IN D. E. Reichle (ed.), Dynamic Properties of Forest Ecosystems, Cambridge University Press, Cambridge, U.K.

- Detling, J. K., W. J. Parton, and H. W. Hunt. 1979a. An empirical model for estimating CO₂ exchange of *Bouteloua gracilis* (H. B. K.) Lag. in the shortgrass prairie. *Oecologia (Berl.)* 33:137-147.
- Detling, J. K., W. J. Parton, and H. W. Hunt. 1979b. A simulation model of *Bouteloua gracilis* biomass dynamics on the North American shortgrass prairie. *Oecologia (Berl.)* 38:167-191.
- Fung, I., K. Prentice, E. Matthews, J. Lerner, and G. Russell. 1983. Three-dimensional tracer model study of atmospheric CO₂: Response to seasonal exchanges with the terrestrial biosphere. *J. Geophys. Res.* 88:1281-1294.
- Furniss, P. R., P. Ferrar, J. W. Morris, and J. J. Bezuidenhout. 1982. A model of savanna litter decomposition. *Ecol. Modelling* 17:33-51.
- Gilmanov, T. G. 1977. Plant submodel in the holistic model of a grassland ecosystem (with special attention to the belowground part). *Ecol. Modelling* 3:149-163.
- Golkin, K. R. (1981). A computer simulation of the carbon, phosphorus, and hydrologic cycles of a pine flatwoods ecosystem. M. S. thesis. University of Florida, Gainesville, Florida.
- Golkin, K. R., and K. C. Ewel. (1984). A computer simulation of the carbon, phosphorus, and hydrologic cycles of a pine flatwoods ecosystem. *Ecol. Modelling* 24:113-136.
- Goodall, D. W. 1981. The modeling of arid ecosystem dynamics. pp. 385-410. IN D. W. Goodall, R. A. Perry, and K. M. W. Howes (eds.), *Arid-land Ecosystems: Structure, Functioning, and Management*, Vol. 2. Cambridge University Press, Cambridge, U.K.

- Goodall, D. W., and C. S. Gist. 1973. Terrestrial models: Calling programs and input/output subroutines. pp. 2.1.3.1-9-2.1.3.1-146. IN US/IBP Desert Biome Reports of 1972 Progress. Vol. 1. Utah State University, Logan.
- Goodall, D. W., R. A. Perry, and K. M. W. Howes (eds.). 1979. Arid-land Ecosystems: Structure, Functioning, and Management. Vol. 1. Cambridge University Press, Cambridge, U.K.
- Hall, C. A. S., C. A. Ekdahl, and D. E. Wartenburg. 1975. A fifteen-year record of biotic metabolism in the Northern Hemisphere. *Nature* 255:136-138.
- Hansen, J., G. Russell, D. Rind, P. Stone, A. Lacis, S. Lebedeff, R. Ruedy, and L. Travis. 1982. Efficient three-dimensional global models for climate studies: Models I and II. *Mon. Weather Rev.* III:609-662.
- Heasley, J. E., W. K. Lauenroth, and T. P. Yorks. 1984. Simulation of SO₂ impacts. pp. 161-184. IN W. K. Lauenroth and E. M. Preston (eds.), *The Effects of SO₂ on a Grassland*. Springer-Verlag, New York.
- Heimann, M., C. D. Keeling, and J. Y. Fung. 1985. Simulating the atmospheric carbon dioxide distribution with a three-dimensional tracer model. IN *Proceedings of the Knoxville Symposium on the Global Carbon Cycle*. (in press).
- Huntley, B. J., and B. H. Walker (eds.). 1982. *Ecology of Tropical Savannas*. Springer-Verlag, Berlin.
- Junge, C. E., and G. Czeplak. 1968. Some aspects of the seasonal variation of carbon dioxide and ozone. *Tellus* 20:422-434.

- Kanninen, M., P. Hari, and S. Kellomaki. 1982. A dynamic model for aboveground growth and dry matter production in a forest community. *J. Appl. Ecol.* 19:465-476.
- King, A. W., and D. L. DeAngelis. 1985. Information for seasonal models of carbon fluxes in terrestrial biomes. ORNL/TM-9404. Oak Ridge National Laboratory, Oak Ridge, Tennessee.
- King, A. W., and D. L. DeAngelis. Information for seasonal models of carbon fluxes in agricultural systems. Oak Ridge National Laboratory, Oak Ridge, Tenn. (in review).
- Krishnamurthy, L. 1978. Herbage dynamics of some semi-arid Indian grazing lands. *Ecol. Modelling* 5:77-81.
- Lieth, H. 1975. Primary production of the major vegetation units of the world. pp. 203-215. IN H. Lieth and R. H. Whittaker (eds.), *Primary Productivity of the Biosphere*. Springer-Verlag, Berlin.
- Lieth, H. 1978. Vegetation and CO₂ changes. pp. 103-109. IN J. Williams (ed.), *Carbon Dioxide, Climate, and Society*. Pergamon Press, Oxford.
- Morris, J. W., J. J. Bezuidenhout, P. Ferrar, J. C. Horne, and M. Judelman. 1978. A first savanna ecosystem model. *Bothalia* 12:547-551.
- Olson, J. S., J. A. Watts, and L. J. Allison. 1983. Carbon in live vegetation of major world ecosystems. ORNL-5862. Oak Ridge National Laboratory, Oak Ridge, Tennessee.

- O'Neill, R. V. 1979. Transmutations across hierarchical levels. pp. 55-78. IN G. S. Innis and R. V. O'Neill (eds.), Systems Analysis of Ecosystems. International Cooperative Publishing House, Fairland, Maryland.
- O'Neill, R. V., D. L. DeAngelis, J. B. Waide, and T. F. H. Allen. A Hierarchical Concept of the Ecosystem. Princeton University Press, Princeton, N. J. (in press).
- Parnas, H., and J. Radford. 1974. A decomposition submodel. US/IBP Desert Biome Research Memorandum 74-64. Utah State University, Logan.
- Parton, W. J. 1976. Abiotic submodel. pp. 12-61. IN G. W. Cole (ed.), ELM: Version 2.0. Range Science Department, Science Series No. 20., Colorado State University, Fort Collins.
- Parton, W. J. 1978. Abiotic section of ELM. pp. 31-53. IN G. S. Innis (ed.), Grassland Simulation Model. Springer-Verlag, New York.
- Parton, W. J., and J. S. Singh. 1976. Simulation of plant biomass on a shortgrass and a tallgrass prairie, with emphasis on belowground processes. US/IBP Grassland Biome Tech. Rep. No. 300. Colorado State University, Fort Collins.
- Parton, W. J., and J. S. Singh. 1984. Adapting a biomass simulation model to a tropical grassland. Ecol. Modelling 23:151-163.
- Parton, W. J., J. S. Singh, and D. C. Coleman. 1978. A model of production and turnover of roots in a shortgrass prairie. J. Appl. Ecol. 44:515-542.

- Pearman, G. I., and P. Hyson. 1981. A global atmospheric diffusion simulation model for atmospheric carbon studies. pp. 227-240. IN B. Bolin (ed.), Carbon Cycle Modelling - SCOPE 16. John Wiley and Sons, New York.
- Pendleton, D. F., J. W. Menke, W. A. Williams, and R. G. Woodmansee. 1983. Annual grassland ecosystem model. *Hilgardia* 51:1-44.
- Reichle, D. E. (ed.) 1981. Dynamic Properties of Forest Ecosystems. Cambridge University Press, Cambridge, U.K.
- Reichle, D. E., R. V. O'Neill, and J. S. Olson (compilers), L. Kern (ed.). 1973. Modeling Forest Ecosystems: Report of International Woodlands Workshop, EDFB-IBP-73-7, Oak Ridge National Laboratory, Oak Ridge, Tenn.
- Schulze, E. D. 1970. Der CO₂ Gaswechsel der Buche (Fagus sylvatica L.) Abhängigkeit von dem Klimafaktoren in Frieland. *Flora* 159:177-232.
- Singh, J. S. A compartment model of herbage dynamics for Indian tropical grasslands. *Oikos* 24:367-372.
- Sollins, P., D. E. Reichle, and J. S. Olson. 1973. Organic matter budget and model for a southern appalachian Liriodendron forest. EDFB-IBP-73-2. Oak Ridge National Laboratory, Oak Ridge, Tenn.
- Stewart, D. W., and E. R. Lemon. 1969. The energy budget of the earth's surface: A simulation of photosynthesis of fieldcorn. U. S. Army ECOM Tech. Rep. 2-68 I-6. U. S. Army Electronics Command, Ft. Huachura, Ariz.
- Terjung, W. H., and P. O'Rourke. 1980. An economical canopy model for use in urban climatology. *Int. J. Biometeorol.* 24:281-291.

- Urban, D. L., R. V. O'Neill, and H. H. Shugart. Landscape ecology: A hierarchical perspective (submitted manuscript).
- Valentine, W. 1974. Terrestrial model: Plant processes (Version IV). US/IBP Desert Biome Research Memorandum 74-50. Utah State University, Logan.
- Whittaker, R. H., and G. E. Likens. 1975. The biosphere and man." pp. 305-328. IN H. Lieth and R. H. Whittaker (eds.), Primary Productivity of the Biosphere. Springer-Verlag, Berlin.
- Wielgolaski, F. E. 1975. Fennoscandian Tundra Ecosystems. Part 2. Animals and Systems Analysis. Springer-Verlag, New York.

INTERNAL DISTRIBUTION

- | | | | |
|--------|------------------|--------|-------------------------------|
| 1. | S. I. Auerbach | 20. | W. M. Post |
| 2. | V. H. Dale | 21. | D. E. Reichle |
| 3-7. | D. L. DeAngelis | 22. | A. M. Solomon |
| 8. | W. R. Emanuel | 23. | J. R. Trabalka |
| 9. | R. H. Gardner | 24. | CDIC Files |
| 10. | S. G. Hildebrand | 25. | Central Research Library |
| 11-15. | A. W. King | 26-40. | ESD Library |
| 16. | J. R. Krummel | 41-42. | Laboratory Records Department |
| 17. | P. J. Mulholland | 43. | Laboratory Records, RC |
| 18. | R. V. O'Neill | 44. | ORNL Patent Office |
| 19. | A. M. Perry, Jr. | 45. | ORNL Y-12 Technical Library |

EXTERNAL DISTRIBUTION

46. Thomas V. Armentano, Director, Biotic Resources Program, Holcomb Research Institute, Butler University, 4600 Sunset Avenue, Indianapolis, IN 46208
47. Robert B. Bacastow, Geological Research Division, Scripps Institution of Oceanography, University of California, 2314 Ritter Hall, A-020, La Jolla, CA 92093
48. Bert Bolin, Arrhenius Laboratory, Department of Meteorology, University of Stockholm, S-106 91 Stockholm, SWEDEN
49. Philippe Bourdeau, Head of Environment, Raw Materials and Materials Technology, Commission of the European Communities, Rue de la Loi 200, Wetstraat 200, 1049 Brussels, BELGIUM
50. Francis P. Bretherton, NCAR/AAP, P. O. Box 3000, Boulder, CO 80307
51. Peter G. Brewer, Department of Chemistry, Woods Hole Oceanographic Institution, Woods Hole, MA 02543
52. Wallace S. Broecker, Lamont-Doherty Geological Observatory of Columbia University, Palisades, NY 10964
53. Sandra Brown, Department of Forestry, University of Illinois, 110 Mumford Hall, 1301 West Gregory Drive, Urbana, IL 61801
54. J. Thomas Callahan, Associate Director, Ecosystem Studies Program, Room 336, 1800 G Street, NW, National Science Foundation, Washington, DC 20550
55. Chen-Tung Arthur Chen, College of Oceanography, Oregon State University, Corvallis, OR 97331
56. Ralph J. Cicerone, NCAR/ACD, P. O. Box 3000, Boulder, CO 80307
57. Roger C. Dahlman, U.S. Department of Energy, Room J-311, ER-12, Washington, DC 20545
58. John A. Eddy, UCAR, P. O. Box 3000, Boulder, CO 80307
59. Prof. Dr. Egon T. Degens, Geologisch-Paläontologisches Institut und Museum, Universität Hamburg, Bundesstrasse 55, D-2000 Hamburg 13, FEDERAL REPUBLIC OF GERMANY

60. Ellen M. Druffel, Department of Chemistry, Woods Hole Oceanographic Institution, Woods Hole, MA 02543
61. Arthur C. Echternacht, Department of Zoology, University of Tennessee, Knoxville, TN 37996
62. Paul G. Falkowski, Oceanographic Sciences Division, Brookhaven National Laboratory, Associated Universities, Inc., Upton, Long Island, NY 11973
63. G. J. Foley, Office of Environmental Process and Effects Research, U.S. Environmental Protection Agency, 401 M Street, SW, RD-682, Washington, DC 20460
64. Hans D. Freyer, Institute of Atmospheric Chemistry, Nuclear Research Center (KFA), D-5170 Julich, FEDERAL REPUBLIC OF GERMANY
65. Inez Yau-Sheung Fung, NASA Goddard Space Flight Center, Institute for Space Studies, 2880 Broadway, New York, NY 10025
66. C. R. Goldman, Professor of Limnology, Director of Tahoe Research Group, Division of Environmental Studies, University of California, Davis, CA 94616
67. Lou Gross, Department of Mathematics, University of Tennessee, Knoxville, TN 37996
68. Charles A. S. Hall, Division of Biological Sciences, Section of Ecology and Systematics, Corson Bldg., 127 Langmuir Hall, Cornell University, Ithaca, NY 14853-0239
69. W. Franklin Harris, Deputy Division Director, Division of Biotic Systems and Resources, National Science Foundation, 1800 G Street, NW, Room 1140, Washington, DC 20550
70. Henry G. Hengeveld, CO₂/Climate Advisor, Canadian Climate Centre, Environment Canada, 4905 Dufferin Street, Downsview, Ontario M3H 5T4, CANADA
71. Bruce B. Hicks, Director, Atmospheric Turbulence and Diffusion Division, National Oceanic and Atmospheric Administration, U.S. Department of Commerce, P.O. Box E, Oak Ridge, TN 37831
72. Martin I. Hoffert, Department of Applied Science, New York University, 26-36 Stuyvesant Street, New York, NY 10003
73. Richard A. Houghton, The Ecosystems Center, Marine Biological Laboratory, 167 Water Street, Woods Hole, MA 02543
74. J. W. Huckabee, Manager, Ecological Studies Program, Environmental Assessment Department, Electric Power Research Institute, 3412 Hillview Avenue, P.O. Box 10412, Palo Alto, CA 94303
75. Boyd A. Hutchison, Atmospheric Turbulence and Diffusion Division, National Oceanic and Atmospheric Administration, U.S. Department of Commerce, P.O. Box E, Oak Ridge, TN 37831
76. Carl F. Jordan, Senior Ecologist, The Institute of Ecology, University of Georgia, Athens, GA 30602
77. George Y. Jordy, Director, Office of Program Analysis, Office of Energy Research, ER-30, G-226, U.S. Department of Energy, Washington, DC 20545
78. Charles D. Keeling, Scripps Institution of Oceanography, University of California-San Diego, 2314 Ritter Hall, A-020, La Jolla, CA 92093

79. F. A. Koomanoff, Director, Carbon Dioxide Research Division, Office of Energy Research, Room J-309, ER-12, U.S. Department of Energy, Washington, DC 20545
80. John A. Laurmann, Executive Scientist, Engineering Sciences, Gas Research Institute, 8600 West Bryn Mawr Avenue, Chicago, IL 60631
81. Prof. Dr. Helmut Lieth, Fachbereich Biologie/Chemie der Universität Osnabrück, Postfach 4469, BarbarasträÙe 11, D-4500 Osnabrück, FEDERAL REPUBLIC OF GERMANY
82. Austin Long, Department of Geosciences, Laboratory of Isotope Geochemistry, The University of Arizona, Tucson, AZ 85721
83. Ariel E. Lugo, Project Leader, U.S. Department of Agriculture, Forest Service, Southern Forest Experiment Station, Institute of Tropical Forestry, P.O. Box AQ, Rio Piedras, PR 00928
84. Gregg Marland, Oak Ridge Associated Universities, Institute for Energy Analysis, P.O. Box 117, Oak Ridge, TN 37831
85. Helen McCammon, Director, Ecological Research Division, Office of Health and Environmental Research, Office of Energy Research, MS-E201, ER-75, Room E-233, Department of Energy, Washington, DC 20545
86. V. Rick McDaniel, Department of Biological Sciences, Arkansas State University, P.O. Box 599, State University, AR 72467
87. Berrien Moore III, Director, Complex Systems Research Center, O'Kane House, University of New Hampshire, Durham, NH 03824
88. Hans Oeschger, Physikalisches Institut, Universität Bern, Sidlerstrasse 5, CH-3012 Bern, SWITZERLAND
89. J. S. Olson, Box 361A, Route 2, Lenior City, TN 37771
90. William S. Osburn, Jr., Ecological Research Division, Office of Health and Environmental Research, Office of Energy Research, MS-E201, EV-33, Room F-216, Department of Energy, Washington, DC 20545
91. H. Gote Ostlund, Rosenstiel School of Marine and Atmospheric Science, Tritium Laboratory, University of Miami, 4600 Rickenbacker Causeway, Miami, FL 33149
92. Ken N. Paige, Department of Biological Sciences, Northern Arizona University, P.O. Box 5640, Flagstaff, AZ 86011
93. J. J. Pastor
94. Eldor A. Paul, Department of Plant and Soil Biology, College of Natural Resources, 108 Hilgard Hall, University of California-Berkeley, Berkeley, CA 94720
95. Graeme I. Pearman, Commonwealth Scientific and Industrial Research Organization, Division of Atmospheric Research, Private Bag No. 1, Mordialloc, Victoria 3195, AUSTRALIA
96. Ralph M. Perhac, Director, Environmental Assessment Department, Electric Power Research Institute, 3412 Hillview Avenue, P.O. Box 10412, Palo Alto, CA 94303
97. James T. Peterson, Director, Geophysical Monitoring for Climatic Change, U.S. Department of Commerce, National Oceanic and Atmospheric Administration, Environmental Research Laboratories, 325 Broadway, Boulder, CO 80303
98. Irwin Remson, Department of Applied Earth Sciences, Stanford University, Stanford, CA 94305

99. Roger R. Revelle, Program in Science, Technology, and Public Affairs (B-007), Scripps Institution of Oceanography, University of California-San Diego, La Jolla, CA 92093
100. John F. Richards, Department of History, Duke University, 6727 College Station, Durham, NC 27708
101. Ralph M. Rotty, Oak Ridge Associated Universities, Institute for Energy Analysis, P.O. Box 117, Oak Ridge, TN 37831
102. William H. Schlesinger, Department of Botany, Duke University, Durham, NC 27708
103. R. J. Stern, Director, Office of Environmental Compliance, MS PE-25, FORRESTAL, U.S. Department of Energy, 1000 Independence Avenue, SW, Washington, DC 20585
104. Boyd R. Strain, Phytotron, Department of Botany, Duke University, Durham, NC 27708
105. Minze Stuiver, Department of Geological Sciences, Quaternary Isotope Laboratory, AK-60, University of Washington, Seattle, WA 98195
106. Eric T. Sundquist, U.S. Department of the Interior, U.S. Geological Survey, 431 National Center, MS-431, Reston, VA 22092
107. Christopher Uhl, College of Science, Department of Biology, 202 Buckhout Laboratory, The Pennsylvania State University, University Park, PA 16802
108. James A. Viecelli, Associate Division Leader, T Division, Physics Department, Lawrence Livermore National Laboratory, P.O. Box 808 (L-71), Livermore, CA 94550
109. Robert L. Watters, Ecological Research Division, Office of Health and Environmental Research, Office of Energy Research, MS-E201, ER-75, Room F-226, Department of Energy, Washington, DC 20545
110. Leonard H. Weinstein, Program Director of Environmental Biology, Cornell University, Boyce Thompson Institute for Plant Research, Ithaca, NY 14853
111. Raymond G. Wilhour, Chief, Air Pollution Effects Branch, Corvallis Environmental Research Laboratory, U.S. Environmental Protection Agency, 200 SW 35th Street, Corvallis, OR 97330
112. Frank J. Wobber, Division of Ecological Research, Office of Health and Environmental Research, Office of Energy Research, MS-E201, Department of Energy, Washington, DC 20545
113. M. Gordon Wolman, The Johns Hopkins University, Department of Geography and Environmental Engineering, Baltimore, MD 21218
114. George M. Woodwell, Director, The Ecosystems Center, Marine Biological Laboratory, 167 Water Street, Woods Hole, MA 02543
115. Paul J. Zinke, Department of Forestry and Natural Resources, Mulford Hall, University of California-Berkeley, Berkeley, CA 94720
116. Office of Assistant Manager for Energy Research and Development, Oak Ridge Operations, P. O. Box E, Department of Energy, Oak Ridge, TN 37831
- 117-143. Technical Information Center, Oak Ridge, TN 37831